



UNIVERSIDADE D  
COIMBRA

João Gonçalo Ereira da Silva

**ENGINEERING AND CHARACTERIZATION OF  
A MOUSE C2-BLOCKING ANTIBODY  
INTRODUCING A PH-DEPENDENT TARGET  
RELEASE**

**Dissertação no âmbito do Mestrado em Biotecnologia  
Farmacêutica orientada pela Dra. Jolien Delaere e pelo Professor  
Doutor João Nuno Sereno de Almeida Moreira e apresentada à  
Faculdade de Farmácia da Universidade de Coimbra**

Julho de 2023



1 2 9 0

FACULDADE DE FARMÁCIA  
UNIVERSIDADE DE  
**COIMBRA**

João Gonçalo Ereira da Silva

**ENGINEERING AND CHARACTERIZATION OF  
A MOUSE C2-BLOCKING ANTIBODY  
INTRODUCING A PH-DEPENDENT TARGET  
RELEASE**

**Dissertação no âmbito do Mestrado em Biotecnologia  
Farmacêutica orientada pela Dra. Jolien Delaere e pelo Professor  
Doutor João Nuno Sereno de Almeida Moreira e apresentada à  
Faculdade de Farmácia da Universidade de Coimbra**

Estágio elaborado na/ Internship performed at argenx



Julho de 2023



# Acknowledgements

I would like to start by thanking the entire argenx-117 team: Inge Van De Walle, Tim Delahaye, Laura Bracke, Karen De Winter and particularly to Jolien Delaere, my direct supervisor, for welcoming me in such an interesting project. I appreciate all of your teachings, guidance and commitment towards my work throughout these months.

Next, I would like to thank Sebastien Verhenne and all argenx, for allowing me to engage in this journey and be part of a cutting-edge company in the vanguard of therapy. Likewise, an appreciation note to all argonauts that shared their knowledge and offered their support during my stay in argenx. I'm certainly proud to have been part of the argonaut family.

I would also like to thank Professor Doctor Nuno Moreira for accepting the role of my faculty supervisor and for always being available to help. To the Faculty of Pharmacy of University of Coimbra, I want to thank for all the knowledge passed on to me during my masters degree.

To my friends in Portugal, that even in distance always demonstrated their support towards me, my experience and my goals, I want to genuinely thank you for your presence and loyalty.

To the friends I gained in Ghent, thank you for helping me making the most out of this experience, I greatly praise the time spent with you and will certainly miss you. Evidently, I could not leave out a special thanks to Claire for walking this path besides me. You absolutely added immensely to this journey.

To my parents and all of my family I would like to thank for always allowing me and encouraging me to follow my dreams, for always believing in my goals and for showing their pride towards me. I certainly acknowledge and appreciate you deeply.

# Contents

Acknowledgements.....	I
List of abbreviations.....	V
List of tables.....	VI
List of figures.....	VII
Abstract.....	IX
Resumo.....	X
Introduction.....	1
1-Complement system.....	1
1.1-Complement activation and general function in the organism.....	1
1.2-Complement system in disease.....	3
1.3-Complement system as therapeutic target.....	4
2-Therapeutic antibodies.....	5
2.1-(IgG) antibody structure.....	6
2.2-Antibody diversity and class switching.....	7
2.3-Mechanisms of action.....	10
3-Engineered Antibodies.....	10
3.1-Enhanced FcRn affinity.....	11
3.2-pH-dependent target release.....	12
5-ARGX-117.....	14
5.1-Mechanism of action.....	14
5.2-Pre-clinical results and clinical status.....	15
Project goals.....	17
Materials.....	18
Equipment.....	18
Material.....	18
Buffers and reagents.....	18
Commercial kits.....	20
Cells.....	20
Proteins/antibodies.....	21

Enzymes .....	21
Serum.....	21
Primers .....	21
Vectors.....	22
Methods .....	23
A-12E08 mutants based on predictive crystal structure .....	23
1-Plasmid generation .....	23
2-Antibody production.....	24
B-Development of antibodies from combinatorial histidine library .....	27
1-DNA cloning.....	27
2-Library cloning .....	30
3-Phage display.....	34
4-Fab production .....	37
C- Antibody characterization.....	38
1-Mouse C2 binding ELISA.....	38
2-Mouse Classical Pathway ELISA.....	38
3-MesoScale Discovery.....	39
4-Peri ELISA .....	40
Results .....	41
A-12E08 mutants based on predictive crystal structure .....	41
1-Plasmid generation .....	41
2-Protein production and purification.....	43
3-Mouse C2 binding ELISA.....	46
4-Mouse Classical Pathway ELISA.....	48
5-MesoScale Discovery.....	51
6-Further analysis of predictive structure .....	53
B-Development of antibodies from combinatorial histidine library .....	57
1-Plasmid preparation .....	57
2-Library construction .....	57
3-Library cloning- Protocol optimization.....	58
4-Phage display and selections.....	64

5-Sequence analysis and peri ELISA.....	70
6- Histidine mutations combination analysis .....	75
Discussion.....	79
References .....	83
Appendix .....	89

# List of abbreviations

CS	Complement system
CP	Classical pathway
LP	Lectin pathway
AP	Alternative pathway
TP	Terminal pathway
MAC	Membrane attack complex
DAMPs	Damage-associated molecular patterns
MBL	Mannose-binding lectin
FB	Factor B
FD	Factor D
PNH	Paroxysmal nocturnal hemoglobinuria
aHUS	Atypical haemolytic uremic syndrome
FDA	Food and Drug Administration
EMA	European Medicines Agency
PK	Pharmacokinetics
PD	Pharmacodynamics
ab	Antibody
mAbs	Monoclonal antibodies
Ig	Immunoglobulin
S2	Sushi 2 epitope
CL	Constant Light domain
CH	Constant Heavy domain
VL	Variable Light domain
VH	Variable Heavy domain
CDRs	Complementarity Determining Region
Fc region	Fragment crystallizable region
FcRn	Neonatal Fc Receptor
Fab	Antigen-binding fragment
His	Histidine
pKa	Acid dissociation constant
pH	Power of Hydrogen; Acidity degree
WT	Wild type

# List of tables

Table 1- Digestion of DNA strings and vectors .....	23
Table 2-Ligation and negative control .....	23
Table 3-Protein purification workflow .....	25
Table 4- First digestion of pCB13 vectors.....	28
Table 5- Digestion of 12E08 VL and VH WT strings.....	28
Table 6 -Ligation of digested pCB13 vectors and digested 12E08 WT strings .....	29
Table 7- Second digestion of vectors (with previously inserted WT chains) .....	30
Table 8 - PCR amplification of 12E08 VH and 12E08 VL synthetic histidine libraries .....	31
Table 9- Libraries digestion from general plasmids .....	31
Table 10- Test-ligation of digested histidine libraries and prepared vectors .....	32
Table 11- Colony PCR protocol.....	32
Table 12- Colony PCR program .....	32
Table 13- Real-ligation of histidine libraries and prepared vectors (with WT chains).....	33
Table 14- Plasmid combination for HEK-293E cell transfection.....	44
Table 15- Plasmid combination for HEK-293E cell transfection for new histidine mutant antibodies production.....	54
Table 16- Overview protocol optimization for library cloning-3 pairs of libraries generated.....	54
Table 17- Digestion protocol for vectors and libraries adapted to Fast Digest enzymes .....	60
Table 18- Further optimized protocol for vector digestion (with WT chain) using FD enzymes.....	61
Table 19-Further optimized protocol for library digestion (PCR product) using FD enzymes .....	62
Table 20- Overview of generated libraries.....	63
Table 21- Conditions selections R1 .....	65
Table 22- Conditions selections R2 .....	66
Table 23- Conditions selections R3 .....	67
Table 24- Conditions selections R4 .....	69
Table 25- Potential mutation positions for VL.....	77
Table 26- Potential mutation positions for VH.....	78

# List of figures

Figure 1- Schematic overview of the complement system (CS) and the different pathways of action .....	1
Figure 2- Representation of the structure of a IgG antibody.....	7
Figure 3- Representation of the V(D)J recombination of a heavy chain.....	8
Figure 4- Schematic representation of the trafficking of an antibody with a pH-dependent target release vs a conventional antibody. ....	13
Figure 5- Schematic representation of the workflow for the preparation of pCB13 vectors to receive HIS libraries. ....	27
Figure 6- Workflow overview after cell transformation .....	34
Figure 7- Predictive crystal structure of 12E08' fab region modelled by Alphafold. ....	42
Figure 8 - 12E08 structure sites where histidine mutations were planned to be introduced. ....	42
Figure 9- Example of the transformation of TOP 10 cells with 12E08 mutant plasmids.....	43
Figure 10- SDS-Page performed as QC for the generated histidine engineered antibodies under reducing and non-reducing conditions.....	45
Figure 11- Schematic representation of a mouse C2 binding ELISA setup .....	47
Figure 12- Mouse C2 binding assay performed for histidine engineered antibodies, .....	47
Figure 13- Schematic representation of a mouse classical pathway ELISA setup .....	49
Figure 14- Mouse classical pathway ELISA assay performed for he histidine engineered antibodies. ....	50
Figure 15- Schematic representation of the MSD setup for the test of a pH-dependent target-release.....	51
Figure 16- Mesoscale discovery performed with all histidine engineered antibodies.....	52
Figure 17- Comparison of the binding profile of mab117_083 upon wash at pH 7.4 vs pH 5.5 .....	53
Figure 18- Comparison of the binding profile of mab117_087 upon wash at pH 7.4 vs pH 5.5 .....	53
Figure 19- Location in 12E08's predictive structure further explored. ....	54
Figure 20- SDS-Page performed as QC for the new generated histidine engineered antibodies under reducing and non-reducing conditions. ....	55
Figure 21- Mesoscale discovery performed with the new histidine engineered antibodies.....	56
Figure 22- Gel electrophoresis of digested vectors with WT chains.....	57
Figure 23- Positions that were mutated (with 10 % probability of histidine).....	58
Figure 24- Gel electrophoresis of the PCR products (amplified libraries).....	58
Figure 25- Gel electrophoresis of the digested libraries. ....	60
Figure 26- Transformation of TG1 electrocompetent cells with 12E08 mutant plasmids from the test ligation.....	62
Figure 27- Transformation of TG1 electrocompetent cells with 12E08 mutant plasmids from ligation .....	63
Figure 28- Spotting of all outputs from Round 1 (R1) of selections.....	65
Figure 29- Spotting of all outputs from Round 2 (R2) of selections.....	67
Figure 30- Spotting of all outputs from Round 3 (R3) of selections.....	68
Figure 31- Spotting of all outputs from Round 4 (R4) of selections .....	69
Figure 32- Optical density of the most pH-dependent clones tested on peri ELISA.....	70
Figure 33- Hotspot analysis of histidine introduction in each position and introduction of histidine in the sequences of the most pH-dependent clones of R4 tested on peri ELISA for VL CDR1.....	71

Figure 34- Hotspot analysis of histidine introduction in each position and introduction of histidine in the sequences of the most pH-dependent clones of R4 tested on peri ELISA for VL CDR2.....	71
Figure 35- Hotspot analysis of histidine introduction in each position and introduction of histidine in the sequences of the most pH-dependent clones of R4 tested on peri ELISA for VL CDR3.....	72
Figure 36- Hotspot analysis of histidine introduction in each position and introduction of histidine in the sequences of the most pH-dependent clones of R4 tested on peri ELISA. ....	73
Figure 37- Hotspot analysis of histidine introduction in each position and introduction of histidine in the sequences of the most pH-dependent clones of R4 tested on peri ELISA for VH CDR1 .....	73
Figure 38- Hotspot analysis of histidine introduction in each position and introduction of histidine in the sequences of the most pH-dependent clones of R4 tested on peri ELISA for VH CDR2.....	74
Figure 39- Hotspot analysis of histidine introduction in each position and introduction of histidine in the sequences of the most pH-dependent clones of R4 tested on peri ELISA for VH CDR3.....	74
Figure 40- Mutation of VH_I31 and VH_A53 in the predictive crystal structure of 12E08 .....	75
Figure 41- Mutation of VH_D101 in the predictive crystal structure of 12E08.....	76
Figure 42- Mutation of VH_I31 and VH_A53 in the predictive crystal structure of 12E08.....	77
Figure 43- Mutation of VH_D101 in the predictive crystal structure of 12E08.....	78

# Abstract

ARGX-117 is a first in class antibody engineered for optimal blockade of the C2 component of the complement system. The therapeutic antibody, developed by argenx, features a pH-dependent target release. This leads to the release of C2 in the endosome for lysosomal degradation, while the antibody travels back into circulation (thanks to an enhanced FcRn binding), free to capture more C2 molecules.

However, the monoclonal antibody is not cross-reactive with mouse, a preferred species as disease model for preclinical pharmacology and safety studies. Therefore, although ARGX-117 is currently under investigation for treatment of different diseases, developing a mouse derivative might enable research for new indications. For this reason, the argenx-117 team developed a mouse C2 blocking antibody (12E08).

Unlike ARGX-117, 12E08 does not show a pH-dependent target release of C2, essential for its recycling properties and longer half-life.

Thus, the purpose of this project is to develop and further optimize, through antibody engineering, a derivative of the mouse C2 blocking antibody, that performs target-release in a pH-dependent manner, to better mimic ARGX-117 mode of action.

To reach that goal, two lines of work were followed: 1-single histidine mutations selected based on the potential interactions with the antigen considering the location on 12E08's predictive crystal structure; 2-generation of combinatorial histidine mutation libraries for the heavy and light chains of 12E08, with a probability of 10% histidine prevalence in all designated positions.

Although, the introduction of single histidine mutations based on the predictive structure of 12E08 did not result in pH-dependent antibodies, the combinatorial histidine mutagenesis libraries proved to be a powerful tool for introduction of a pH-dependent target release. The data generated reveals important insights about the most implicated positions in such feature as well as the most promising combinations to mutate.

Therefore, this thesis provides important hints towards the development of a full pH-dependent mouse C2-blocking antibody that can be used for accurate *in vivo* studies in mice, allowing the search for new potential indications.

# Resumo

ARGX-117 é um anticorpo inovador projetado para o bloqueio ótimo do componente C2 do sistema do complemento. O anticorpo terapêutico, desenvolvido pela argenx, apresenta uma liberação do alvo dependente de pH. Isto leva a que o C2 seja liberto no endossoma para degradação lisossomal, enquanto que o anticorpo viaja de volta à circulação (devido a ligação aumentada ao FcRn), livre para capturar mais moléculas de C2.

No entanto, o anticorpo monoclonal não apresenta reatividade cruzada com murganho/ratinho, que é uma espécie de preferencia como modelo de doença para estudos pré-clínicos.

Assim sendo, embora o ARGX-117 esteja atualmente a ser estudado para diferentes doenças, o desenvolvimento de um derivado para murganho pode permitir a investigação de novas indicações. Por esta razão, a equipa do argenx-117 desenvolveu um anticorpo bloqueador de C2 de murganho, o 12E08.

Contudo, ao contrário do ARGX-117, o 12E08 não apresenta uma liberação de C2 dependente de pH, essencial pelas suas propriedades de reciclagem e aumento de semi-vida.

Assim, o objetivo deste projeto é desenvolver e otimizar, através da engenharia de anticorpos, um derivado do anticorpo bloqueador de C2 de murganho, que liberte o alvo de uma forma dependente do pH, para melhor imitar o modo de ação de ARGX-117.

Com esse intuito, duas linhas de trabalho foram seguidas: 1-mutações únicas de histidina selecionadas com base nas potenciais interações com o antigénio, tendo em conta a localização na estrutura cristalina preditiva do 12E08; 2-geração de bibliotecas combinatórias de mutações de histidina para a cadeia pesada e leves de 12E08, com uma probabilidade de prevalência de histidina de 10% em cada posição designada.

Embora a introdução de mutações únicas de histidina baseadas na estrutura preditiva de 12E08 não tenha resultado em anticorpos dependentes de pH, as bibliotecas combinatórias de mutagénese de histidina provaram ser uma ferramenta poderosa para a introdução de dependência de pH. Os dados gerados revelam informações importantes sobre as potenciais posições envolvidas na introdução da característica, bem como as combinações mais promissoras para introduzir mutações.

Desta forma, esta dissertação fornece indicações importantes para chegar ao desenvolvimento de um anticorpo bloqueador de C2 de murganho, dependente de pH,

que pode ser usado para estudos in vivo mais precisos em murganho, permitindo a exploração de novas potenciais indicações.



CP is activated primarily upon antibody recognition, however, an antibody-independent trigger is also possible. (Duncan e Winter, 1988) In the first case, specific antibodies from the adaptive immune system recognize and bind to a pathogens' cell surface. The Fc regions of these antibodies can then be recognized by C1, a complement protein complex consisting of protein C1q, C1r and C1s. The binding of C1q to the antibody leads to the activation of subunits C1r and C1s (serine proteases). C1s proceeds to cleave the next protein in the CP cascade, C4, originating C4a and C4b. Deposited C4b will attract C2 to bind and C1s will cleave C2b off, resulting in C4bC2b complex. This complex, also known as C3 convertase, follows to cleave C3, generating C3a (with proinflammatory properties) and C3b (opsonin). (Galvan, Greenlee-Wacker e Bohlsion, 2012; Kishore et al., 2004)

From the formation of C3 convertase, the terminal pathway (TP) of complement begins. Each C3 convertase can cleave multiple C3 molecules, leading towards an abundance of C3b. When there is enough C3b, it can bind to the C4bC2b complex, forming the C4bC2bC3b complex (= C5 convertase). The formed C5 convertase then cleaves circulating C5 into C5a (a pro-inflammatory fragment) and C5b – which is the starting point for the assembly of the Membrane Attack Complex (MAC). (Hadders et al., 2012)

The antibody-independent scenario, however, relies on the capability of C1 to recognize multiple potential danger molecules, including surface-bound pentraxins and damage-associated molecular patterns (DAMPs). After this initial C1 binding, CP activation proceeds in the same manner as described above. (Fraser e Tenner, 2008)

The LP, on the other hand, is activated when pattern recognition molecules (PRMs) such as mannose-binding lectin (MBL), collectins and ficolins bind to pathogen-associated molecular patterns (PAMPs), such as D-mannose, N-acetyl-D-glucosamine, or acetyl groups, usually present on bacteria or viruses. These PRMs form complexes with MASP1, MASP2 and MASP3 (serine proteases) that are able to activate C2 and C4 resulting in the same C3 convertase (C4bC2a) generated in CP. (Banda et al., 2010; Chen e Wallis, 2001)

Contrary to the described CP and LP, AP is spontaneously activated as a result of C3 hydrolysis, happening at a constant rate. This leads to a conformational change of C3 that allows binding to Factor B (FB). Factor D (FD) then cleaves FB into Bb and Ba resulting in the soluble C3 convertase C3(H<sub>2</sub>O)Bb and, subsequently, soluble C3 convertase is able to cleave more C3. As a result of that cleavage, C3b deposits on target surfaces originating the complex C3bBb, which is the membrane bound AP C3 convertase. The cascade then continues similarly to the CP and LP cascade. Furthermore, other forms of activation of

the AP such as lipopolysaccharides on cell walls of Gram-negative bacteria, are also known. (Pangburn, Schreiber e Müller-Eberhard, 1981; Rooijakkers et al., 2009)

Additionally, AP can amplify CP and LP, from the formation of C3 convertase. This amplification can happen in the fluid phase, with the covalent binding of two C3b molecules with IgG, forming C3b2-IgG that then binds bivalently to properdin. These complexes promote the binding of FB (then cleaved by FD), resulting in properdin-stabilized C3 convertase, with a half-life more than 100 times longer than free C3b, as these molecules become partially protected from inactivation. Alternatively, on cell surfaces, C3b binds to thioesters and forms clusters that can also bivalently bind to properdin and recruit FB and FD, ultimately resulting in the additional C3 convertase and promote the amplification loop. (Harboe e Mollnes, 2008; Janeway CA Jr, 2001; Lutz e Jelezarova, 2006)

Despite the differences in activation trigger, in all three pathways C5b proceeds to bind to C6 and C7, leading to a hydrophobic site of C7 to be exposed and allowing binding of soluble C8. The complex with C8 behaves similarly and also exposes a hydrophobic site, making the partial penetration of C8 in the membrane possible. This entire complex promotes the polymerization of C9 which can completely penetrate the membrane, forming a pore and, consequently - as there can be up to 22 C9 molecules in one MAC complex- promoting cell lysis. In addition, this MAC complex can also be sublytic, performing other roles such as protein synthesis and apoptosis (Podack, 1984).

## 1.2-Complement system in disease

Although the CS is key in protecting the organism from invading pathogens, it is clear that when dysregulated and working incorrectly, CS can lead to pathology development.

On one hand complement can be under activated, creating an immunodeficient scenario with reduced pathogen protection that ultimately results in an increased risk of severe infections. These deficiencies are often genetic and can occur in different components of any pathway or even involve positive regulators of CS. These dysregulations result in particularly severe pathologies when associated with AP or the terminal pathway. (Figuerola e Densen, 1991; Grumach e Kirschfink, 2014)

In case of C2 deficiency, for example, a higher recurrency of bacterial infections arises, but also a higher risk of developing systemic lupus erythematosus (SLE). (Manne e Narayana, 2018; Pickering et al., 2001) However, in C1 or C4 deficiencies, this correlation is much higher.

Remarkably, the fact that a complement deficiency is related to an autoimmunity scenario (although the obvious outcome would be an immunodeficient disease), relies on complement's protective role against autoimmunity, through clearance mechanisms. Nevertheless, the presence of complement can also contribute to tissue injury/inflammation, giving CS a dual role in disease. (Cook e Botto, 2006; Sjöholm et al., 2006)

On that note, it is also important to highlight the excessive activation of the CS, which can result in an exacerbated response of the immune system, causing aggravated or even chronic inflammation and autoimmune diseases.(Ricklin, Reis e Lambris, 2016; Vlam et al., 2015)

In multifocal motor neuropathy (MMN), for example, IgM anti-GM1 antibodies trigger the activation of the CP, leading to complement deposition and consequent disruption of sodium channel clusters through MAC. Such mechanism assists the promotion of progressive axonal loss and severe weakness, characteristic of MMN. (Cook e Botto, 2006; Vlam et al., 2015)

### 1.3-Complement system as therapeutic target

Considering the role of CS in health and disease, the interest in targeting it with therapeutic purpose is decipherable.

The approval of anti-C5 antibody Eculizumab for the treatment of Paroxysmal nocturnal hemoglobinuria (PNH) in 2007 by the FDA and EMA and later for the treatment of atypical hemolytic uremic syndrome (aHUS), highlighted the importance of targeting complement and further demonstrated the potential of complement-targeting therapies in humans. (Rother et al., 2007; Wong, Goodship e Kavanagh, 2013)

However, despite the decades of research, very few complement inhibitors get to late-stage clinical studies. As of august 2022, only 9 complement targeting therapies were approved by FDA: Cinryze, Enjaymo, Ruconest and Berinert inhibiting C1, SYFOVRE™ and

Empaveli inhibiting C3 and Eculizumab, Ravulizumab and Avacopan inhibiting C5.(Complement Inhibitors as Therapeutic Agents, 2022)

This is likely due to the fact that there are still concerns and limitations regarding therapies targeting the CS.

Firstly, complement proteins that could act as therapy targets show a high turnover rate and are usually present in very high concentrations, especially in acute scenarios of inflammation, which is often translated into the need of high dosage of therapy for the expected outcome. (Tange et al., 2018) (Harris, 2018)

Moreover, blocking CS in diseases where it is over-expressed can result in unwanted side effects, since blocking CS also means blocking an important part of the immune system and leaves the organism prone to infection. (Socié et al., 2019) Additionally, the unclear biological disease mechanisms and role of CS can also make the selection of a specific target and potential indications challenging.

Therefore, approaches that address such challenges should continue to be the object of research and improvement as the potential of complement-targeting therapies is clear.

## 2-Therapeutic antibodies

As part of the adaptive immune system, the organism generates a humoral response to protect itself from pathogens. The humoral response is characterized by the production of antibodies -highly specific immunoglobulin proteins- by B cells.

As antibodies represent an opportunity to target multiple factors with precision and accuracy, the application of these molecules in a clinical setting became a source of interest, evidently, also to target complement factors.

However, the generation of antibodies for therapeutic purposes only became possible in 1975, when Kohler and Milstein developed the hybridoma method, a lymphocyte (from animals after immunization) and myeloma cell-fusion that provided immortal clones, making the production of larger amounts of mAbs possible. (KÖHLER e MILSTEIN, 1975) In present day, alternatives to the hybridoma method can be found, such as recombinant production of antibodies by transfection of mammalian cells or library construction from

B cell RNA and consequent phage display for antibody selection.(Sheets et al., 1998; Wurm, 2004)

## 2.1-(IgG) antibody structure

The great majority of monoclonal antibodies (mAbs) used for therapeutic purposes until present date are immunoglobulin class G proteins (IgG). (Mould e Meibohm, 2016) (Geist, Zheng e Xu, 2021)

Monoclonal antibodies all have a basic and fundamental structure, represented in **Error! Reference source not found.** They are large molecules (~150 kDa) with a characteristic Y shape, consisting of two polypeptide heavy chains and two polypeptide light chains, connected through a bisulfide bridge.

Each heavy chain has three constant regions (CH1, CH2, CH3) and one variable region (VH). The light chain, however, exists in two different formats in mammals, type lambda ( $\lambda$ ) and type kappa ( $\kappa$ ), both with only one constant region (CL) and one variable region (VL). The molecule can also be characterized by the definition of a fragment crystallizable (Fc) region and an antigen binding fragment (Fab). The Fc region corresponds to the CH2 and CH3 of each heavy chain, where the binding to cell surface receptors, such as FcRn, Fc $\gamma$  or even molecules within the CS, happens. Fab regions correspond to the CH1 of the heavy chains and CL of the light chains, together with the variable regions of both chains. (Ryman e Meibohm, 2017)

Within the variable regions of the antibody, there are hypervariable regions, formed by 3 complementarity determining regions (CDRs) in each chain. CDRs are responsible for the high-specificity of the antibody to the respective antigen and, therefore, the combination of the 3 CDRs from light and heavy chain form the antibody binding site (paratope), specifically complementary to the binding site of the antigen (epitope). (Akbar et al., 2021; Inbar, Hochman e Givol, 1972)

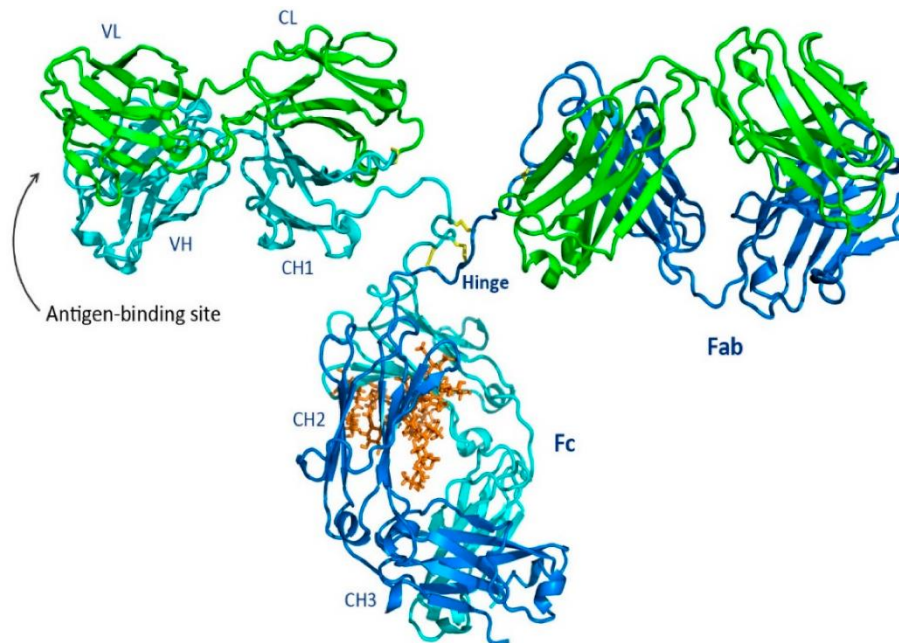


Figure 2- Representation of the structure of a IgG antibody (Chiu et al., 2019)

## 2.2-Antibody diversity and class switching

Upon the encounter of an antigen (potential pathogen), the corresponding B cell is activated (as each B cell recognizes a specific antigen) and the activated B cell goes through an expansion process, originating millions of cell clones that produce specific antibodies against the antigen. This process is called monoclonal expansion, which then, originates monoclonal antibodies.(Burnet, 1959)

Therefore, to be able to defend the organism against thousands of different and rapidly evolving pathogens and to cover the wide range of potential threats, an incredible variety of specific antibodies is needed. For that reason, a large number of genes would be expected to code for these protective antibodies, however, the mechanisms involved in antibody diversity are very particular and can meet the goal with a reduced number of genes.

Three different gene loci in different chromosomes encode for antibodies, one for heavy chain, one for kappa (K) light chain and one for lambda ( $\lambda$ ) light chain. In each loci, there is a variable region with different types of segments, variant (V), junction (J) and an extra segment, diversity (D), for the heavy chain. Additionally, constant segments are also present in each chain.

Within each fragment type there is diversity of fragments, and the variable region of each chain is formed by the random recombination of different segments (V-D-J in the case of heavy chain and V-J for light chain) as observed in Figure 3. (Tonegawa, 1983)

Moreover, during the recombination of the different fragments, additional nucleotides can be added in between fragments, which particularly affects the CDR3 loop (the region between V and J fragments), making CDR3 the most diverse region in antibodies. (Antibody Diversity, 2012)

The constant region is then combined with the newly-formed variable region through RNA splicing, (Antibody Diversity, 2012) and the subsequent pairing between a light chain and a heavy chain, further expands the diversity of antibodies that can be generated.

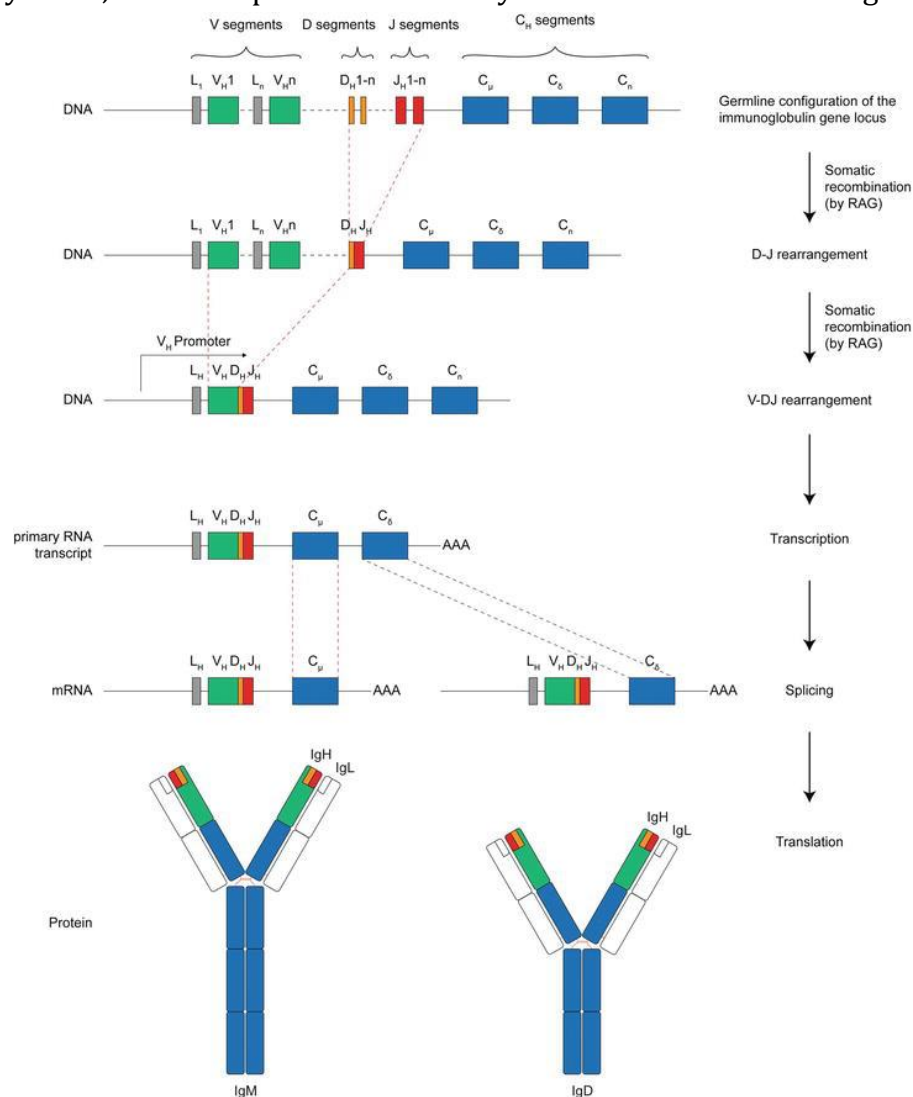


Figure 3- Representation of the V(D)J recombination of a heavy chain. The random recombination of the different segments leads to antibody diversity. (Backhaus, 2018)

The constant segments of the heavy chain determine the class of the antibody. (Amendt et al., 2021) Initially, non-activated B cells express only  $\mu$  chain and  $\delta$  chain, originating IgM and IgD antibodies, that act as transmembrane proteins, as part of the B cell receptor (BCR). Only when B cell activation occurs, as a consequence of antigen presentation by T cells, does the class switch recombination process happens. (Sathe e Cusick, 2022)

Upon the encounter of an antigen, T cells secrete specific cytokines that trigger the recombination process in at particular site. The activation-induced cytidine deaminase (AID) converts cytidine to uracil (in the location triggered by cytokines), and DNA uracil glycosylase digests the uracil residues out. In an attempt to fix the breaks in the DNA, repair machinery leaves out the digested part (with most of the isotope chains) and by the non-homologous end joining (NHEJ) mechanism, connects the variable part with the next constant region. Clearly, this process is also dependent on the location of the chain, since previously excised chains cannot be included, making the class switching irreversible.(Gearhart, 2002; Taeye, de, Rispens e Vidarsson, 2019)

At this point, different classes of antibody can be produced (IgA, IgE and IgG).

While IgD is not abundant and it seems to only play a role in B cell maturation (Amendt et al., 2021), IgM is characteristically a first line of defense class , as they are polyreactive antibodies, binding to a broader range of antigens but with low affinity. Because of its pentameric structure, IgMs are also a powerful CS activators (via CP). (Boes, 2000)

IgA, on the other hand, is mostly known for its important role in mucosal immunity and promotion of agglomeration of microorganisms for an easier clearance for the pathogens (Li, Jin e Chen, 2020).While IgE is associated with immune defense against parasitic pathogens and allergic response through degranulation of basophiles and mast cells and consequent release of pro-inflammatory cytokines and histamine.(Mukai et al., 2016)

Lastly, IgGs can be divided into four different subclasses (IgG 1-4).They are capable of interacting with hematopoietic cells or stimulate the activation of CS through interaction and activation of C1q, resulting in target opsonization or formation of MAC. IgGs are also the only class that can cross the placenta, making them the main responsible for fetal humoral immune protection. (Nimmerjahn e Ravetch, 2008; Vidarsson, Dekkers e Rispens, 2014)

### 2.3-Mechanisms of action

The application of antibodies in a therapeutic setting can be done in distinct ways and serve different purposes.

By binding to a receptor, the antibody itself can act as an antagonist, blocking the binding site for its ligand. This neutralization mechanism can result in loss of cellular activity, inhibition of cell proliferation or blockade of many other cellular pathways. (Cavallo, Calogero e Forni, 2007; Ferrara et al., 2007)

On the other hand, an agonistic function is also possible by replicating the behavior of the native ligand. Through this mechanism, the physiological activity of the receptor is enhanced, leading for example, to stimulation of anticancer immunity.(Hahn *et al.*, 2017; Mayes, Hance e Hoos, 2018)

The therapeutic antibody can also operate as a mediator for immune cell-recruiting in a process called antibody-dependent cell-mediated cytotoxicity (ADCC). During this process, the antigen-binding site (paratope) of the antibody recognizes and binds to an antigen present on the cell surface. The exposed Fc region of the antibody subsequently interacts with receptors of cells such as natural killer (NK) cells or macrophages that lyse and phagocytose the cell. (Zafir-Lavie, Michaeli e Reiter, 2007)

In a similar way, the formed immune complex can bind to the C1 complex via the Fc region of the antibody. The CP cascade will be initiated leading to complement-dependent cytotoxicity (CDC). This process results in the attack of the cell membrane by MAC and, thus, in cell lysis and opsonization.

### 3-Engineered Antibodies

With the goal of changing the pharmacokinetic/ pharmacodynamic profile, manipulating target affinity or to even better suit disease biology, antibodies can be molecularly engineered to generate molecules with stronger and/or different capabilities.

Besides the engineering processes for chimeric or humanized antibodies, where CDRs are combined with human variable region framework sequences, to maintain target specificity but reduce immunogenicity, many other forms of antibody modification have been studied to further improve clinical efficacy. (Lo, Leger e Hock, 2014)

The most common form of antibody engineering with the aim to modulate pharmacokinetic properties are Fc modulations. Other technologies can be explored for affinity, maturation and optimization. Examples are random mutation introduction by chain shuffling or CDR randomization. These techniques are followed by phage display and selections. (Chiu e Gilliland, 2016; Yélamos, 2022) Such technologies can also be applied to the modulation of the pharmacokinetic profile by, for example, lowering the isoelectric point or introducing pH-dependency.(Igawa et al., 2010; Igawa, Mimoto e Hattori, 2014)

Moreover, next-generation antibodies with a wide range of different properties and applications are also being explored, such as bispecific antibodies, antibody–drug conjugates, antibody fusion protein or nano-antibodies. (Lo, Leger e Hock, 2014; Yélamos, 2022). Enhanced FcRn affinity and pH-dependent target release are examples of antibody engineering that will be further explored in following chapters.

### 3.1-Enhanced FcRn affinity

Normally involved in the transfer of humoral immunity from the mother to the neonate, the neonatal Fc receptor (FcRn) is also known to extend IgG antibodies half-life through IgG recycling (which is one of the reasons for the preferred choice of IgG antibodies for therapy). The binding of FcRn (a MHC class I-related receptor) and IgG is known to be weak at a neutral pH (physiological pH 7.4) but strong at an acidic pH (pH 6.0). This is due to the hydrophobic interactions between anionic (negatively charged) residues on FcRn and positively charged titratable histidine residues on Fc region.(Martin et al., 2001)

As depicted in Figure 4, during the process of pinocytosis by an endothelial cell the Fc region of the IgG antibody binds to FcRn. Once in the endosome, at an acidic pH of around 6.0, the binding between IgG and FcRn is strong enough to keep the antibody from lysosomal degradation and instead, can be recycled back to the cell surface and to circulation. (Rodewald, 1976; Roopenian e Akilesh, 2007)

Because FcRn affinity can influence pharmacokinetic (PK) properties of therapeutic antibodies, through the mechanism just explained, there has been an increased interest in engineering IgGs to further enhance their affinity to FcRn. With this alteration, the half-life of the molecule is further increased, prolonging the PK effect and/or reducing the necessary dose of administration. (Hinton et al., 2004; Rodewald, 1976; Roopenian e Akilesh, 2007)

An example of Fc engineering that aims to increase the affinity of the Fc region of antibodies to FcRn is the NHance™ technology. The technology was developed by Dr. Sally Ward (University of Texas Southwestern Medical Center) and is currently under an exclusive global license by argenx.

### 3.2-pH-dependent target release

Many therapeutic antibodies, even when able to escape the FcRn degradation route, remain in complex with the antigen. This results in no antigen degradation, antibody-antigen complex buildup and makes the capture of other target molecules impossible, ultimately leading to the need of higher dosing of antibody.(Igawa, Mimoto e Hattori, 2014)

However, this can be prevented by engineering the antibody to have a pH-dependent target release behavior. An example is represented in Figure 4. The antibody binds its target at pH 7, enters the cell by endocytosis and the antibody-antigen complex goes into the endosome, where pH is lower (pH 5.5 to 6). Through the pH-dependent target release property, the antigen is released from the antibody and proceeds to lysosomal degradation. The antibody stays bound to FcRn until it is finally recycled back into circulation, free to further capture target molecules.

To modulate pH-dependency in antigen release, the introduction of histidine's is a commonly chosen approach(Ito et al., 1992; Klaus e Deshmukh, 2021; Laughlin e Horn,

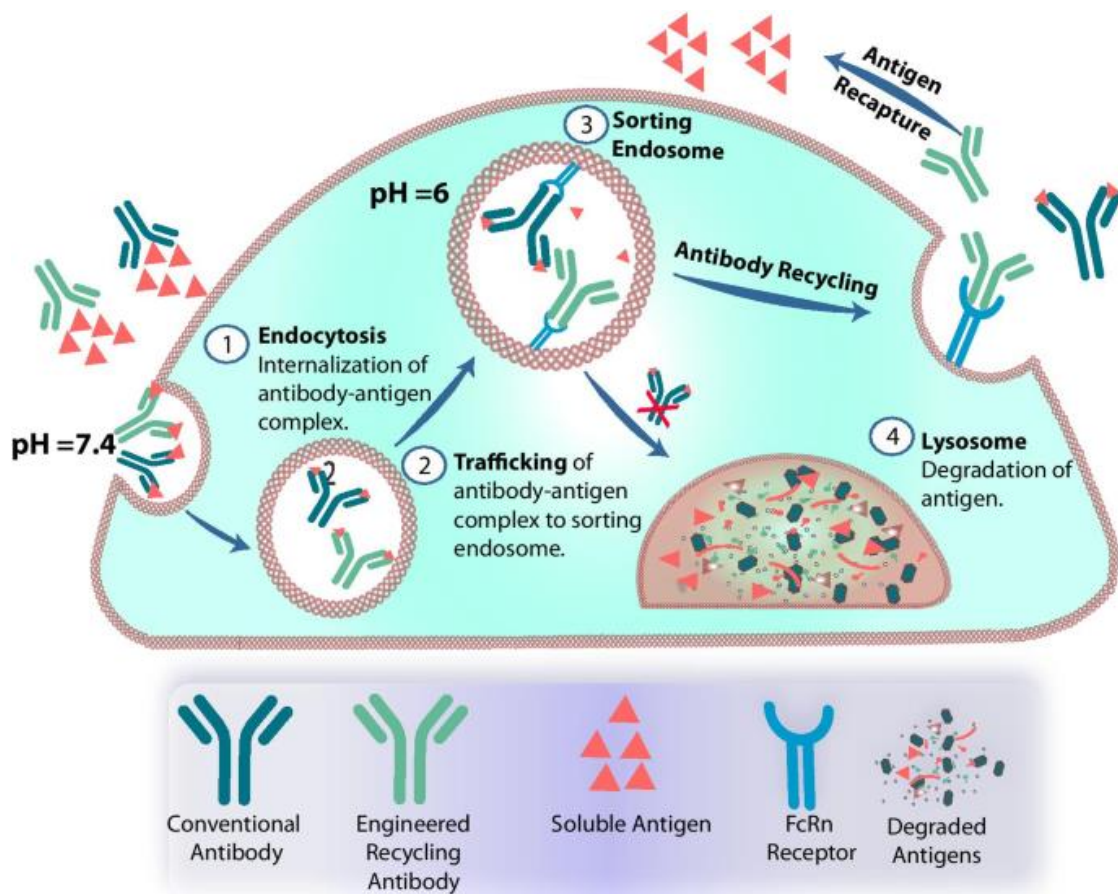


Figure 4- Schematic representation of the trafficking of an antibody with a pH-dependent target release vs a conventional antibody. The pH-dependent antibody is able to dissociate from the target in the endosome (where the pH is acidic, 5.5-6) and proceed back into circulation in a free format, while the second remains in complex with the antigen and is not able to capture more target molecules. (Klaus e Deshmukh, 2021)

2022; Murtaugh et al., 2011), as the amino acid is usually involved in naturally occurring pH-dependent protein-protein interactions. (Vaughn e Bjorkman, 1998)

The mechanism behind the histidine's feature relies on its ability for ionic receptiveness at different pHs. As histidine contains an imidazole side chain with a pKa of around 6.0, it means that at an acidic pH, protons are easily accepted and the protonation of the side chain is favored, resulting in positively charged histidine's. In antibodies, upon the protonation of the amino acid, interactions become repulsive and the antibody-antigen interaction can be destabilized, potentially leading to antigen release. (Liao et al., 2013) (Igawa, Mimoto e Hattori, 2014)

Other positively charged amino acids, such as lysine and arginine are protonated at pH 10 or even 12. Therefore, there is no change in protonation state between acidic and neutral condition and, consequently, the shift to a repulsive interaction does not align with the pH values of interest, as the interactions would be expected to maintain the same repulsive behavior in both conditions. (Shen, 2019)

Because of this protonation difference of histidine at physiological pH compared to low pH, various attempts are made to create histidine mutant IgG antibodies with the conviction of developing antibodies that release the antigen at acidic pH, which in the organism translates into a target release in the endosome. (Murtaugh et al., 2011) It has been demonstrated, however, that introducing pH-dependency in antibodies is often associated with affinity loss and the functional capacity might be compromised. Because of that, further affinity maturation of the antibodies might be necessary. (Devanaboyina et al., 2013; Igawa, Mimoto e Hattori, 2014) Nevertheless, by combining a recycling mechanism by enhancing the affinity of the Fc region of the IgG antibody to FcRn with a pH dependent target-release through histidine mutations, it is possible to achieve an improved “sweeping” therapeutic antibody with a much longer circulation time. (Igawa et al., 2013)

## 5-ARGX-117

ARGX-117 is a first -in-class therapeutic antibody targeting and blocking the Sushi2 domain (S2) of complement factor C2, inhibiting both LP and CP, that was developed by argenx and is currently in phase 2 clinical trials. (Walle, Van de et al., 2021)

### 5.1-Mechanism of action

ARGX-117 is a humanized monoclonal antibody that binds with a sub-nanomolar affinity to the C2 component of the CS.

By targeting C2, ARGX-117 makes the interaction of C2 and C4 impossible, blocking classical and lectin pathway, but leaving alternative pathway untouched. By doing so, the antibody is able to down-regulate CS without leaving the patient totally pathogen-vulnerable and infection-prone, as AP continues functioning properly. Additionally, by blocking upstream C3, ARGX-117 is able to prevent inflammatory responses associated with C3a, C5a and sub lytic MAC.

Moreover, besides having CP mildest disease phenotype when deficient, C2 is also one of the complement factors that occurs in the lowest concentration in circulation, making a good target for complement inhibition.

The antibody was Fc engineered with H433K and N434F mutations (NHance™) that enhance/increase Fc affinity to FcRn at low pH (5.5-6), resulting in a more effective rescue of the antibody from lysosomal degradation and allowing the therapeutic IgG to be recycled back in circulation- which translates in a longer half-life. Additionally, LALA mutations (L234A, L235A) were also introduced in the antibody, to minimize the effector function of the Fc.

Furthermore, the ARGX-117 antibody features intrinsic calcium and pH-dependent binding properties, capturing C2 and efficiently releasing it in the endosome for lysosomal degradation, returning into circulation free to capture more target molecules. (Walle, Van de et al., 2021)

Overall, ARGX-117 effectively captures C2 due to a strong affinity to the target, escapes lysosomal degradation due to Fc-NHance mutations, releases the antigen in the endosome because of pH-dependent faculties and travels back into circulation to continuously capture C2. Therefore, with its features, ARGX-117 is a novel sweeping/recycling complement-targeting therapeutic antibody.

## 5.2-Pre-clinical results and clinical status

Upon the administration of 80mg/kg of ARGX-117 in cynomolgus monkeys, extended to a maintenance dose of 20mg/kg at day 8, CP showed to be completely inhibited for at least 7 weeks, and the free C2 levels were demonstrated to be undetectable for that period. (Walle, Van de et al., 2021)

These results show great therapeutic potential and, in humans, results could be expected to be even more favorable dose-wise, since experiments with serum of both species show that a higher concentration (2-fold) of ARGX-117 is necessary to achieve CP inhibition in cynomolgus monkeys compared to humans.(Walle, Van de et al., 2021)

Also worth mentioning are the clinical trials phase 2 of ARGX-117 as of 2023, for the treatment of multifocal motor neuropathy (MMN) and preclinical studies in delayed graft function after kidney transplant (DGF) and dermatomyositis (DM).

With its properties, ARGX-117 can theoretically have a beneficial therapeutic effect for every patient where CP and/or LP of CS play a significant role in disease biology.

# Project goals

ARGX-117, an anti-C2 human IgG1 NHance-LALA antibody with calcium dependent target binding and pH-dependent target release, does not show cross-reactivity with mouse C2. Mouse is a preferred species for preclinical pharmacology and safety studies for various reasons. Firstly, because it is an ethically preferred model over species such as cynomolgus monkey or pig, secondly because of the lower volume of treatment necessary to administer (and therefore, to produce) for pre-clinical studies. Lastly, because most disease models are represented in mice.

Although ARGX-117 is already in clinical trials, developing a mouse derivative might enable research for new indications due to the above-mentioned reasons

For that, the ARGX-117 team has developed a mouse C2 blocking antibody (12E08). However, unlike ARGX-117, this molecule does not show pH- or calcium-dependence.

The purpose of this project is to develop and further optimize, through antibody engineering, a derivative of the mouse C2 blocking antibody, that performs target-release in a pH-dependent manner to better mimic ARGX-117 mode of action.

To reach that goal, two lines of work were traced.

The first approach relies on the predictive model (via AlphaFold) of 12E08 crystal structure. Based on the model, CDR regions of the antibody will be studied at an amino acid level. This is done in order to select sites that can potentially generate a repulsive interaction with antigen at an acidic condition, when mutating amino acids within these regions to histidine. In the selected sites, single histidine mutations will be inserted, replacing the original amino acids. The engineered antibodies will then be characterized on affinity and function assays to study pH-dependency, binding and blocking functionality.

The second approach is inspired by an article (Schröter *et al.*, 2015). Based on the study, combinatorial histidine mutation libraries will be generated for the heavy and light chains of the 12E08 clone, with a probability of 10% histidine prevalence in all designated positions. The libraries will then proceed to phage display selections. Obtained clones will be sequenced to study histidine enrichment and fabs produced for characterization of pH-dependency on ELISA. The data will be pulled together in search of potential correlations of position patterns in histidine introduction and an pH-dependent behavior.

# Materials

## Equipment

BioTek automated platewasher 96-well (405TS)
Tecan EVO Spectrometer
Thermocycler
NanoDrop 2000
BioRad Micropulser
Thermoblock
Chemidoc MP imaging system
GeneSnap from Syngene
Epson perfection V370 Photo: imager for agar plates

## Material

Product	Supplier	Cat N°
96-well Half Area Clear Flat Bottom Polystyrene High Bind Microplate	Corning	3690
96-well clear V-bottom Not treated polypropylene storage microplate (V-bottom)	Falcon	353263
96 wells plate Flat Bottom	Costar	3596
96/2000 µL Protein LoBind - deep well plate	Eppendorf	0030504305
Standard MSD plates (Multi Array 96 well plate)	Meso Scale Discovery	L15XA-3
Pierce centrifuge columns	Thermo Scientific	N.WA313396
LB medium	Made in house	N.A.
2TY medium	Made in house	N.A.
5 ml gravity flow column	Thermo Scientific	89896
Ultra-4 Centrifugal Filter Unit with Ultracel-10	Amicon	UFC503096
20% Mini-PROTEAN TGX Stain-Free gels	Biorad	4568093
Gene Pulser cuvette 0.1 cm	Biorad	1652089

## Buffers and reagents

Product	Supplier	Cat N°	Remarks
1x PBS	PanReac AppliChem	A0964	Made in house
1x PBS-T (PBS + 0.05% (v/v) Tween20)	Made in house	N.A.	Washing buffer
PBS/1%casein	Bio-Rad	1610783	Blocking buffer
TMB	CHEM LAB	CL07	Substrate
0.5 M H2SO4	CHEM LAB	CL05-2615-1000	Stop Solution
Carbonate buffer	Thermo Scientific	28382	made in house, sodium carbonate and sodium bicarbonate, 0.1M, PH=9.6 (BupH Carbonate-Bicarbonate buffer packs)
Lonza BioWhittaker Veronal buffer 5x (VB)	Fisher Scientific	12-624E	N.A.
Sodium chloride (NaCl)	Chem-Lab NV	CL00.1429.1000	Used to make 1M NaCl in 1x VB
MgEGTA (0.1M)	Complement Technology	B106	N.A.
EDTA	ITW Reagents	A4892,0100	Used to make EDTA (0.1M) pH = 8

Tris Buffered Saline (TBS) 10X	Fisher bioreagents	BP2471-1	Used to make TBS 1X
Tween 20	Chem-lab	CL00.2097.0500-500ml	N.A.
Bovine Serum Albumin (BSA) for cell culture 7,5%	SIGMA	SLCH7496	Used to make 1% BSA in 1X TBS pH 7.4
Citric Acid C6H8O7	Sigma	C7129-500g	Used to make citrate buffer pH 5.5 in 0,05% tw20 and CPB
Sodium Citrate C6H5O7Na3	Sigma	S4641-1kg	Used to make citrate buffer pH 5.5 in 0,05% tw20
1x TBS pH 7.4 (0,05%Tween 20)	Made in house	N.A.	Buffer 1
1% BSA in 1X TBS pH 7.4	Made in house	N.A.	Buffer 2
0.1 % BSA in 1xTBS pH7.4	Made in house	N.A.	Buffer 3
citrate buffer pH 5.5 in 0,05% tw20	Made in house	N.A.	Buffer 13
MSD read buffer T (4X) with surfactant	Meso Scale Discovery	R92TC-2	diluted 1/2 in MQ water before use)
10 x Tango Buffer (with BSA)	Thermo Scientific	BY5-01321328	N.A.
DTT 10 mM	Thermo Scientific	P/NY00147	N.A.
UltraPure Agarose	Invitrogen	16500-500	Used to make 1% and 1,2% agarose
TAE buffer 50x for molecular biology	ITW Reagents	A4686,1000	Used to make 1X TAE Buffer
Midori Green Advance	Filter Service	371MG18062	N.A.
Gel loading dye, orange (6X)	Life Technologies Europe	01327327	N.A.
Gene ruler DNA ladder mix	Life Technologies Europe	01192976	N.A.
T4 DNA ligase buffer 10 X	Thermo Scientific	B69-00881869	N.A.
Ampicillin (100 mg/mL)	Sigma-Aldrich	A9518	N.A.
Glucose 60%	Made in house	N.A.	N.A.
Glucose 20%	Sigma-Aldrich	G8270	
Recovery cell culture freezing medium	Fisher Scientific BVBA	2322925	N.A.
Protein loading dye (laemmli sample buffer) with DTT (4x)	Bio-Rad	1610747	Aliquoted in house
Protein loading dye (laemmli sample buffer) without DTT (4x)	Bio-Rad	1610747	Aliquoted in house
Tris/glycine/Sds Buffer 10X	Bio-Rad	1610772	Used to make 1xTGS
Precision Plus Protein Unstained Standards	Bio-Rad	1610396	N.A.
Taq Buffer (10x, NHSO4-)	Merck life Science	SLCL3987	N.A.
50 mM MgCl2	Thermo Scientific	00889513	N.A.
dNTP Mix (2mM)	Thermo Scientific	R0241-00169665	N.A.
dNTP Mix (10 mM)	Life Technologies Europe	2414668	N.A.
Polyethylenimine Max (PEI Max)	Polyscience	24765	ready to use at 1mg/mL
FreeStyle™ 293 Expression Medium	Life Technologies Europe BV	12338-026	N.A.
Opti-MEM™ Medium	Life Technologies Europe BV	11058021	N.A.
HyPep™ 4601N	Kerry	PHBT23	1L freestyle medium + 100 gram HyPep™ 4601N .

LB+AMP	Made in house	N.A.	LB medium with ampicillin 1/1000 diluted
LB+AMP+GLU	Made in house	N.A.	LB medium with ampicillin 1/1000 diluted and 2% glucose
2TY+AMP+GLU	Made in house	N.A.	2TY medium with ampicillin 1/1000 diluted and 2% glucose
2TY+AMP+KAN	Made in house	N.A.	2TY medium with ampicillin 1/1000 and kanamycin 1/1000 diluted
HF buffer (5 X)	Life Technologies Europe	F-530L	N.A.
Readyload	Invitrogen	1504998	N.A.
CPA (Citrate_phosphate_acetate) pH 5,5	N.A.	N.A.	10 mM sodium citrate, 10 mM sodium phosphate, 10 mM sodium acetate and 115 mM NaCl
Kanamycin (25 mg/mL)	Sigma-Aldrich	K4000	N.A.
Helperphage VCSM13, 1x10 <sup>13</sup> /mL	N.A.	N.A.	N.A.
Trypsin (10 mg/mL in 1xPBS)	Merck Life sciences	T1426	N.A.
Dried skimmed milk	Marvel	92964	Used to make 2% Marvel in 1xPBS and 0,2% Marvel in 1xPBS
AEBSF (4mg/mL)	Sigma-Aldrich	A8456-25MG	N.A.
20% PEG (PEG6000), 2.5M NaCl	N.A.	N.A.	N.A.
PEG6000	CalBiochem	528877	N.A.
IPTG	Life Technologies Europe B.V.	01004800	N.A.
Disodium phosphate Na <sub>2</sub> HPO <sub>4</sub>	Chem-lab	CL00.1463.1000	Used to make CPB pH 5,5
CPB pH 5,5	Made in house	N.A.	Disodium phosphate + citric acid
CPB pH 5,5 + Tween 0,05%	Made in house	N.A.	N.A.

## Commercial kits

Product	Supplier	Cat N°
NucleoSpin Gel and PCR clean-up Kit	Machery-Nagel	740609
Plasmid DNA purification (NucleoBond Xtra Midi/Maxi)	Machery-Nagel	740410.100

## Cells

Product	Supplier	Cat N°
HEK-293E cells (human embryonic kidney cells- Uprotein express)	Made in house	N.A.
TOP10 E. Coli competent cells	Lucigen	Further developed in-house
TG1 Electrocompetent Cells	Immunosource B.V.	31224

## Proteins/antibodies

Product	Supplier	Cat N°
DAMPO (Peroxidase AffiniPure Donkey Anti-Mouse IgG (H+L))	Jackson ImmunoResearch Europe	715-035-150
Recombinant mouse C2 (C2-(his)N mouse)	U-Protein Express BV	Batch 3070
Mouse IgG: Purified mouse IgG	Sanbio B.V.	PMP01- 157729
Anti-C3 antibody: Anti mouse complement component C3, biotin (Clone RmC11H9, rat IgG2a)	Sanbio B.V.	CL7503B
Strep-HRP: Peroxidase-conjugated Streptavidin	Jackson ImmunoResearch	016-030-084
MSD SULFO-TAG anti-mouse antibody (goat)	Made in house	W00211235S
Mouse Sushi2 (mFb-mC2Sushi2_(his)N)	U-Protein Express BV	Batch 4349
Human C2 (C2-(his)N human)	Abcam B.V.	Batch 4409
Human C1 Complex (PURE)	Complement Technology	A098
HRP - Rabbit Anti-c-myc	Sanbio B.V.	20
Anti-Myc tag antibody [9E10] (Alexa Fluor® 647)	Abcam B.V.	GR3324576-1

## Enzymes

Enzyme	Supplier	Cat N°	Cutting site
BsmBI (10 U/μL)	Thermo Scientific	ER045	5' C G T C T C N1 ↓ 3' 3' G C A G A G N5 ↑ 5'
ApaLI (10 U/μL)	Thermo Scientific	ER0041	5' G ↓ T G C A C 3' 3' C A C G T ↑ G 5'
AvrII (10 U/μL)	Thermo Scientific	ER1561	5' C ↓ C T A G G 3' 3' G G A T C ↑ C 5'
NcoI (10 U/μL)	Thermo Scientific	ER0572	5' C ↓ C A T G G 3' 3' G G T A C ↑ C 5'
NheI (10 U/μL)	Thermo Scientific	ER0972	5' G ↓ C T A G C 3' 3' C G A T C ↑ G 5'
T4 DNA Ligase (5 U/μL)	Thermo Scientific	EL0011	(Not a restriction enzyme)
Jumpstart Taq DNA Polymerase	Merck life Science	SLCL3987	(Not a restriction enzyme)
Phusion High-Fidelity DNA polymerase	Life Technologies Europe	F-530L	(Not a restriction enzyme)

## Serum

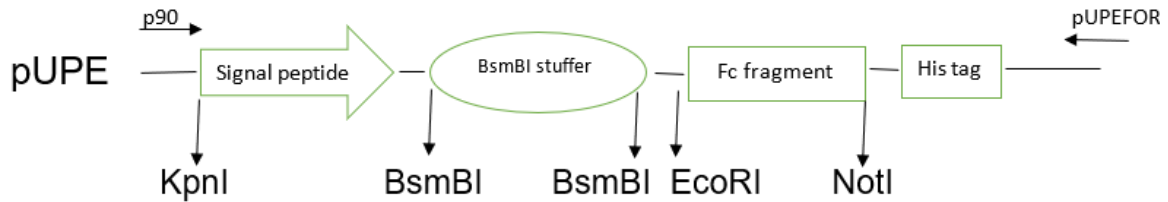
- Complement preserved serum: Mouse complement serum BALB/c (Cat N° IGMSBCSER10ML, lot39518)

## Primers

Name	Sequence
P90	CTTTCTCTCCACAGGTGTCCACTCCCAGTTC
PupeForward	TGTAATCCAGAGGTTGATTGCG
M13R	GAGCGGATAACAATTTACACAGG
pelB3	GCGCCAATTCTATTTCAAGG
MPE25	TTTCTGTATGAGGTTTGTGCTA

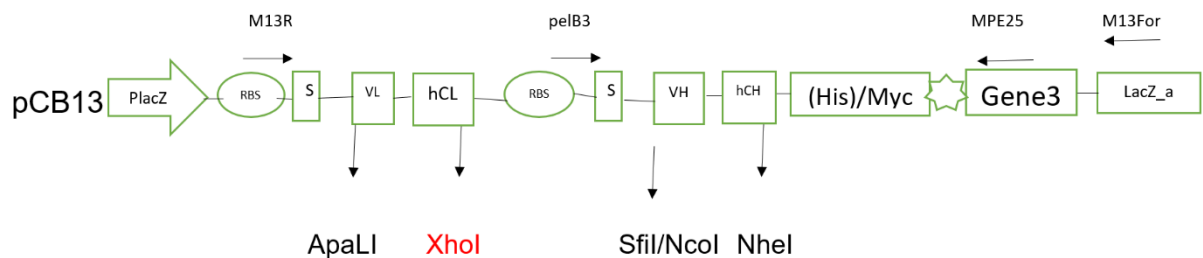
## Vectors

1. pUPEX mammalian expression vectors (pUPEX 35 and pUPEX 201 (mIgG2b-DANA))



Vector pUPEX 201 has a mIgG2b backbone, common between the two mouse strains of interest (BALB/c and C57BL/6), and contains the mouse IgG2b heavy chain constant domain. To the vector, DANA (D265A, N297A) mutations were added to avoid effector functions of the Fc-tail (FcD) of the antibody (e.g. ADCC, CDC). Vector pUPEX35 contains the mouse lambda light chain constant domain. Both vectors have BsmBI cutting sites for the insertion of variable regions, as well as ampicillin resistance gene.

2. pCB13 phagemid vector



Vector pCB13, an in-house developed vector, is a phagemid vector containing a gene 3 that in this case is linked to a fab. The linked gen3-fab is used for expression of the fab on the phage, allowing phage display. In this vector, the constant domains of the fab are human, both for light and heavy chains. Additionally, the vector contains ampicillin resistance gene.

A LAC operon is also present, allowing the regulation of expression of the vector. With the LAC operon cells can only express the vector in the presence of lactose. As glucose competes with lactose, lactose is not produced when glucose is added, resulting in non-expression of the vector. This allows a simple turn-off of the vector expression by adding glucose and a switch on of the vector by leaving glucose out of the medium and adding IPTG (molecular mimic of allolactose).

# Methods

## A-12E08 mutants based on predictive crystal structure

### 1-Plasmid generation

#### 1.1-DNA cloning

DNA strings (1.1-Construct design) were delivered in a lyophilized formulation and were reconstituted in MilliQ to a concentration of 20 ng/ $\mu$ L. Thereafter, strings were digested for 2h at 37°C. Next to this, the plasmid vectors that were to receive the string material were also digested for 2h at 37°C, see Table 1.

Table 1- Digestion of DNA strings and vectors

Digestion of DNA strings		
DNA	20	ng/ $\mu$ L
Tango Buffer (10x)	2	$\mu$ L
DTT (10mM)	2	$\mu$ L
BsmBI (10 U/ $\mu$ l)	0,5	$\mu$ L
MQ	X	$\mu$ L
Total volume	20	$\mu$ L

Digestion of vectors		
Vector	5,0	$\mu$ g
BsmBI (10 U/ $\mu$ l)	2	$\mu$ L
Tango buffer (10x)	20	$\mu$ L
DTT (10mM)	20	$\mu$ L
MQ	X	$\mu$ L
Total volume	200	$\mu$ L

After digestion, vectors were separated from the excised material through agarose gel electrophoresis in 1% agarose + 5  $\mu$ L Midori/ 100 mL 1% agarose.

All digested material was purified using the NucleoSpin Gel and PCR clean-up Kit according to protocol and yield was measured via nanodrop (260 nm).

The material was then ready for ligation, that proceeded as shown in Table 2.

Table 2-Ligation and negative control

Vector	10 ng	Vector	10 ng
Insert	50 ng	Insert	0 $\mu$ L
T4 Buffer (10x)	1 $\mu$ L	T4 Buffer (10x)	1 $\mu$ L
T4 DNA Ligase	1 $\mu$ L	T4 DNA Ligase	1 $\mu$ L
MQ	0 $\mu$ L	MQ	X $\mu$ L
Total volume	10 $\mu$ L	Total volume	10 $\mu$ L

Vector pUPEX201(mIgG2b backbone) received the VH strings and pUPEX35 (mClambda) received the VL strings.

After incubation, the ligation product was transformed into TOP10 *E. coli* cells through heat shock. 50 µL of cells were added to the ligation product of each construct and incubated in the following manner:

- 5 mins on ice
- 90 secs at 42°C
- 2 mins on ice

Cells were plated on LB agar dishes with ampicillin and grown at 37°C until next morning.

After overnight (ON) incubation, 100 µL/well LB+ ampicillin (LB+AMP) was added to a 96-well flat bottom plate and multiple colonies per plasmid were picked from agar plate (one colony/well) in a sterile manner. Bacteria were grown 3-4 hours shaking at 37°C and 5 µL of the bacterial suspension was inoculated in a 96-well LGC agar+AMP plate to send for MTP (microtiter plates) Sanger sequencing with P90 primer, at LGC Genomics (Germany).

The sequences (see 1-Plasmid generation) were then aligned with the respective 12E08 WT chain through Clone Manager 9 Software and the plasmids that showed the right insert sequence were further grown. From each mutant, 20 µL of bacterial culture/clone was grown in 100 mL LB+AMP at 37°C shaking ON. On the following day midiprep was performed via Plasmid DNA purification protocol and DNA was quantified via nanodrop (260 nm), see appendix.

Obtained purified DNA material was sent for sequencing in Eppendorf's with 100 ng/µL of DNA (in a final volume of 10 µL ) and 4 µL of primer P90 and pUPEForward to confirm the sequence of the entire plasmid. Plasmids were stored at -20°C.

## 2-Antibody production

### 2.1-Cell transfection

On the day of transfection, HEK-293 cells were at 0.5 - 0.8 x10<sup>6</sup> cells per mL in plain Freestyle medium. For every 50 mL cells was added:

- 25 µg DNA
- 2 mL Opti-MEM™ (40 µL Opti-MEM™ medium/mL of cell culture)

- 75  $\mu\text{L}$  =  $\mu\text{g}$  PEI Max (PEI Max is at 1 mg/mL; 1,5  $\mu\text{g}$  of PEI/mL of cell culture)- positively charged polymer that binds to DNA and promotes DNA entrance in the cells

The mixture was incubated for 10 minutes at room temperature and transferred to the HEK cell culture. 4 hours later, 1/20 V/V of HyPep™ 4601N , a source of L-glutamine essential for protein biosynthesis, was added to the cells as supplement. The culture was incubated for 6 days at 37°C with 5% CO<sub>2</sub> at 110 rpm.

## 2.2-Protein purification

Six days post transfection, produced antibodies were purified from HEK cell culture through protein purification protocol:

Medium was harvested and centrifuged for 10 minutes at 1000 g. Supernatant of the transfected cell culture was harvested (as antibodies are secreted to extracellular space) and pellet was discarded. To every 50 mL of supernatant, 500  $\mu\text{L}$  of prewashed protein A beads were added. Protein A beads are stored at 50% in ethanol, therefore, they must be washed 3 x with PBS to not damage the binding ability.

The suspension was left to rotate for 2 hours at 4 °C (25 rpm/min) to allow binding of antibodies to the beads and spun down at 1800 rpm, for 2 min, at 4 °C with an acceleration(a)=9, deacceleration(d) =7 and the supernatant was discarded.

Beads were washed with 5 mL 1 x PBS and transferred to 5 mL gravity flow column. The following steps as described in Table 3.

*Table 3-Protein purification workflow*

2nd wash	5 mL	PBS containing 500mM NaCl
3rd wash	5 mL	1 x PBS
4th wash	5 mL	5 mL 0.5X PBS containing 150mM NaCl
Elution	2mL	20 mM citrate, 150 mM NaCl pH=3
Neutralization	200 $\mu\text{L}$	1M KH <sub>2</sub> PO <sub>4</sub> /K <sub>2</sub> HPO <sub>4</sub> pH=8

Purified antibodies went through dialysis with Amicon Ultra-4 Centrifugal Filter Unit with Ultracel-10 membrane for buffer exchange into PBS (Millipore, Merck).

Concentration was measured on nanodrop (280 nm) and an extinction factor (/1.51) was applied to obtain the real concentration of the antibodies.

### *2.3- SDS-Page QC*

To confirm the integrity of the produced antibodies, SDS-Page was performed as quality control.

Protein samples were diluted in MilliQ to obtain 0.1 µg/µL (make > 30 µL). To 15 µL of each sample 5 µL loading dye (Laemmli) with DTT (reduced condition) was added and to the other 15 µL of each sample 5 µL loading dye (Laemmli) without DTT (non-reduced condition) was added.

- Samples were vortexed, spun down and denatured at 95 °C in the thermoblock for 10 minutes. Denatured samples were again spun down and loaded to a Mini-PROTEAN TGX Stain-Free gels in an electrophoresis chamber with 1X TGS buffer. Protein standard (ladder: Precision Plus Unstained Protein Standard) was also loaded and the samples were left to run 10 min at 90 V to allow proper stacking and 25 min at 250 V.
- After the run, the gel was placed in Chemidoc MP imaging system to subject the gel to UV-light. As the used stain-free gels emit fluorescence upon exposure to UV light and have a trihalo compound that binds to tryptophan residues (present in proteins), an image was obtained containing black bands where proteins are present.

## B-Development of antibodies from combinatorial histidine library

### 1-DNA cloning

#### 1.1-Vector preparation

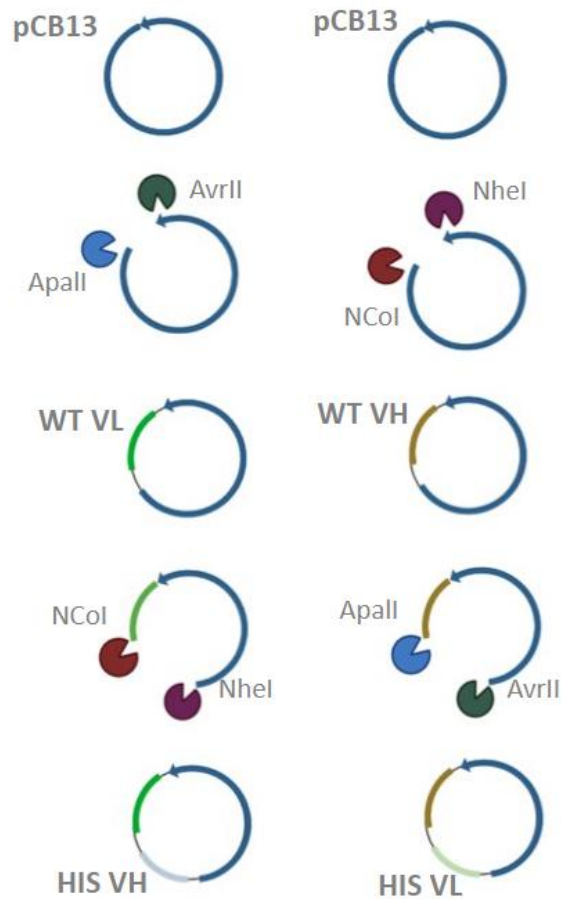


Figure 5- Schematic representation of the workflow for the preparation of pCB13 vectors to receive HIS libraries.

To obtain the initial plasmid, from glycerol stock, 20  $\mu$ L of cells transformed with pCB13 were grown at 37°C shaking ON in LB+AMP+GLU.

On the following day, midiprep was performed via Plasmid DNA purification (NucleoBond Xtra Midi/Maxi) kit accordingly to the corresponding protocol and DNA was quantified via nanodrop (260 nm). Midiprepped material was sent for sequencing with 10  $\mu$ L DNA and 4  $\mu$ L of primer (5 $\mu$ M) M13R and pelB3 at LGC Genomics.

### *First digestion of the vector*

Plasmid were digested for 3h at 37°C, pCB13 vector was planned to receive: Plasmid 1: 12E08 WT VL + HIS library VH; Plasmid 2: 12E08 WT VH + HIS library VL, as depicted in Table 4.

*Table 4- First digestion of pCB13 vectors*

<b>Plasmid 1</b>	<b>Double-digestion</b>		<b>Plasmid 2</b>	<b>Double-digestion</b>	
Vector	15	µg	Vector	15	µg
AvrII	5	µL	NcoI	5	µL
ApalI	5	µL	NheI	5	µL
Tango buffer (10x)	30	µL	Tango buffer (10x)	30	µL
MQ	X	µL	MQ	X	µL
Total volume	300	µL	Total volume	300	µL

The vectors were separated from the excised material through agarose gel electrophoresis (in 1% agarose + 5µl Midori/ 100 mL agarose) and DNA was purified via the PCR clean-up and gel extraction kit (Macherey-Nagel). Yield was measured via nanodrop (260 nm).

### *Digestion of 12E08 WT strings*

The wild-type variable domains of the light and heavy chains of 12E08 were ordered from Twist with flanking regions: light chain with AvrII and ApaLI cutting sites and heavy chain with NcoI and NheI cutting sites.

Strings were delivered in a lyophilized formulation and were reconstituted in MilliQ to a concentration of 20 ng/µL. Strings were digested for 2h at 37°C, see Table 5.

*Table 5- Digestion of 12E08 VL and VH WT strings*

<b>WT VL inserts</b>			<b>WT VH inserts</b>		
DNA	20	ng/µL	DNA	20	ng/µL
Tango buffer (10x)	2	µL	Tango buffer (10x)	2	µL
AvrII	0,5	µL	NcoI	0,5	µL
ApalI	0,5	µL	NheI	0,5	µL
MQ	X	µL	MQ	X	µL
Total volume	20	µL	Total volume	20	µL

DNA was purified via the PCR clean-up and gel extraction kit (Macherey-Nagel). Yield was measured via nanodrop (260 nm).

#### *Ligation with 12E08 WT strings*

The material was then ready for ligation (Plasmid 1 + WT VL insert; Plasmid 2+ WT VH insert), performed as shown in Table 6.

*Table 6 -Ligation of digested pCB13 vectors and digested 12E08 WT strings*

Vector	10	ng
Insert	50	ng
Tango buffer (10x)	1,5	μL
Ligase	1	μL
MQ	X	μL
Total	15	μL

1h at RT

TG1 competent cells were transformed with generated plasmid by electroporation.

For that, 50μl of TG1 cells was added to the clean ligation product (eluted in MQ at 72°C). The mixture was transferred to cuvettes and cells were rapidly pulsed to create pores in cell membrane and allow the plasmid to enter the TG1. Recovery medium was immediately added and transformed cells were grown for 30 minutes at 37°C, shaking. Cells were plated on agar plates and grown ON at 37°C.

Cells were plated on LB agar dishes with ampicillin and grown at 37°C until next morning.

After ON incubation, 100 μL LB+AMP+GLU was added to a 96-well flat bottom plate and multiple colonies per plasmid were picked from agar plate (1 colony/well) in a sterile manner. Bacteria was grown 3-4 hours shaking at 37°C and 5 μL of the bacterial suspension was inoculated in a 96-well LGC agar+AMP plate to send for MTP (microtiter plates) Sanger sequencing with P90 primer, at LGC Genomics (Germany).

The sequences were then aligned with the respective WT chain through Clone Manager 9 Software and the plasmids that showed the right insert sequence to further grown. From each correct mutant 20 μL of bacterial culture/clone was grown in 100 mL LB+ AMP at

37°C shaking ON. On the following day, midiprep was performed via Plasmid DNA purification protocol and DNA was quantified via nanodrop (260 nm).

Obtained purified DNA material was sent for sequencing in Eppendorf's with 100 ng/μL of DNA (in a final volume of 10 μL ) and 4 μL of primer pelB3 in case of VH strings or primer M13R in case of VL strings.

### *Second digestion of vectors*

Produced pCB13 vectors with one WT chain were digested for 3h at 37°C, as depicted in Table 7.

*Table 7- Second digestion of vectors (with previously inserted WT chains)*

<b>Plasmid 1 with VL WT</b>			<b>Plasmid 2 with VH WT</b>		
Vector	25	μg	Vector	25	μg
NcoI	5	μL	AvrII	5	μL
NheI	5	μL	ApalI	5	μL
Tango buffer (10x)	30	μL	Tango buffer (10x)	30	μL
MQ	X	μL	MQ	X	μL
Total volume	300	μL	Total volume	300	μL

Digested vectors were separated from excision through agarose gel electrophoresis (in 1,2% agarose + 5μl Midori/ 100 mL agarose) and DNA was cleaned via PCR clean-up and gel extraction kit.

### *2-Library cloning*

12E08 VH and 12E08 VL synthetic His libraries were delivered in general plasmids.

Based on calculations to determine how much DNA was necessary to cover 10x the library size, PCR was performed with 2 μL of DNA of each library, as described in Table 8.

Table 8 - PCR amplification of 12E08 VH and 12E08 VL synthetic histidine libraries

DNA	2	μL
P90	15	μL
PupeF	15	μL
dNTPs 10mM	10	μL
5xHF buffer	60	μL
Phusion enzyme	15	μL
MQ	183	μL
Total	300	μL

A small volume (10 μL) of the PCR product was run through agarose gel electrophoresis (in 1% agarose + 5μl Midori/ 100 mL agarose) for QC of amplification. Remaining DNA was purified via the PCR clean-up and gel extraction kit (Macherey-Nagel). Yield was measured via nanodrop (260 nm).

### Library digestion and ligation

Libraries were digested from general plasmid for 1h30 at 37°C, see Table 9.

Table 9- Libraries digestion from general plasmids

VL library			VH library		
DNA	3	μg	DNA	3	μg
Tango buffer (10x)	30	μL	Tango buffer (10x)	30	μL
AvrII	6	μL	NcoI	6	μL
ApalI	6	μL	NheI	6	μL
MQ	X	μL	MQ	X	μL
Total	300	μL	Total	300	μL

Digested libraries were separated from non-digested material through agarose gel electrophoresis (in 1,2% agarose + 5μl Midori/ 100 mL agarose) and DNA was cleaned via PCR clean-up and gel extraction kit.

A test ligation was performed, as shown in Table 10, for 2h at room temperature (RT) with small volumes of vector and inserts to verify the efficacy of the ligation with the prepared material. Negative controls for each vector (without insert) were taken along.

Table 10- Test-ligation of digested histidine libraries and prepared vectors

Vector pCB13 with WT chain	50	ng
Insert (library)	25	ng
Ligation buffer 10x	2	μL
T4 DNA ligase	0,5	μL
MQ	X	μL
Total	20	μL

Electrocompetent TG1 cells were transformed with generated plasmid through electroporation as (described in Ligation with 12E08 WT strings)

Colony PCR was performed, as described in Table 11 and Table 12, to assess insert rate: 1 μl of 1/10 diluted grown culture (in MQ) was used.

Table 11- Colony PCR protocol

DNA/Bact	1	μL
M13R (5 μM)	0,75	μL
MP25 (5 μM)	0,75	μL
Taq Buffer (10x, N <sub>H</sub> SO <sub>4</sub> <sup>-</sup> )	1,5	μL
MgCl <sub>2</sub>	1,5	μL
dNTP (2mM)	1,5	μL
Readyload	1,5	μL
Taq enzyme	0,1	μL
H <sub>2</sub> O	6,4	μL
Total	15	μL

Table 12- Colony PCR program

Lid temperature 98°C

Preheating on	
1: 98°C	2 min
2: 98°C	30s
3: 55 °C	30s
4: 72 °C	2min back to step 2 for 32x
5: 72 °C	5min
6: 4 °C	pause

Material was run through agarose gel electrophoresis in 1% agarose + 5 μL Midori/ 100 mL agarose.

After confirmation from test ligation, the real ligation took place as shown in Table 13.

Table 13- Real-ligation of histidine libraries and prepared vectors (with WT chains)

Vector pCB13 with WT chain	1	µg
Insert (library)	0,5	µg
Ligation buffer 10x	20	µL
T4 DNA ligase	5	µL
MQ	X	µL
Total	200	µL

Electrocompetent TG1 cells were transformed with generated plasmid through electroporation (as described in Library digestion and ligation). To 50 µL of TG1 cells, 30 µL of the cleaned ligation product were added and 50 µL more of TG1 cells were added. For each library, the mix was divided over 3 precooled cuvettes and electroporated. Cells were recovered in 1 mL of recovery medium per cuvette + 1 mL used to rinse the 3 cuvettes and transferred to 15 mL tubes (4 mL in total per library). Tubes were put at 37°C shaking for 30 mins.

After incubation, for each library a 10<sup>-3</sup> dilution was made (5 µL from the transformation product added to 5 mL of 2TY+AMP+GLU medium). From 10<sup>-3</sup> dilution, a serial dilution 1/10 was performed on a 96 wells V-bottom plate with LB+AMP+GLU, as depicted in Figure 6.

5 µL of each dilution were spotted on petri dishes and incubated ON at 37° C to assess library size.

Additionally, 20 µL ad 100 µL of the 10<sup>-3</sup> dilution were plated on petri dishes and incubated ON at 37° C. Colony PCR was performed and colonies were sent for MTP Sanger sequencing to assess insert rate.

The remaining recovered cultures (before dilution) was inoculated in 300 mL of 2TY+AMP+GLU medium and incubate at 37°C (110 rpm) for 9h for library expansion.

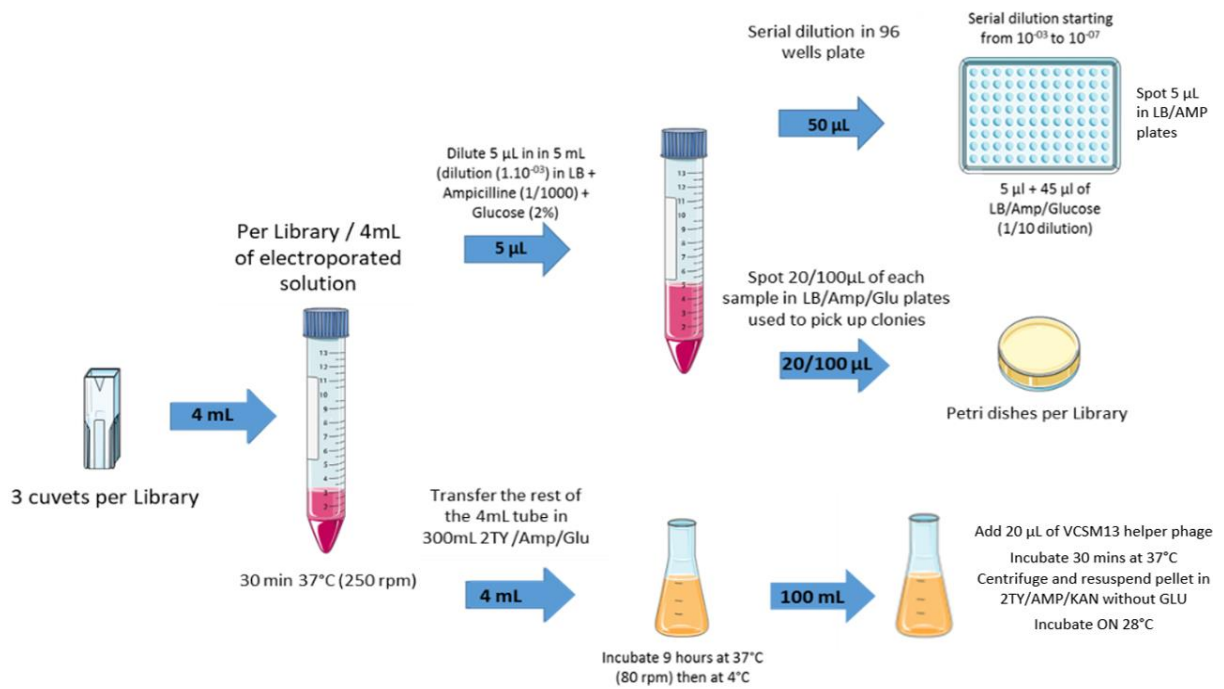


Figure 6- Workflow overview after cell transformation: Spotting of serial dilution of libraries, plating libraries on petri dishes; inoculation for library expansion.

After incubation, the libraries were saturated and glycerol stocks were prepared. 100 mL of the expanded library were centrifuged for 15 minutes at 4700 rpm at 4°C and supernatant was discarded. Pellet was resuspended in a final volume of 8 mL of TY/Amp/Glu + 4 mL of 60% glycerol.

### 3-Phage display

#### Day 1

##### 1-Phage production

- From the saturated library, enough volume covering at least 10 times of the library size was added to 150 mL 2TY+AMP+GLU, aiming to a start OD<sub>600nm</sub> of 0.05. The culture was grown at 37°C until OD<sub>600nm</sub> 0.5
- To 100 mL of culture ( $4^{10}$  cells) 40 μL of helper phage ( $1^{13}$ /mL) were added (phage/bacteria ratio should be 10:1 for more than 95% infection) and incubated 30 minutes shaking (110 rpm) at 37°C (phage infection).
- Culture was centrifuged 10 minutes at max speed at RT and the supernatant was removed. Pellet was resuspended in 10 mL 2TY+AMP+KAN and transferred to a

1L baffled flask containing 190 mL 2TY+AMP+KAN The culture was incubated ON at 28°C, 110 rpm (phage production).

- Note that, for subsequent rounds the protocol was performed in the following manner:
- Rescue culture was added to 15 mL 2TY+AMP+GLU, aiming to a start OD<sub>600nm</sub> of 0.05. The culture was grown at 37°C until OD<sub>600nm</sub> 0.5.
- To 10 mL of culture, 4 µL helper phage ( $1^{13}$ /mL) were added and incubated 30 minutes shaking (110 rpm) at 37°C.
- Culture was centrifuged 10 minutes at max speed at RT and the supernatant was removed. Pellet was resuspended in 10 mL 2TY+AMP+KAN and transferred to a 250 mL baffled flask containing 40 mL 2TY+AMP+KAN and incubated ON t at 28°C, 110 rpm.

## 2-Selection preparation

- To prepare for selections, a 96 well selection plate (Maxisorp) was coated with 100 µL of antigen of interest (AG) diluted in 1xPBS and incubated ON at 4°C.
- One colony of a previously plated TG1 cells was inoculated in 10 mL LB medium and incubated ON at 37°C, 120 rpm.

## Day 2

### 1-Input phage

- Phage production cultures were centrifuged 45 minutes at max speed at 4°C and 40 mL of supernatant was transferred to a falcon tube with 10 mL ice cold 20%PEG/2.5M NaCl and incubated on ice for 30 minutes (phage precipitation).
- The mix was centrifuged at max speed at 4°C and supernatant was discarded.
- Pellet was resuspended 1 mL ice-cold 1xPBS and transferred to a new 2 mL Eppendorf tube
- Eppendorf tubes were centrifuged 3 minutes at max speed at 4°C, supernatant was removed and pellet was transferred to a new Eppendorf tube with 250 µL ice-cold 20% PEG/2.5M NaCl and incubated for 10 minutes on ice.
- Eppendorf tubes were centrifuged for 3 minutes at max speed at 4°C and supernatant was carefully removed. The pellet was resuspended in 1 mL 1xPBS,

centrifuged 3 minutes at max speed at 4°C and supernatant was transferred to a new Eppendorf tube.

- The samples in the v bottom plate are the input phage.

## 2-Selection and output phage

- Previously coated plate was washed 3 times with 1xPBS 0.05% tween20
- Plate was blocked with 250 µL 1xPBS+ 2% marvel for at least 2 hours (shaking at RT).
- Blocking buffer was removed and 100 µL/well of phage (1/10 diluted in 2% marvel for R0 and 1/100 diluted in 2% marvel for subsequent rounds) and incubated for 2 hours at RT, 450 rpm shaking.
- Supernatant was removed and plate was washed 5 times with 200µL 1xPBS 0.05% tween20 and the final wash was incubated 5 minutes shaking. The process was repeated 3 times (total washes = 15)
- Plate was eluted with 150 µL of the elution option, shaking at 450 rpm
- The samples were transferred to a new 96 well V-bottom plate. In case the elution option is trypsin, the corresponding wells in the new plate contained 7.5 µL AEBSF (4 mg/mL) (trypsin inhibitor).
- The samples in the v bottom plate are the output phage.

## 3-TG1 culture

ON TG1 culture was diluted 1/100 in 50 mL LB medium, aiming to a start an OD<sub>600nm</sub> of 0.05. The culture was grown at 37°C until OD<sub>600nm</sub> of 0.5. (As negative control, 10 mL of this mix were transferred into a 50 mL falcon tube and 10 µL of ampicillin were added).

## 4-Rescue cultures

75 µL of every output phage was added to 500 µL of previously cultured TG1 cells at OD 0.5 (Negative control included: no phage added) and incubated 30 minutes standing at 37°C

After incubation, 2TY+AMP+GLU was added up to 10 mL and grown ON at 37°C, 110 rpm.

#### 5- Dilution and spotting of phage

##### Input phage

1. In a 96-well V-bottom plate, 50  $\mu$ L 2TY medium was added to 12 wells per input phage sample plus one extra row for the negative control.
2. A serial dilution of 1/10 for every input phage was performed
3. 50  $\mu$ L of previously cultured TG1 cells at OD 0.5 were added to each well and the plate was incubated for 30 minutes standing at 37°C
4. 5  $\mu$ L from the last 8 dilutions were spotted on an LB+AMP+GLU agar plate and incubated ON at 37°C.

##### Output phage

1. In a 96-well V-bottom plate, 50  $\mu$ L 2TY medium was added to 6 wells per input phage sample plus one extra row for the negative control.
2. A serial dilution of 1/10 for every output phage was performed
3. 50  $\mu$ L of previously cultured TG1 cells at OD 0.5 were added to each well and the plate was incubated for 30 minutes standing at 37°C
4. 5  $\mu$ L from each dilution were spotted on an LB+AMP+GLU agar plate and incubated ON at 37°C.

Additionally, 10 and 100  $\mu$ L of relevant rescues were plated on LB+AMP+GLU agar plates. Colonies were picked to a 96 well plate with 2TY+AMP+GLU medium and sent for sequencing as described . The same plates were used to proceed to Fab production.

#### 4-Fab production

To 750  $\mu$ L 2TY/AMP/GLU medium in a 96- deep well plate, 37.5  $\mu$ L of bacteria from masterplate culture (plate where colonies of output phage were picked) and grown at 37°C until afternoon. 250  $\mu$ L of 2TY/AMP/IPTG mix medium were added and plates was incubated ON at 26°C shaking, to induce Fab production.

On the following day the described workflow followed:

- Plates were centrifuged at max speed for 15 min
- Supernatants were discarded and pellet was placed at -20°C for around 3h
- Plates were moved to -80°C for 1h
- Pellet was thawed and resuspended in 120 µL PBS/well
- Pellet was resuspended by vortex and incubated for 1h at RT shaking
- Suspension was transferred to a V-bottom plate and centrifuged at max speed for 15 min
- Supernatant (periplasmic material) was transferred to a new V-bottom plate and stored at -20°C

## C- Antibody characterization

### 1-Mouse C2 binding ELISA

A high binding half area 96 well plate was coated with recombinant mouse C2 (target) at 1 µg/mL in PBS (50 µL/well) ON at 4°C. The plate was blocked with PBS/1% casein (100 µL/well) for 1 hour at RT shaking. Samples were diluted in PBS in a low binding plate through a dilution series, 50 µL of each dilution was transferred to the assay plate (high binding) and incubated for 1 hour at RT shaking. 50 µL of DAMPO 1/50000 diluted in PBS was loaded to detect the sample antibody and incubated for 1 hour at RT shaking. Next, 50 µL of TMB was loaded to the plate and incubated for 10 minutes at RT shielded from light and 50 µL H<sub>2</sub>SO<sub>4</sub> was loaded to each well to stop the reaction.

### 2-Mouse Classical Pathway ELISA

50 µL/well of mouse IgG at 10 µg/mL was coated in a high binding half area 96 well plate and incubated ON at 4°C. On the next day, plate was blocked with 100 µL of PBS/1% casein and incubated for 1 hour at RT while shaking.

In a low binding plate, the dilution series of the antibodies were prepared in 100% mouse complement preserved serum and preincubated for 15 minutes on ice.

This was followed by the dilution of the serum to 10% in buffer (1x VB + 150 mM NaCl in 1x VB).

25  $\mu\text{L}$  of each sample was loaded to the high binding plate and incubated for 1 hour at RT while shaking. Afterwards, 25  $\mu\text{L}$  of Anti-C3 antibody diluted 1/600 in PBS-T was loaded and incubated for 1 hour at RT shaking, followed by 25  $\mu\text{L}$  of STRP-HRP diluted 1/300 000 in PBS-T incubated for 1 hour at RT shaking. Finally, 25  $\mu\text{L}$  of TMB was loaded to each well and incubated for 10 minutes at RT, shielded from light and 25  $\mu\text{L}$  of  $\text{H}_2\text{SO}_4$  to each well were added to stop the enzymatic reaction.

### 3-MesoScale Discovery

A MSD plate was coated with 25  $\mu\text{L}$  recombinant mouse C2 at 1  $\mu\text{g}/\text{mL}$  (30  $\mu\text{L}$  per well in 1X PBS) and incubated ON at 4°C.

After the incubation period, the plate was washed 3 times with 1x TBS pH 7.4 (0,05%Tween 20) (150  $\mu\text{L}$  per well) and blocked with 1% BSA in 1X TBS pH 7.4 (150  $\mu\text{L}$  per well). The plate was incubated with blocking buffer for 1 hour at RT shaking.

Meanwhile, the antibodies to be tested were diluted in a serial dilution 1/5 in 0.1 % BSA in 1xTBS pH 7.4 in a low binding plate, in a duplicate way (2 times dilution series for each antibody).

After incubation time, the plate was washed 3 times with 1x TBS pH 7.4 (0,05%Tween 20) and 25  $\mu\text{L}$  of the diluted antibodies were transferred to the assay plate (high-binding). The plate was left to incubate 1 hour at RT shaking.

After 1 hour, one of the (duplicate) dilution series of each antibody was washed 3 times with 1x TBS pH 7.4 (0,05%Tween 20) and the duplicates were washed 3 times with citrate pH 5.5 in 0,05%Tween20. A fourth wash was performed with the same buffer previously used (150  $\mu\text{L}$  per well) and incubated for 5 minutes shaking at RT. All wells were then washed with 1X TBS pH 7.4 (0,05%Tween 20) (150  $\mu\text{L}$  per well) and 25  $\mu\text{L}$  per well of Goat anti-Ms Fc-Sulfo conjugated in PBS/0.1% BSA (pH 7.4) (1/1000 dilution) was added and incubated for 1 hour at RT shaking.

Finally, the plate was washed 5 times with 1X TBS pH 7.4 (0,05%Tween 20) (150  $\mu\text{L}$  per well) and 150  $\mu\text{L}$  of Reading buffer/well (With surfactant, dilution 1/2 in MQ water) was added. The plate was immediately placed on MSD plate reader.

#### 4-Peri ELISA

Working in duplicate, high binding half area 96 well plates were coated with recombinant mouse C2 (target) at 1 µg/mL in PBS (50 µL/well) ON at 4°C. The plates were blocked with PBS/1% casein (100 µL/well) for 2 hours at RT shaking. In a low binding dilution plate, peris were diluted 1/10 in PBS/0,1% casein and 50 µL of each dilution was transferred to each assay plate (high binding) and incubated for 1 hour at RT shaking.

After 1 hour, one plate was 4 times washed with 1x PBS 0,05% Tween pH 7.4 and the other (duplicate) was washed 4 times with CPB 0.05% Tween20 pH 5.5. A fifth wash with the correspondent buffer was performed and left to incubate 10 mins shaking. Both plates were then washed with 1x PBS 0,05% Tween pH 7.4.

50 µL of Rabbit anti-Myc HRP (1/2000) diluted in PBS/0,1% casein were added to the plates and left to incubate for 1hour at RT shaking. Next, 50 µL of TMB was loaded to the plate and incubated for 10 minutes at RT shielded from light and 50 µL H<sub>2</sub>SO<sub>4</sub> was loaded to each well to stop the reaction.

Alternatively, 50 µL of Anti-Myc tag antibody (1/1000) diluted in PBS/0,1% casein can be added and left to incubate for 1 hour at RT shaking. After 1 hour 50 µL of DAMPO (1/50000) diluted in PBS/0,1% casein are loaded and the protocol proceed similarly to loading of TMB and H<sub>2</sub>SO<sub>4</sub>.

# Results

## A-12E08 mutants based on predictive crystal structure

### 1-Plasmid generation

#### *1.1-Construct design*

The introduction of histidine's in antibodies is known to play a duality of binding and repulsing the antigen in a pH-dependent manner by the mechanisms previously explained (3.2-pH-dependent target release). Because of this feature, it was decided to introduce histidine mutations in the CDR regions of the mouse 12E08 anti-C2 antibody (as these CDR regions are most involved in antigen-antibody binding). Hypothesis is that, this way, a pH-dependent target release ability might be introduced into the 12E08 antibody.

A predictive model of 12E08's crystal structure (fab region), represented in Figure 7, was studied in search of potential sites for histidine mutations. The selection of those sites was based on the theoretical probability of generating a positively charged site by introducing a histidine mutation, strong enough to destabilize the interaction with the antigen at acidic pH, due to repulsion. Moreover, it was hoped that the interaction would be conserved at neutral pH. For that three premises were considered (Figure 8):

- 1- The first and most considered hypothesis was that mutating an aminoacid close to a positively charged aminoacid (arginine or lysine) to a histidine, allows the occurrence of a positively charged pocket ( Figures A-1,4,5,6, 7 and B-1,3,4)
- 2- A second hypothesis was based on the idea that an aminoacid in the CDRs with an upwards direction might be interacting with the antigen. Therefore, if mutated to a histidine, once in an acidic pH (5,5) the aminoacid is presumably able to clash with the target and lead to the unbinding of the antibody. ( Figures A-3)
- 3- The last hypothesis was established based on the pi-stacking of aromatic amino acids seen in ARGX-117 molecule and is believed to be involved in pH-dependency. For that the combination of tryptophane and histidine (FIG A-2) and histidine with histidine (FIG B 2) were explored.

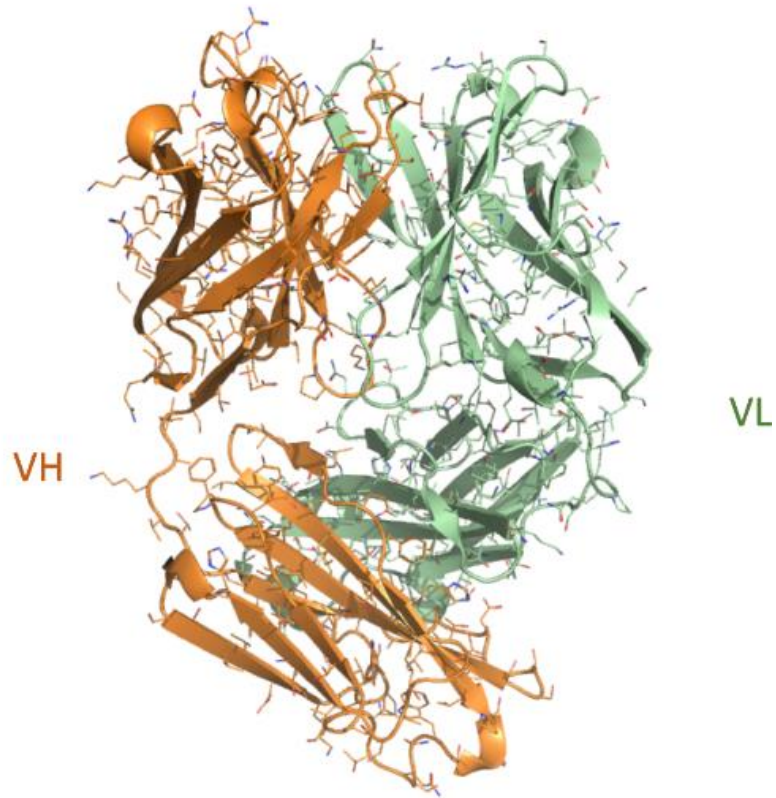


Figure 7-Predictive crystal structure of 12E08' fab region modelled by AlphaFold.

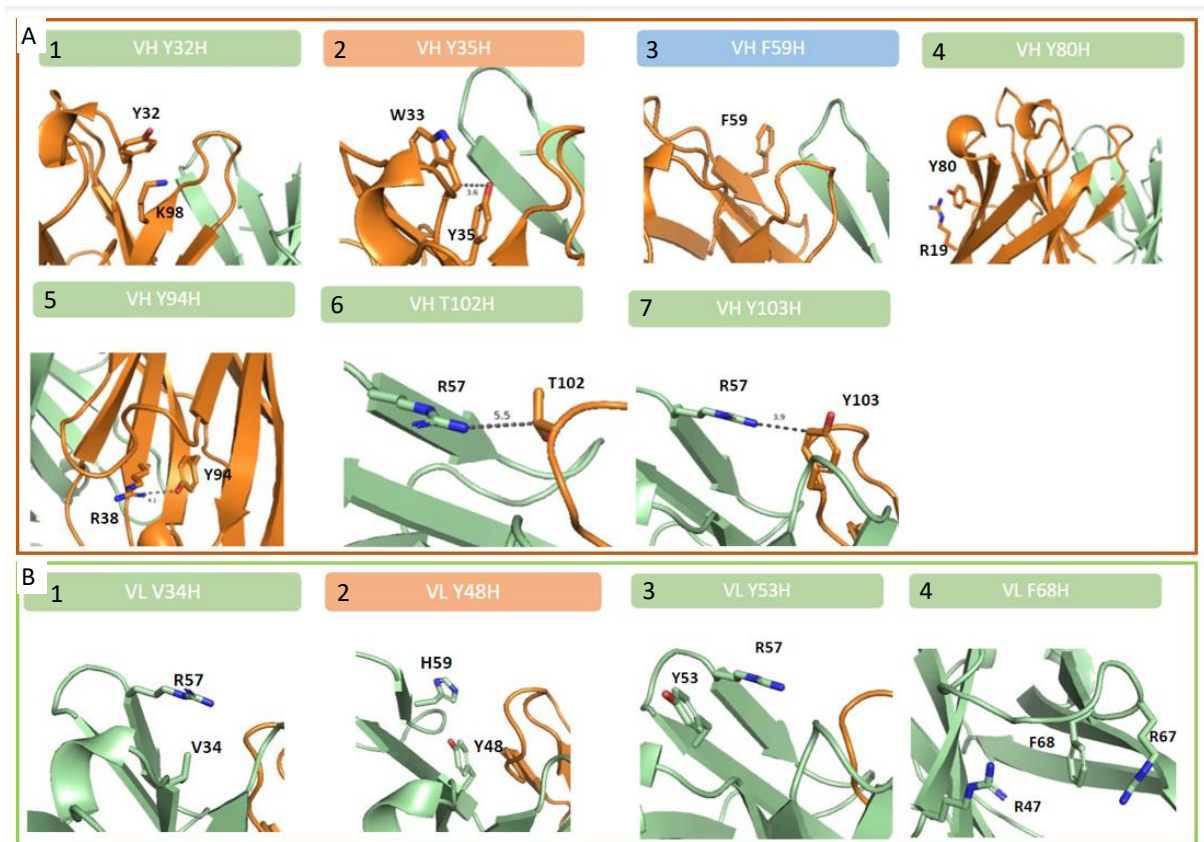


Figure 8 - 12E08 structure sites where histidine mutations were planned to be introduced. A-12E08 heavy chain CDRs sites; B-12E08 light chain CDRs sites.

11 potential mutation sites in both heavy and light chain variable regions (VH and VL) were selected (Figure 8) and 11 DNA strings were constructed and ordered from Twist Bioscience (USA) with BsmBI cutting sites on both 3' and 5' end.

### 1.2-DNA cloning

After proper digestion, the ligation of pUPEX 201 with VH strings and pUPEX35 with VL strings was performed as described above (1.1-DNA cloning) and *E. coli* cells were transformed with the generated plasmids.

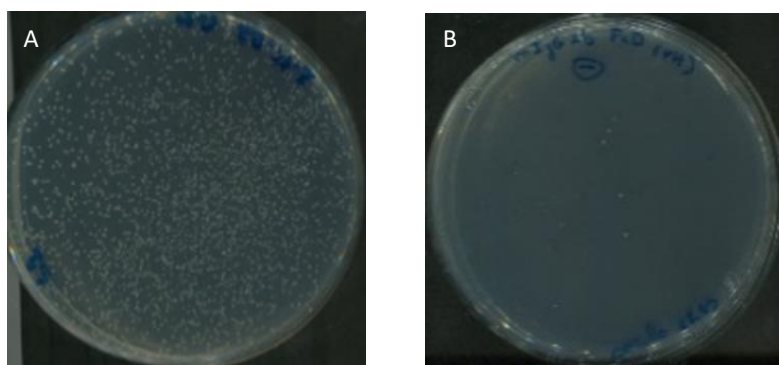


Figure 9- Example of the transformation of TOP 10 cells with 12E08 mutant plasmids from the ligation of: A-a single histidine mutant (or WT) chain and the correspondent vector (pUPEX 201(mIgG2b)-DANA) for VH strings and pUPEX35 for VL strings); B-negative controls (digested vectors ligated with only MQ). Image taken with Epson perfection V370 Photo image after O/N incubation.

Transformed cells were plated on LB agar dishes with ampicillin for positive selection of cells that were successfully transformed and acquired the new plasmid (that contains ampicillin resistance gene).

For every transformation there was growth of colonies, except for the negative control plates, where MQ was added to the ligation mixture instead of insert. Therefore, for every plasmid, the ligation and transformation were demonstrated to be successful and the controls behaved as expected.

Midiprep was performed and 12 plasmids with the correct sequence were produced.

### 2-Protein production and purification

Upon the successful production and purification of plasmids with single histidine mutations, HEK293 cell transfection took place.

To produce 12E08 mutant antibodies with only one HIS mutation compared to WT, each light chain mutant needed to be combined with heavy chain WT and vice versa, as shown in Table 14.

Table 14- Plasmid combination for HEK-293E cell transfection

	Plasmid VH	Plasmid VL
1	VH12E8_Y94H	VL12E08 pUPEX35 (mClambda) (WT)
2	VH12E8_Y103H	VL12E08 pUPEX35 (mClambda) (WT)
3	VH12E8_F59H	VL12E08 pUPEX35 (mClambda) (WT)
4	VH12E8_T102H	VL12E08 pUPEX35 (mClambda) (WT)
5	VH12E8_Y32H	VL12E08 pUPEX35 (mClambda) (WT)
6	VH12E8_Y35H	VL12E08 pUPEX35 (mClambda) (WT)
7	VH12E8_Y80H	VL12E08 pUPEX35 (mClambda) (WT)
8	VH12E08 mIgG2b DANA (WT)	VL12E8_F68H
9	VH12E08 mIgG2b DANA (WT)	VL12E8_V34H
10	VH12E08 mIgG2b DANA (WT)	VL12E8_Y48H
11	VH12E08 mIgG2b DANA (WT)	VL12E8_Y53H
12	VH12E08 mIgG2b DANA (WT)	VL12E08 pUPEX35 (mClambda) (WT)

6 days after, protein was purified and an SDS-P was performed as antibody quality control. The results are demonstrated in Figure 10.

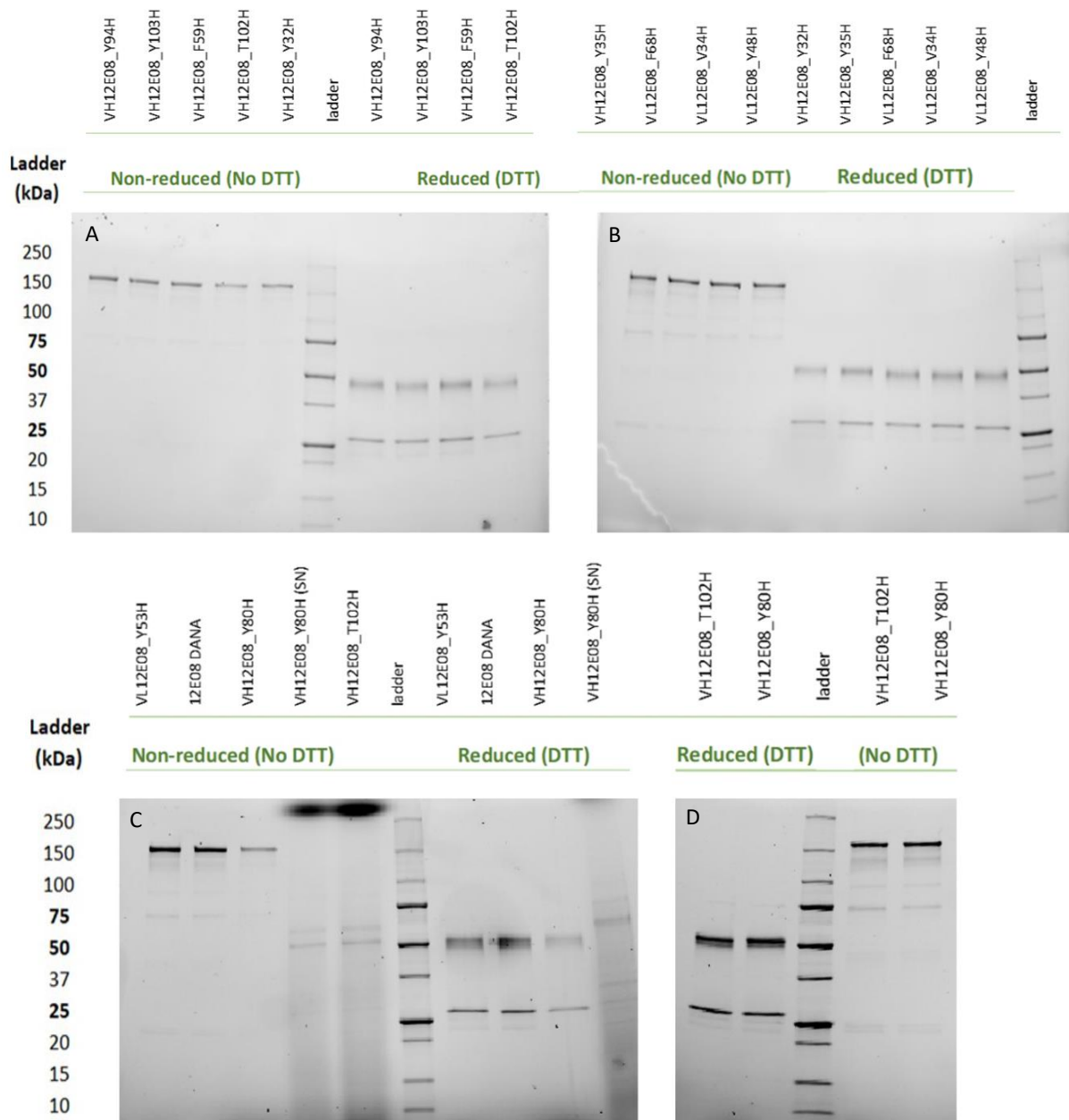


Figure 10- A,B- SDS-Page performed as QC for the generated histidine engineered antibodies under reducing and non-reducing conditions. C shows the SDS-Page where supernatant from the growing culture of two antibodies (VH12E08\_T102H ; VH12E08\_Y80H ) was taken along, because of low concentrations measured on nanodrop after purification. The wells loaded with supernatant show a dark band likely due to medium component. D show the SDS-Page for the repetition of antibody production for the two antibodies with low yield.

In the non-reduction situation only a band of 150Da was present (around the size of a full IgG antibody) with no unspecific bands showing up and in the reduced situation, only one band of around 50 Da and one of around 25 Da were present (corresponding to heavy and light chains respectively, as DTT breaks disulphide bonds). As this was also without any unspecific bands, it is concluded that 12 antibodies (11 histidine-mutant antibodies and one WT) were generated as depicted in Table 15.

Table 15-Internally attributed names to the produced histidine engineered antibodies and their corresponding mutations

VH12E08	
mab117_076	Y94H
mab117_087	Y103H
mab117_077	F59H
mab117_078	T102H
mab117_079	Y32H
mab117_080	Y35H
mab117_081	Y80H
VL12E08	
mab117_082	F68H
mab117_083	V34H
mab117_084	Y48H
mab117_085	Y53H
12E08 WT	
mab117_086	mIgG2b DANA

### 3-Mouse C2 binding ELISA

In order to characterize the previously generated 12E08 histidine-mutant antibodies and understand their binding profile to their target (mouse C2), a mouse C2 binding ELISA was performed, as depicted in Figure 11.

The concept of this binding ELISA is to coat the target (mouse C2), block the plate to avoid unspecific binding and add the newly generated 12E08 mutant antibodies. Antibodies that have the ability to bind to recombinant mouse C2, will stay bound to the C2 coated on the plate and will not be washed away on the following washing steps. After, a detection antibody is added, which will bind to the mouse Fc region of the 12E08 mutants (as they are in mIgG2b DANA backbone). The anti-mouse antibody is labelled with the enzyme peroxidase. When TMB - the substrate for the enzyme - is added, the enzymatic reaction takes place, making the samples change color from colorless to blue. This reaction is stopped with an acidic solution, that leads to a second change of color to yellow and the optical density is immediately read. The bigger the affinity to C2, the bigger the binding of anti-mouse antibody with peroxidase and, consequently, the higher the optical density values.

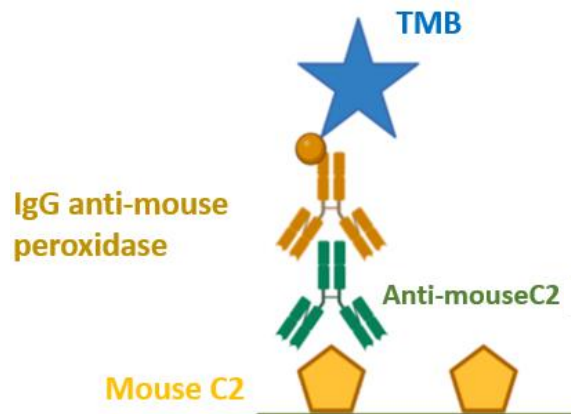


Figure 11- Schematic representation of a mouse C2 binding ELISA setup

The experiment was performed for 6 of the generated histidine engineered antibodies, together with 12E08 mIgG2b-DANA WT and Mota mIgG2b DANA as a negative control.

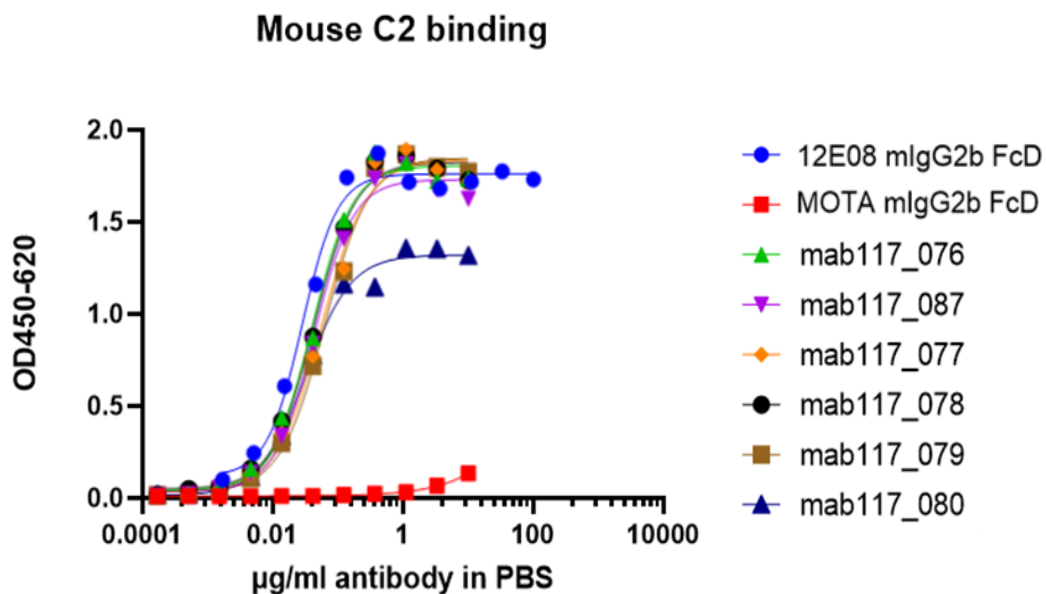


Figure 12-Mouse C2 binding assay performed for 6 of the histidine engineered antibodies, with 12E08-DANA and a non-C2 binder (MOTA mIgG2b), assay performed for a concentration range between 10 µg/mL and 0,0195 µg/mL (Note that 12E08 DANA and Mota DANA were not diluted 1/10, therefore, the starting concentration in the dilution series was 10X higher than the other antibodies. This difference was plotted in the final graph). For more details about the antibodies (mutations present in each antibody) see Table 15.

As visualized in Figure 12, the assay was performed successfully, showing no binding of the negative control (Mota mIgG2b DANA) to the coated recombinant C2. All 12E08 histidine-mutant antibodies tested showed binding to C2.

mab117\_080 (VH12E08\_Y35H) showed a lower affinity to the target at the higher concentrations, however, this is likely due to a technical mistake, as the antibody shows the same profile as the other antibodies in a repetition of the experiment.

It was decided that the data of mab117\_080 could later be confirmed on MSD, as the assay also allows the assessment of binding.

#### 4-Mouse Classical Pathway ELISA

A mouse CP activation ELISA assay was performed to understand the functional profile of the engineered antibodies, as shown in Figure 13.

The objective of the mouse CP assay is to understand if the antibodies can actively block CP activation. The idea is to coat mouse IgG antibodies as CP is mainly activated upon the recognition of the Fc region of antibodies by C1. With this strategy it is possible to mimic the activation of CP.

Additionally, in such setup, 4 controls are taken along:

- Wells with only 10% serum and no antibodies, where CP activation should not be blocked and therefore a signal should be detected
- Wells with 10% serum and MgEGTA, as EGTA only allows alternative pathway activation by specifically chelating calcium (leading to lack ionized calcium) and, therefore, blocking the calcium dependent steps of both CP and LP. (Prez, Des *et al.*, 1975) (Johnson, Capraro e Parks, 2008) (Garred, Tenner e Mollnes, 2021) Consequently, no signal should be detected;
- Wells with 10% serum and EDTA, as treatment with EDTA, similarly to MgEGTA, blocks the calcium dependent steps of both CP and LP. But additionally, EDTA can also chelate magnesium, leading to the inhibition of the formation of AP C3 convertase, which is a magnesium-dependent step, resulting in the blockage of AP and therefore, blocking the entire system. (Banin, Brady e Greenberg, 2006; James, 1982) Consequently, no signal should be detected
- Uncoated wells with 10% serum, that should not show a signal, as the trigger for the activation of CP (mouse IgGs) is not present.

The plate is then blocked to avoid unspecific binding and the 12E08 mutant antibodies are serially diluted in 100% mouse serum in order to visualize a dilution effect. Then, the serum with the antibodies is transferred to the assay plate and an anti-C3 antibody is

loaded. If the new antibodies are able to block C2, the cascade is not able to proceed and C3 will not be deposited. Therefore, anti-C3 will not be able to bind to anything and is washed away. A STREP-HRP antibody is added to detect anti-C3 antibody, followed by the substrate and the enzymatic reaction is then stopped with an acidic solution. The optical density is immediately read.

The better the antibodies are able to block CP activation, the less C3 is deposited and consequently the lower the optical density values.

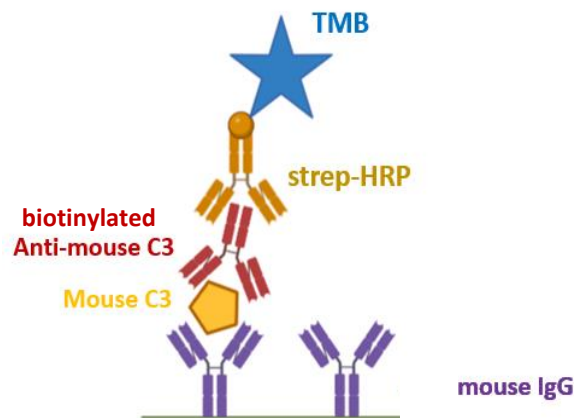
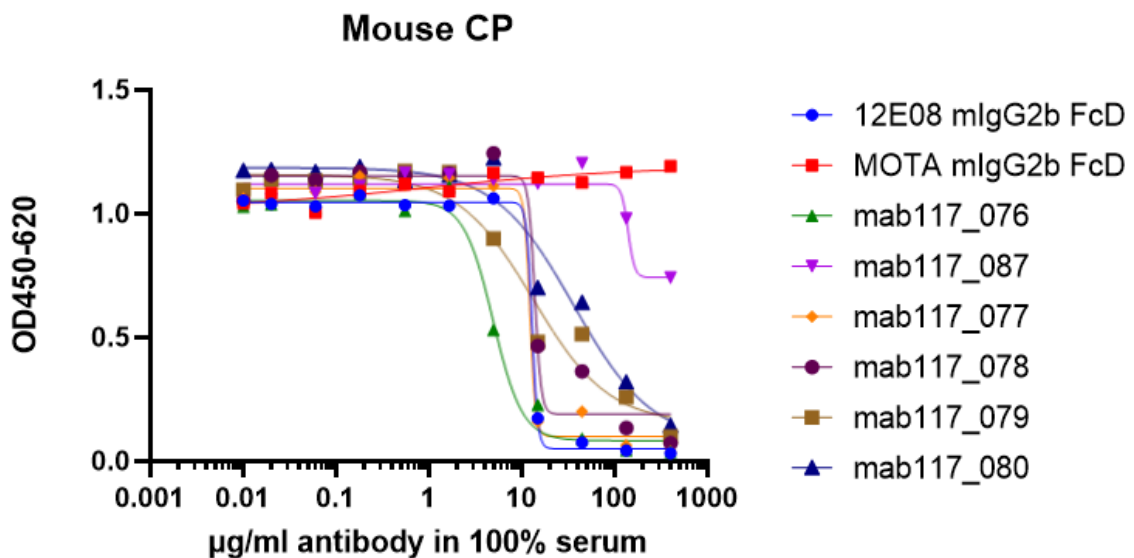


Figure 13- Schematic representation of a mouse classical pathway ELISA setup

All 12E08 mutant antibodies were tested, together with 12E08 mIgG2b-DANA WT for comparison and Mota mIgG2b DANA as control.



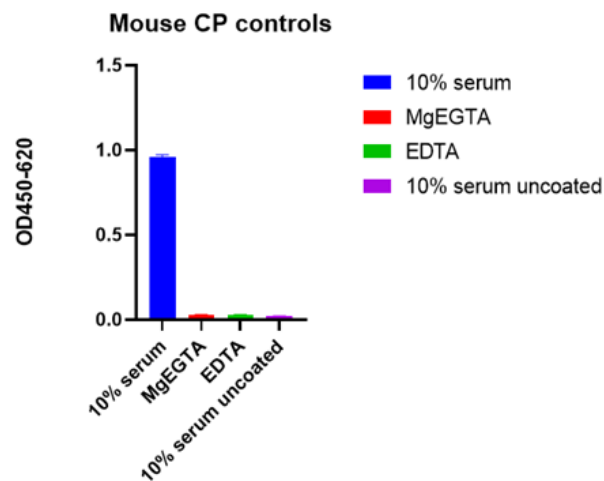
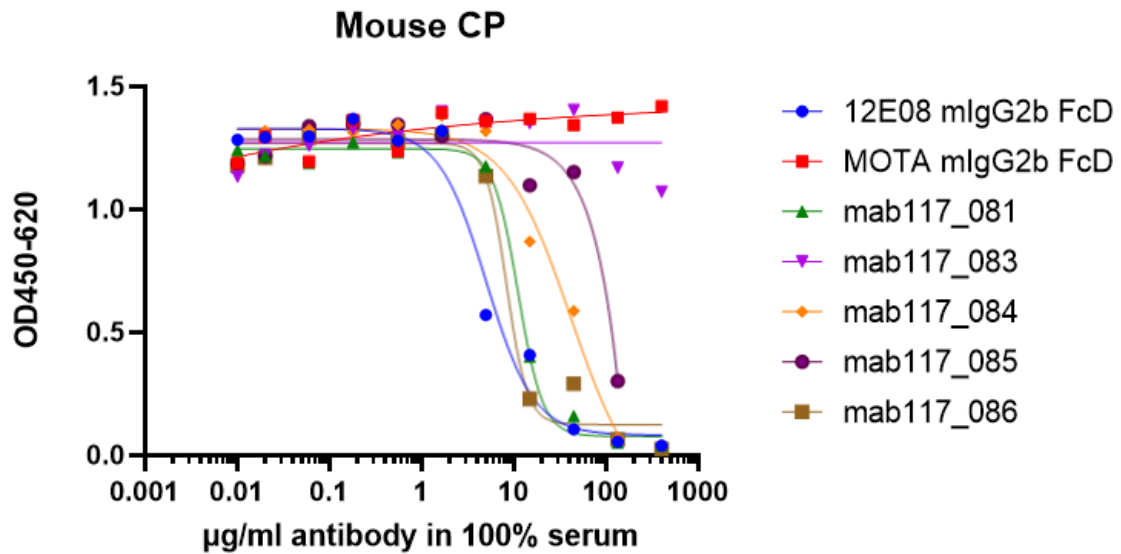


Figure 14- Mouse classical pathway ELISA assay performed for a random selection of the histidine engineered antibodies. In a low binding plate, the dilution series of the antibodies were prepared in 100% mouse complement preserved serum and preincubated for 15 mins on ice. This was followed by the dilution of the serum to 10% in buffer. 10% serum without antibody sample, MgEGTA, EDTA and 10% serum in uncoated wells were used as controls. For more details about the antibodies (mutations present in each antibody) see Table 15.

Figure 14 shows that the assay was performed successfully, demonstrated by the controls (MgEGTA leaving only alternative pathway activated - should not show a signal as the assay should only activate CP, EDTA blocking CP, AP and LP- should not show a signal, 10% serum uncoated- should not show a signal because the coating (Mouse IgG) is not present).

Although with a different profile from 12E08 DANA, all antibodies tested still block mouse CP activation. mab117\_087 and mab117\_083 showed the biggest loss in blocking capacity.

## 5-MesoScale Discovery

As the objective of the project is to generate antibodies that bind to C2 at a pH of 7.4 but release the target at a pH of 5.5, MesoScale Discovery (MSD) was the selected assay to test this feature as it allows the setup of two conditions in parallel (acidic and neutral pH) in a more sensitive assay than ELISA.

In this setup (Figure 15), the target (mouse C2) is coated and unspecific binding sites are blocked (at pH 7.4). Antibodies are diluted in a pH 7.4 condition, brought to the assay plate in duplicate and allowed to bind to the coating. Afterwards, one of the duplicates is washed with a pH 7.4 buffer and the other with a pH 5.5 buffer. An anti-mouse antibody (sulfo-conjugated) is added to detect the Fc region of the antibodies, followed by the reading buffer with surfactant to promote the enzymatic reaction.

C2 binders with pH-dependent target release are expected to stay bound to the coating at pH 7.4 but to unbind and be washed away at pH 5.5, therefore pH-dependent antibodies should show high reading values at a pH 7.4 but lower reading values at pH 5.5.

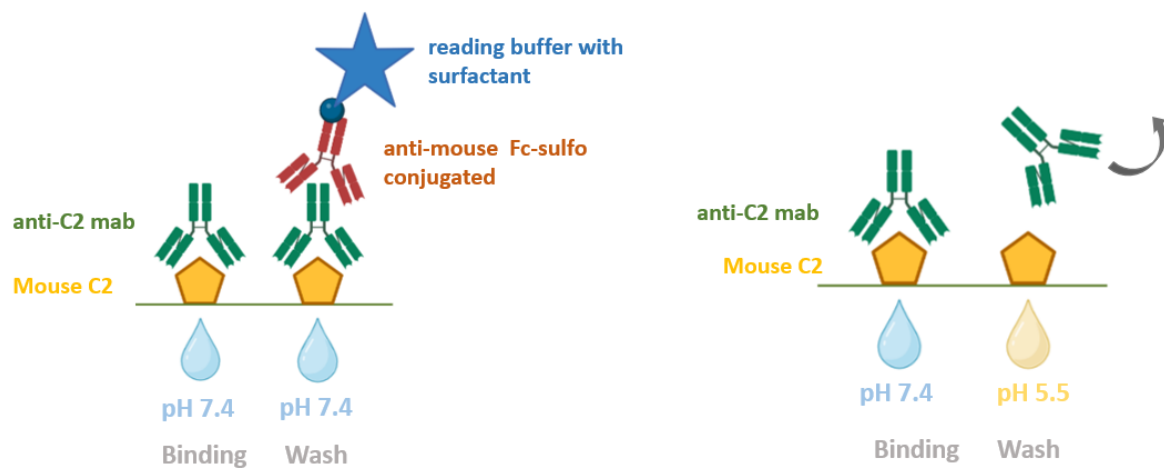
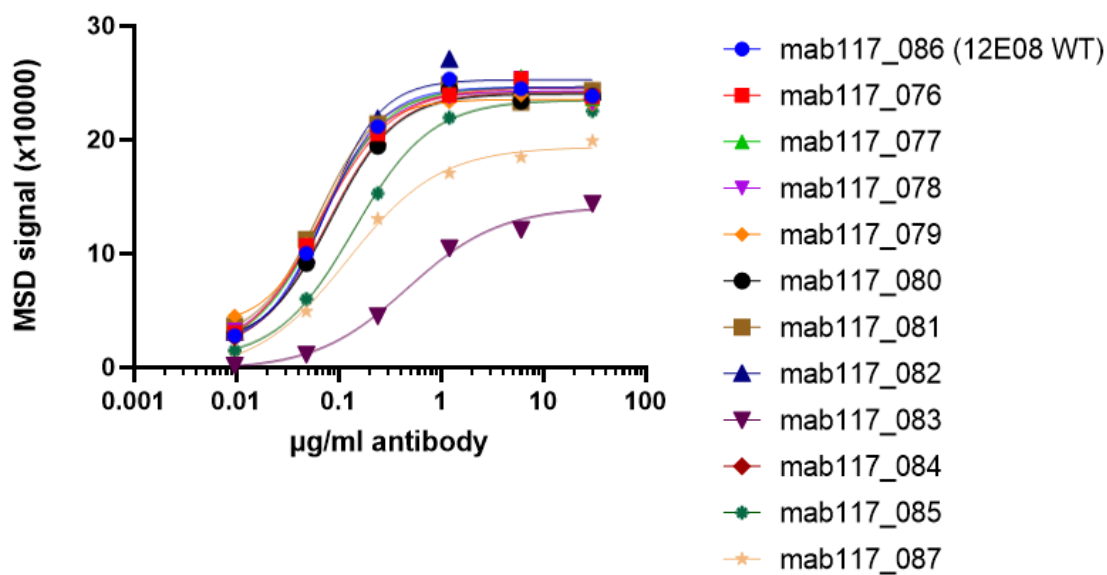


Figure 15- Schematic representation of the MSD setup for the test of a pH-dependent target-release, with two conditions in parallel (antibodies washed at pH 7.7 vs washed at pH 5.5)

All 12E08 mutant antibodies were tested, together with 12E08 mIgG2b-DANA WT.

### Mouse C2 binding MSD (pH 7.4/ pH 7.4)



### Mouse C2 binding MSD (pH 7.4/ pH 5.5)

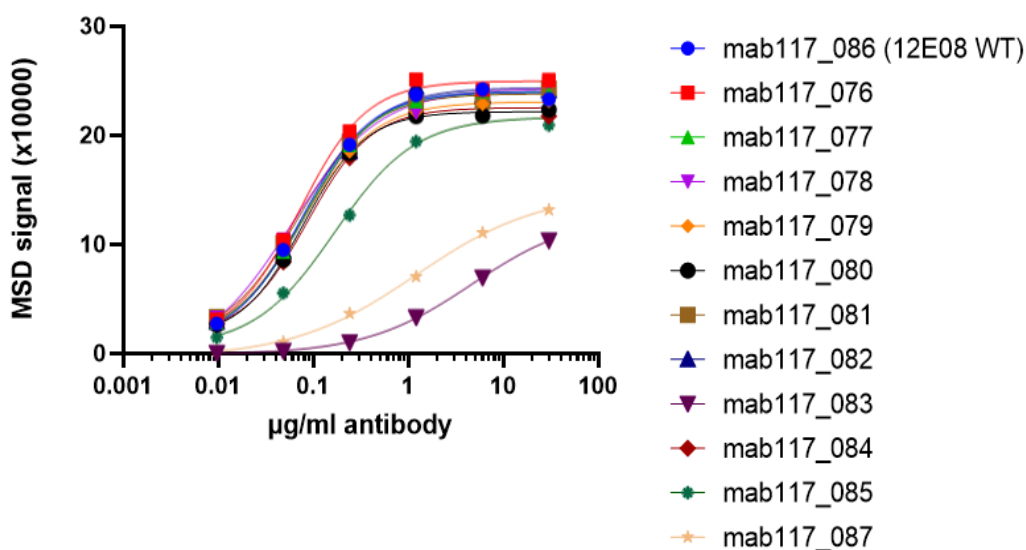


Figure 16- Mesoscale discovery performed with all histidine engineered antibodies, comparing a condition of wash at a pH of 7.4 and wash as a pH of 5.5. 12E08 DANA was taken along as reference. A dilution series of 1/5 was performed.

In case of the presence of a pH-dependent target-release antibody, the binding profile should be lower in the acidic condition comparing to the neutral, as the expected would be that the antibody unbinds C2 (target).

With that premise, in Figure 16, it was observed that two antibodies, mab117\_087 (12E08\_Y103H) and mab117\_083 (12E08\_V34H), show some level of pH-dependent target release (better visualized in Figure 18 and Figure 17).

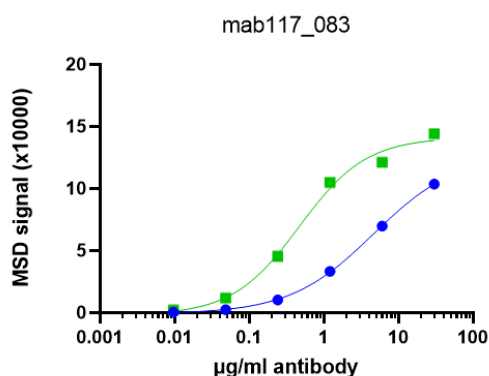


Figure 18-Comparison of the binding profile of mab117\_083 upon wash at pH 7.4 vs pH 5.5

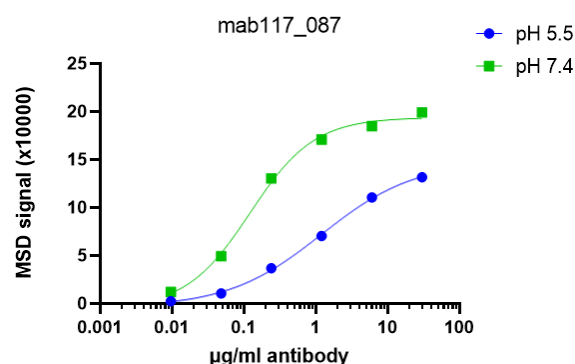


Figure 17-Comparison of the binding profile of mab117\_087 upon wash at pH 7.4 vs pH 5.5

However, this was also associated with binding loss. The data correlates with past experiments where both antibodies show some loss of function (blocking ability). Even though it could be interesting to further explore these antibodies, in particular mab117\_087, as the slight loss of binding could be compensated by the recycling of the molecule (due to pH-dependency), the functional assay demonstrates that blocking was too compromised for that option to be viable.

Therefore, other options to introduce pH-dependency in 12E08 were explored.

#### 6-Further analysis of predictive structure

A deeper dive into the predicted 12E08 structural model (determined via Alphafold) indicated VH T102 and VL Y48 (both single mutated to histidine with no impact on C2 binding in MSD) to be close to each other and near VL His59. It was discussed that although the single point mutations did not result in any pH-dependent target release, a combination of both might create a positively charged pocket able to cause enough repulsion and lead to antibody destabilization, represented in Figure 19.

Further, VH S100 seems to point towards VL His59 so also this residue will be mutated to a histidine and combinations with both VH T102H and VL Y48H will be tested.

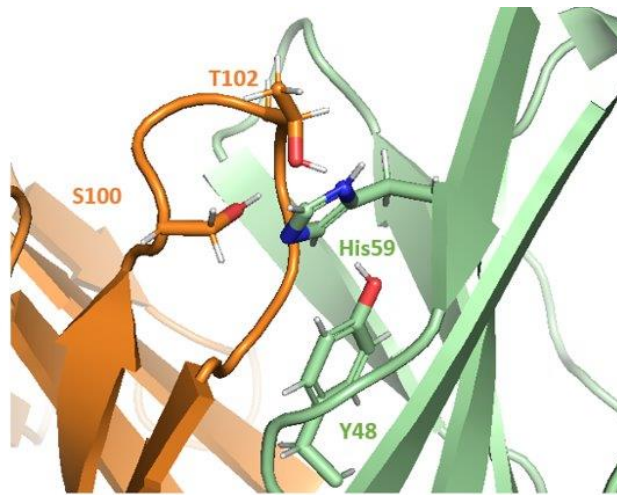


Figure 19- Location in 12E08's predictive structure further explored, as combination of histidine mutations in this sites were thought to be able to create a positively charged pocket and lead to a pH-dependent target release.

For this, 2 additional gene blocks were ordered and recloned in pUPEX 201 (mIgG2b backbone) and the process of plasmid production was repeated for the mentioned mutant combinations.

The digestion, ligation and transformation steps were performed as described above.

Both constructs showed colony growth, and the negative control was free of colonies, therefore, colonies were sent for MTP sequencing and showed that the correct strings were successfully inserted in the mIgG2b-DANA vector.

Next, HEK293 cells were transfected with the combination of the previously purified plasmids as shown in Table 16.

Table 16- Plasmid combination for HEK-293E cell transfection for new histidine mutant antibodies production

	Plasmid VH	Plasmid VL
1	VH12E8_S100H	12E08 WT pUPEX35 (mClambda)
2	VH12E8_T102H	VL12E8_Y48H
3	VH12E8_S100H	VL12E8_Y48H
4	VH12E8_S100H_T102H	12E08 WT pUPEX35 (mClambda)
5	VH12E8_S100H_T102H	VL12E8_Y48H

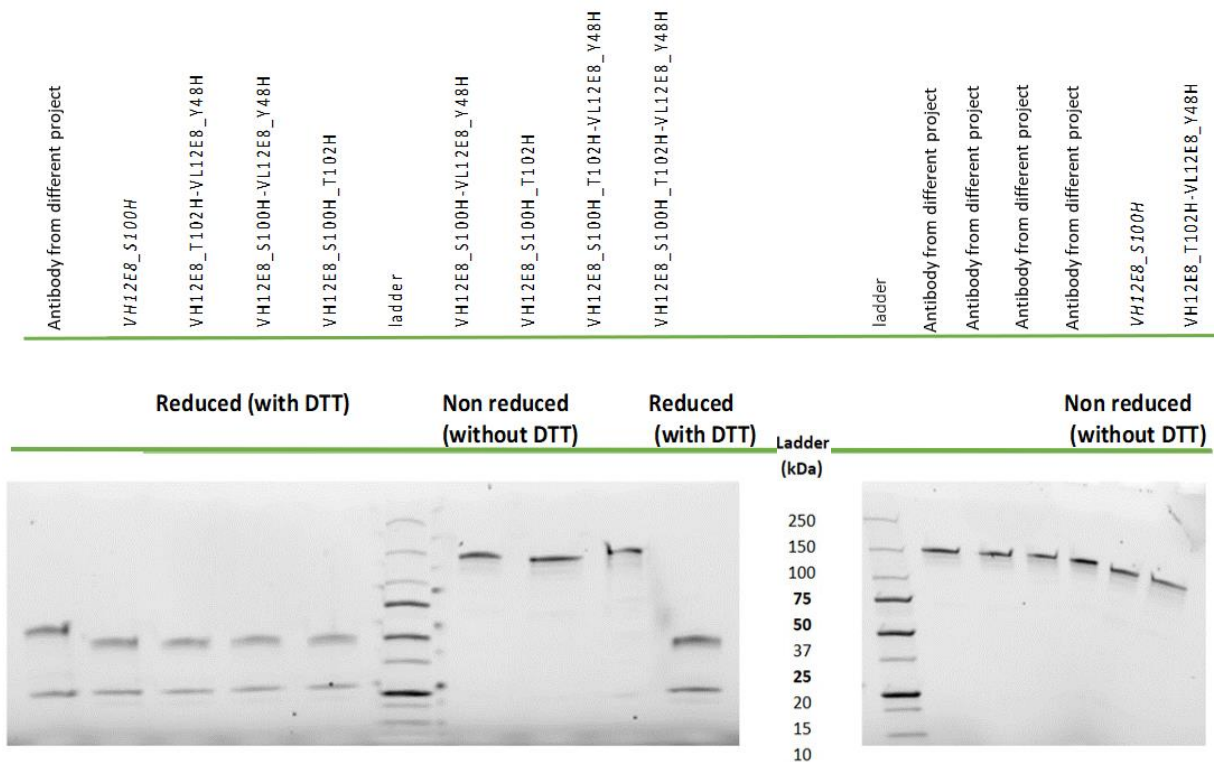


Figure 20-SDS-Page performed as QC for the new generated histidine engineered antibodies under reducing and non-reducing conditions.

Six days after transfection, protein purification took place and an SDS-PAGE was performed as antibody quality control. The results are shown in Figure 20.

Once again, in the non-reduction situation only a band of 150kDa was present (around the size of a full IgG antibody) with no unspecific bands showing up and in the reduced situation, only one band of around 50 kDa and one of around 25 kDa were present (corresponding to heavy and light chains respectively) also without any unspecific bands. It was concluded that 5 histidine-engineered antibodies were generated.

Mesoscale Discovery (MSD) assay was performed with the newly produced antibodies to screen for pH-dependency. For this assay, 12E08 WT mIgG2b DANA was taken along as a control and the most promising antibody tested previously (VH12E08\_Y103) was taken along for comparison with the new mutants.

Table 17- Internally attributed names to the produced histidine engineered antibodies and their corresponding mutations

mab117_089	VH12E8_S100H
mab117_090	VH12E8_T102H-VL12E8_Y48H
mab117_091	VH12E8_S100H-VL12E8_Y48H
mab117_092	VH12E8_S100H_T102H
mab117_093	VH12E8_S100H_T102H-VL12E8_Y48H

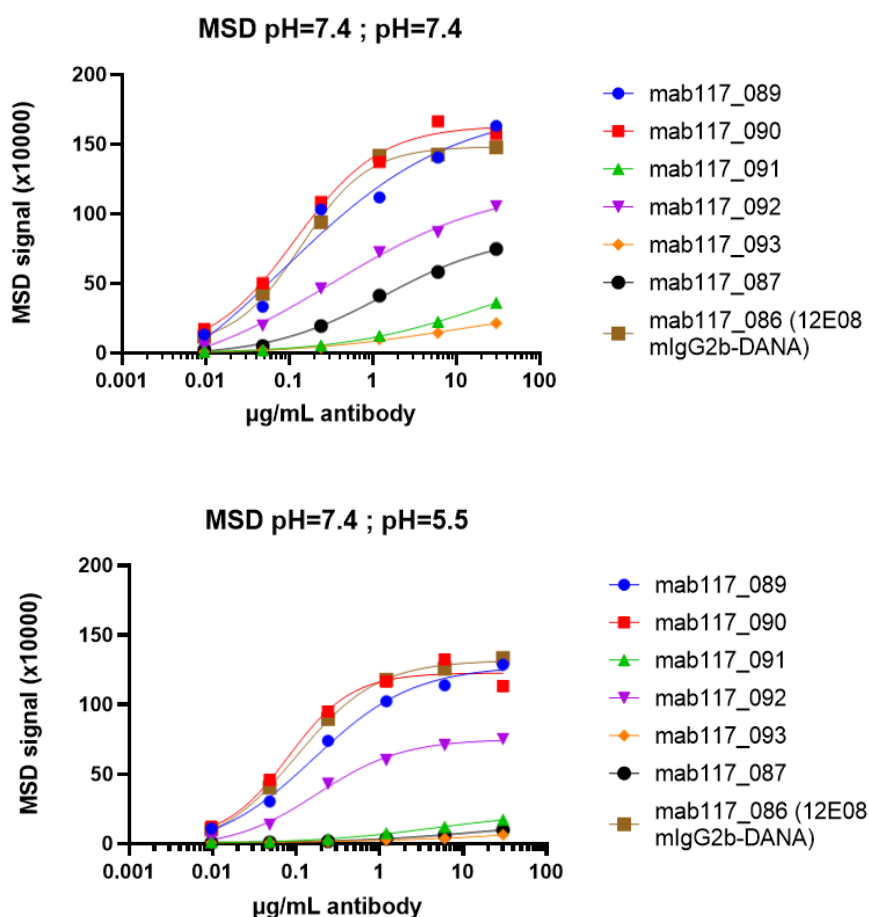


Figure 21-Mesoscale discovery performed with the new histidine engineered antibodies, comparing a condition of wash at a pH of 7.4 and wash as a pH of 5.5. 12E08 DANA was taken along as reference and the previous most promising antibody (VH12E08-Y103) was also taken along for comparison.

A binding profile different (lower) than 12E08 WT was observed for many engineered antibodies. Moreover, the binding profiles seem to be similar between pH= 7.4 and pH=5.5, suggesting a non-pH-dependent behavior. The previously produced VH12E08\_Y103 remained the only pH-dependent antibody but, demonstrating a great loss in binding capacity.

## B-Development of antibodies from combinatorial histidine library

### 1-Plasmid preparation

As an alternative way to develop a pH-dependent target-release mouse C2-blocking antibody (12E08 derivative) a library construction (a large repertoire of different DNA fragments cloned into vectors) approach was followed.

Firstly, a phagemid vector (pCB13) received one 12E08 WT chain and then, the corresponding library chain was inserted (pCB13 + 12E08 VH WT + 12E08 VL HIS; pCB13+ 12E08 VL WT + 12E08 VH HIS) as depicted in Figure 5.

For that, both vectors and chain were digested with the corresponding enzymes.

Ligation took place and the new plasmids were midprepped and digested with the opposite enzymes (as described in Second digestion of vectors), and were ready to receive the libraries.

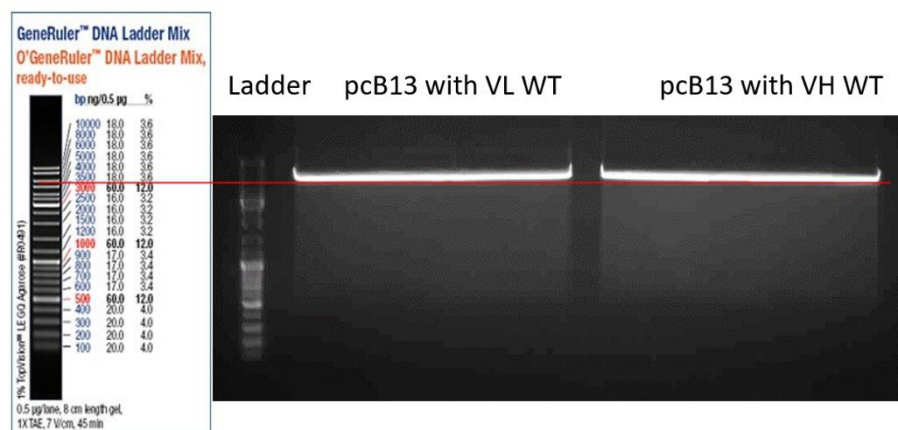


Figure 22- Gel electrophoresis of digested vectors with WT chains (around 5600 bp)

### 2-Library construction

12E08 VL and 12E08 VH libraries were constructed (ordered from GenScript) with a 10% probably of an histidine mutation (amino acid substitution) in every designated position of the three CDRs of each chain, using Trimer technology. See Figure 23.

Trimer technology uses trimer phosphoramidites (trinucleotides), for an oligonucleotide-directed mutagenesis. As trimers are trinucleotides, the technology allows the synthesis of oligonucleotides, not via an individual nucleotide structuring, but in a codon fashion.



attempting on library cloning in the vector are summarized in Table 18- Overview protocol optimization for library cloning-3 pairs of libraries generated.

Table 18- Overview protocol optimization for library cloning-3 pairs of libraries generated

Library	Protocol	Result	QC experiments performed		Outcome
1st libraries	Regular enzymes	Small library size Low insert rate	<ul style="list-style-type: none"> <li>- WT-WT ligation was tested</li> <li>- Start from the new vectors (with one WT chain already inserted)</li> <li>- Sequence the entire vector (with inserts)</li> <li>- Ligation with digested material known to have a successful bacterial transformation</li> </ul>		<ul style="list-style-type: none"> <li>- Bacterial transformation for a VH WT- VL WT vector showed less growth than expected, in spite of most sequences being correct.</li> <li>- Sequences were fully correct for both vectors</li> <li>- Ligation for known material showed a lot less colonies than expected, and according to colony PCR, the insert rate was not optimal</li> </ul>
2nd libraries	<ul style="list-style-type: none"> <li>-Fast Digest enzymes</li> <li>-New batch of agar plates</li> <li>-Ligation buffer as new as possible</li> </ul>	Small library size Low insert rate	Condition 1 Condition 2 Condition 3 Condition 4	New ligase buffer + hard shaking New ligase buffer + DNA treatment + hard shaking New ligase buffer + ON ligation + DNA treatment + hard shaking) New ligase buffer + ON ligation + heat inactivation + DNA treatment + hard shaking	All conditions showed a substantial improvement in number of colonies (in particular condition 1 and 3), therefore, condition 1 (simpler option) was used to proceed.
3rd libraries	<ul style="list-style-type: none"> <li>-Vectors and plasmids were again digested</li> <li>-Volume of enzymes and digestion time optimized</li> <li>-Fast digest enzymes</li> <li>-Condition 1</li> </ul>	Bigger library size Better insert rate	-		Proceed with libraries

In a first attempt, even though the test ligation and transformation were not optimal, the protocol was followed (as described in 2-Library cloning) and VH and VL libraries were generated. However, in this experiment, the lack of colonies in the spotting plates indicated that the generated libraries were too small to cover the expected diversity and sequences showed that only around 50% of the sequenced clones had correct sequence (low insert rate).

Multiple QCs were performed, as described in Table 18, and results showed that vector sequences were correct but ligation and transformation steps were compromised.

Consequently, two main changes were planned for the following experiments: use a new batch of agar plates and fresh ligation buffer. Additionally, fast digest enzymes were used in the following experiments to make the digestion as efficient as possible.

Therefore, the protocol was adapted to Fast Digest enzymes, as shown in Table 19.

Table 19- Digestion protocol for vectors and libraries adapted to Fast Digest enzymes

pCB13 with WT chains			Inserts (libraries)		
Plasmid	25	μg	PCR product	3	μg
10X FD Buffer green	40	μL	10X FD Buffer green	30	μL
Enzyme 1	20	μL	Enzyme 1	10	μL
Enzyme 2	20	μL	Enzyme 2	10	μL
MQ water	X	μL	MQ water	X	μL
Total	400	μL	Total	300	μL

3h at 37°C

1h30 at 37°C

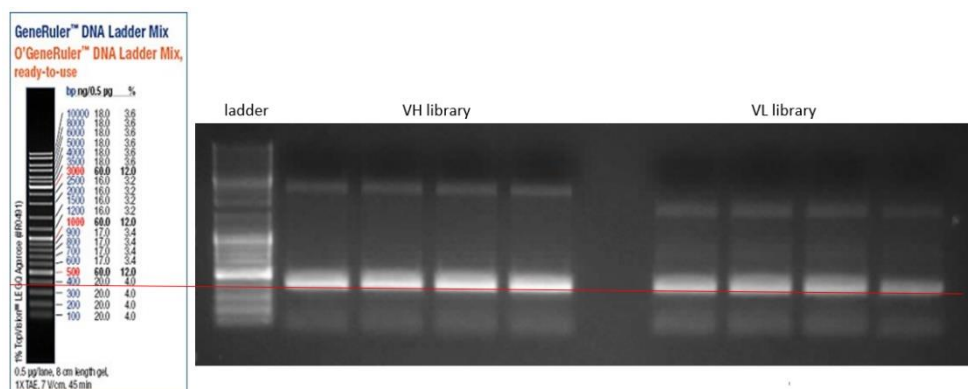


Figure 25- Gel electrophoresis of the digested libraries. Bands at the expected size (around 350 bp)

The other steps of the protocol were followed as previously described.

Test ligation was performed and the results, even though not optimal, appeared slightly improved. However, for the real ligation, results were less convincing, with less colony growth in streaked plates and spotting plates only showing 1 or 2 colonies. Therefore, it was concluded that the generated library size was again smaller than expected. Additionally, colony PCR showed an insert rate of around 50 % (data not shown).

Based on the non-optimal results, one more attempt to optimize the ligation and transformation steps was made. For that, different conditions were tested, as shown in Table 18, and condition 1 was chosen to be used in following experiments (New ligase buffer + hard shaking).

Because of lack of DNA material to proceed with the repetition of the protocol with condition 1, the vectors and plasmids were again digested according to the Fast Digest protocol. These digestions were also optimized and the volume of enzymes was increased (compared to last experiment) based on the product information manual for all fast digest enzymes to achieve an optimal digestion of all material and digestion time was lowered, also based on the recommended time in the manual to avoid star activity, see Table 20 and Table 21.

*Table 20- Further optimized protocol for vector digestion (with WT chain) using FD enzymes*

PCB13_with VH WT			PCB13_VL		
Plasmid	25	µg	Plasmid	25	µg
10X FD Buffer green	50	µL	10X FD Buffer green	50	µL
FD ApaLI	25	µL	FD NcoI	25	µL
FD AvrII	25	µL	FD NheI	25	µL
MQ water	X	µL	MQ water	X	µL
Total	500	µL	Total	500	µL

1h at 37°C

Table 21-Further optimized protocol for library digestion (PCR product) using FD enzymes

VL			VH		
PCR product	3	μg	PCR product	3	μg
10X FD Buffer green	30	μL	10X FD Buffer green	30	μL
FD ApaLI	15	μL	FD NcoI	15	μL
FD avrII	15	μL	FD NheI	15	μL
MQ water	X	μL	MQ water	X	μL
Total	300	μL	Total	300	μL

1h at 37°C

Therefore, a new experiment was performed according to the optimized Fast Digest protocol and condition 1 (new ligase buffer and hard shaking).

Test ligation pointed to transformation improvement (see Figure 26) and the experiment proceeded to real ligation.

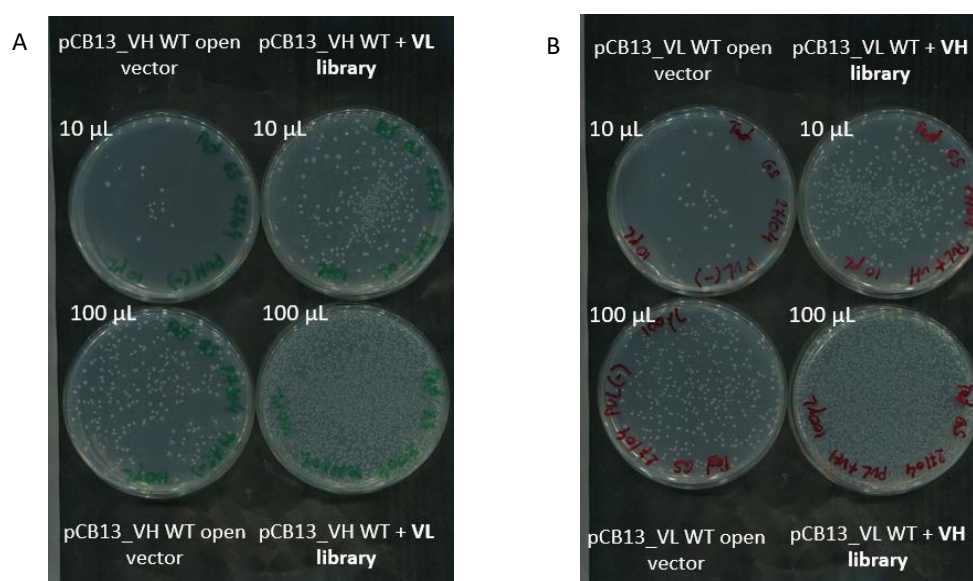


Figure 26- Transformation of TG1 electrocompetent cells with 12E08 mutant plasmids from the test ligation (small volumes were used) of: A-pCB13 with previously inserted VH WT, ligated with the VL library; B- pCB13 with previously inserted VL WT, ligated with the VH library. Corresponding negative controls (open vectors) are also present.

Images taken with Epson perfection V370 Photo image after O/N incubation.

The real ligation, however, only showed 1 or 2 colonies once again for the spotting plates. However, streaked material seemed slightly improved, see Figure 27.

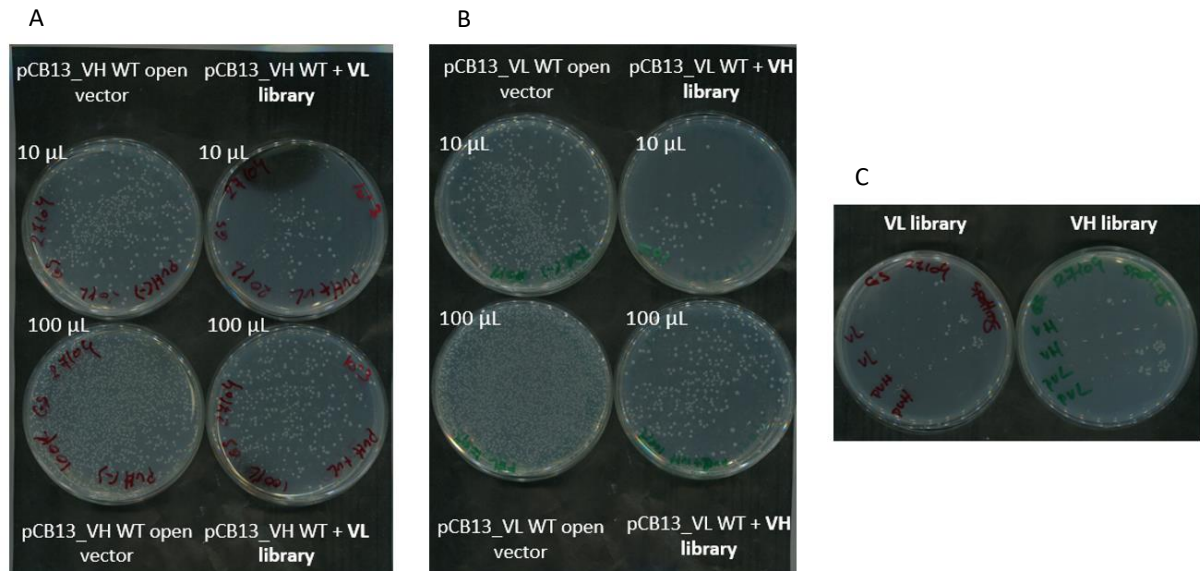


Figure 27- Transformation of TG1 electrocompetent cells with 12E08 mutant plasmids from ligation of: A- pCB13 with previously inserted VH WT, ligated with the VL library; B- pCB13 with previously inserted VL WT, ligated with the VH library. Corresponding negative controls (open vectors) are also present. C- Spotting of the dilution series (1/10) from an initial 10<sup>-3</sup> dilution of both libraries.

Images taken with Epson perfection V370 Photo image after O/N incubation.

A comparison between the 3 pairs of libraries was made, as depicted in Table 22.

The library size was assessed, not based on the number of colonies on spotting plate, but the number of colonies on the plates where 20 µL or 100 µL were plated. The insert rate was assessed based on sequence analysis.

Table 22- Overview of generated libraries

	1st libraries		2nd libraries		3rd libraries	
	VH	VL	VH	VL	VH	VL
Library size (based on nr colonies)	4,20E+06	1,00E+07	1,04E+06	4,00E+06	1,00E+07	1,40E+07
Insert rate (%)	≈60%*1	≈75%*1	≈55%	≈60%	≈70%	≈70%

\*1- Only 8 clones were sequenced

After comparing the data of the libraries generated, it was decided to proceed with the third libraries as they show a bigger library size and a better insert rate.

Generated libraries then proceeded to phage display in order to be able to select for pH dependent clones.

#### 4-Phage display and selections

Phage display is a commonly used technology for the high-throughput screening of protein interactions from large libraries, that relies on the genetic manipulation of bacteriophage viruses (obligate intracellular parasites of bacteria) to express peptides on their surface. This alteration creates a link between the phenotype (peptide/antibody) on the surface of the particle and the packaged genetic information encoding for that phenotype, inside the phage. (Pande, Szewczyk e Grover, 2010)

In case of phagemid vectors, an additional helper phage is needed, as the phagemid contains the genetic information encoding for gene 3 fused with a protein (in this case, a Fab region) but lack all the other phage proteins necessary for the assembly of functional particles. Therefore, this information is supplied by a helper phage. The WT gene 3 is also present in the helper phage, making the preparations heterogeneous (displaying both recombinant and WT protein), however, the helper phage is defective in replication as result of packaging signal disablement. For that reason, the number of WT protein should be substantially reduced compared to recombinant protein. (Chasteen et al., 2006)

Additionally, the helper phage also carries an antibiotic resistance gene, different from the phagemid vector. (In this case the phagemid vector carries an ampicillin resistance gene while the helper phage's carries resistance for kanamycin). This way, it is possible to select bacteria with both phagemid vector and helper phage, resulting in functional particles that display protein of interest.(Chasteen et al., 2006)

The selection itself has a simple principle: when a protein target is immobilized in a surface, a phage displaying a protein that is able to bind to such target stays bound to the target, while non-binding or low affine clones are washed way.

Because of the phenotype-genotype association previously mentioned, while selecting binders through the displayed protein, the encoding gene is also automatically selected,

which makes it possible to proceed with further rounds of selection to obtain the clones of interest.

For the first round (R1) 10 µg/mL of the corresponding coating was used, accordingly to the layout, for each library. The setup is described in Table 23.

Table 23- Conditions selections R1

Coating (10 µg/mL)	Elution buffer	Elution time
mouse C2	Trypsin (pH ≈7.4)	20 mins
mouse sushi-2	Trypsin (pH ≈7.4)	20 mins
mouse sushi-2	CPA (pH ≈ 5.5)	30 mins
irrelevant (human C2)	Trypsin (pH ≈7.4)	20 mins
PBS	Trypsin (pH ≈7.4)	20 mins

For R1, the goal was to select sequences from the libraries that had affinity to the target C2, and specifically to Sushi2 epitope. As libraries derived from 12E08 (mouse C2 binder), it was expected that clones would maintain the affinity to C2. Therefore, it was decided to include already in R1, an acidic elution (CPA pH ≈ 5.5) to select for a pH-dependent target release.

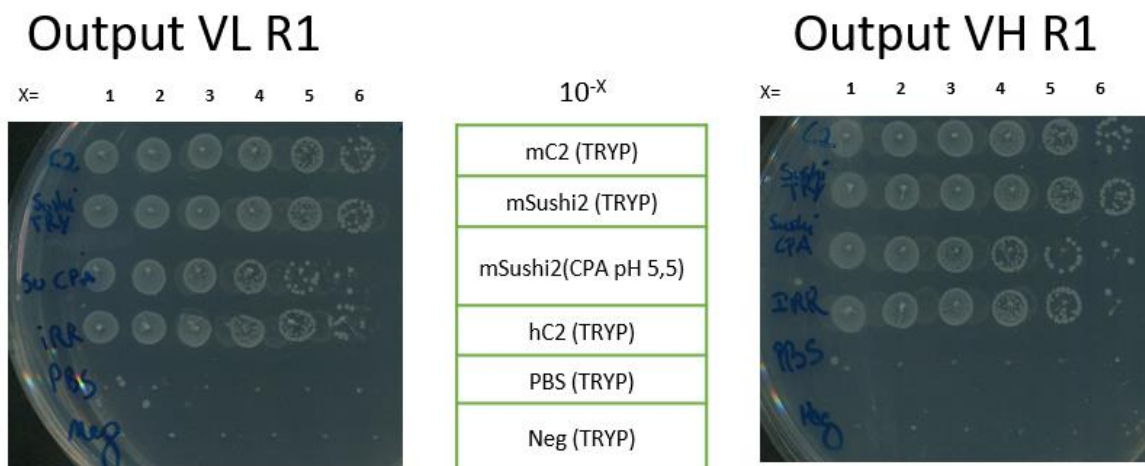


Figure 28-Spotting of the dilution series (from 10<sup>-1</sup> to 10<sup>-6</sup>) of all outputs from Round 1 (R1) of selections, for VL (left) and VH (right).

Already in R1, there was a visible difference between mSushi2-TRYP condition and mSushi2-CPA (less colonies in the second condition), see Figure 28. This shows that there is a specific selection for pH dependent clones in the CPA condition.

As a negative control for unspecific binding, an irrelevant protein was used on the setup. Therefore, a molecule different from the target, where binding is not expected should be used.

However, the results obtained in R1 showed that the “irrelevant” protein condition (human C2) shows many binders. This was further investigated and previously generated data (data not shown) pointed towards the fact that 12E08 is cross-reactive with human. For following rounds, a different protein (human C1 (hC1)) was used as irrelevant protein.

R2 proceeded from the CPA elution (30 mins) rescues from each library and the following conditions were performed (See Table 24):

*Table 24- Conditions selections R2*

<b>Coating (1 µg/mL)</b>	<b>Elution buffer</b>	<b>Elution time</b>
mouse sushi-2	Trypsin (pH ≈7.4)	20 mins
mouse sushi-2	CPA (pH ≈ 5.5)	10 mins
mouse sushi-2	CPA (pH ≈ 5.5)	30 mins
irrelevant (human C1)	Trypsin (pH ≈7.4)	20 mins
PBS	Trypsin (pH ≈7.4)	20 mins

In R2, a 10X lower concentration of coating was used, in order to select for stronger binders. As there is less target to bind, there is competition for binding and only more affine binder are able to bind.

Additionally, mC2 coating was left out, as the previous data showed the presence of C2 binders and, more importantly, to sushi2 epitope.

In this round, different times of acidic elution (CPA pH ≈ 5,5) were compared, as a longer time of elution might lead to the elution of binders with less potent pH-dependency. By reducing the elution time, there is a selection towards stronger pH-dependent clones

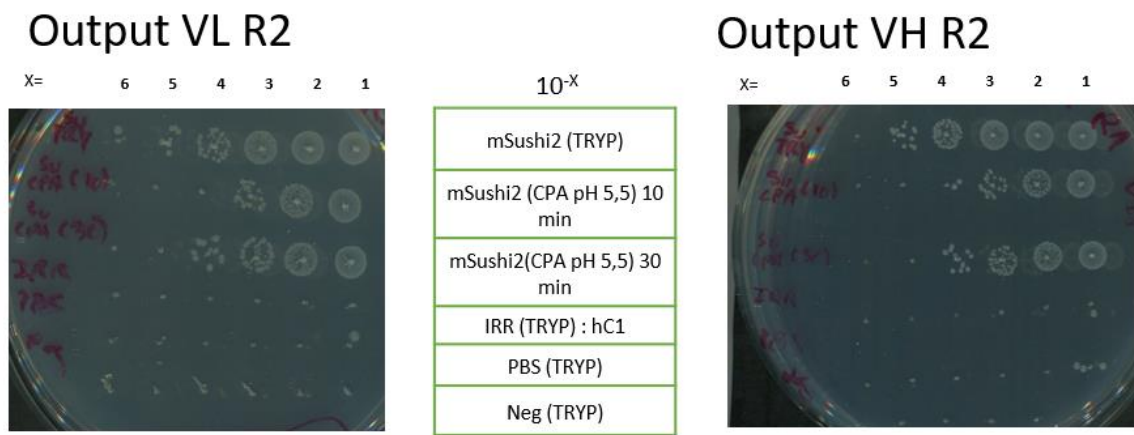


Figure 29- Spotting of the dilution series (from  $10^{-1}$  to  $10^{-6}$ ) of all outputs from Round 2 (R2) of selections, for VL (left) and VH (right).

Once again, a visible difference between mSushi2-TRYP condition and mSushi2-CPA, hinting a selection for pH dependent clones.

Additionally, a noticeable difference is seen between CPA elution for 30 mins and CPA elution for 10 mins (Figure 29).

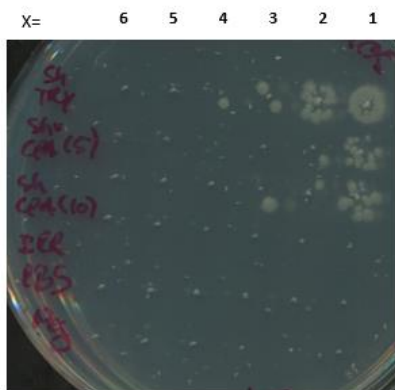
A R3 was performed from the CPA elution (10 mins) rescues from each library with the setup described in Table 25.

Table 25- Conditions selections R3

Coating (0,1 $\mu\text{g}/\text{mL}$ )	Elution buffer	Elution time
mouse sushi-2	Trypsin (pH $\approx 7.4$ )	20 mins
mouse sushi-2	CPA (pH $\approx 5.5$ )	5 mins
mouse sushi-2	CPA (pH $\approx 5.5$ )	10 mins
irrelevant (human C1)	Trypsin (pH $\approx 7.4$ )	20 mins
PBS	Trypsin (pH $\approx 7.4$ )	20 mins

For R3, coating concentration was further decreased 10X from R2 to select for stronger binders and the acidic elution times was also decreased (10 min vs 5 min elution) for a bigger pH-dependency selection.

## Output VL R3



10<sup>-x</sup>

mSushi2 (TRYP)
mSushi2 (CPA pH 5,5) 5 mins
mSushi2 (CPA pH 5,5) 10 mins
IRR (TRYP) : hC1
PBS (TRYP)
Neg (TRP)

## Output VH R3

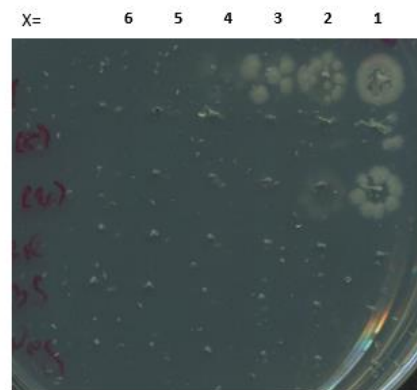


Figure 30-Spotting of the dilution series (from  $10^{-1}$  to  $10^{-6}$ ) of all outputs from Round 3 (R3) of selections, for VL (left) and VH (right).

From elution with CPA for 10 mins to 5 min, a difference is again clearly visible. (Figure 30).

The results suggest an efficient selection for strong binders with strong pH-dependent target release properties. For this reason, selections were stopped and fab production was initiated from the 5 minutes CPA elution rescues (for VH and VL).

Therefore, in following experiments clones were sequenced (in search for positions where histidine's were enriched histidine) and fabs produced. The peri material (fabs) was tested for pH-dependency on an ELISA setup (see 4-Peri ELISA).

In ELISA, some clones showed pH-dependent target-release, as the OD values were high for condition pH 7.4 but low for condition pH 5.5 (less binding detected). Moreover, sequence analysis showed an enrichment in histidine's in certain positions, but not optimally evident. (Data not shown).

Therefore, it was concluded that there was still too much diversity to correlate the pH-dependent feature to sequence patterns in histidine positions.

Therefore, a further round of selections was performed (R4) with 5 mins CPA elution with or without off-rate wash (for 2 hours) with mouse sushi-2.

Off-rate is the rate at which the peptide (Fab) and the target molecule disassociate from each other. By adding the target molecule in solution, there is a competition for binding of the coated target or the target in solution. Therefore, if the peptide-target complex is not stable and the peptide dissociates from the coated target at any point, it will likely bind to the target in solution instead of showing an on and off binding to the coating and

potentially be bound to the target at the moment of the next washing. Hence, with the off-rate wash, less stable clones are washed away and clone that are more stable are saved. The setup is described in Table 26.

Table 26- Conditions selections R4

Coating (0,1 µg/mL)	Elution buffer	Elution time	Off-rate wash
mouse sushi-2	Trypsin (pH ≈7.4)	20 mins	mouse sushi-2 (1 µg/mL)
			buffer
mouse sushi-2	CPA (pH ≈ 5.5)	5 mins	mouse sushi-2 (1 µg/mL)
			buffer
irrelevant (human C1)	Trypsin (pH ≈7.4)	20 mins	mouse sushi-2 (1 µg/mL)
			buffer
PBS	Trypsin (pH ≈7.4)	20 mins	mouse sushi-2 (1 µg/mL)
			buffer

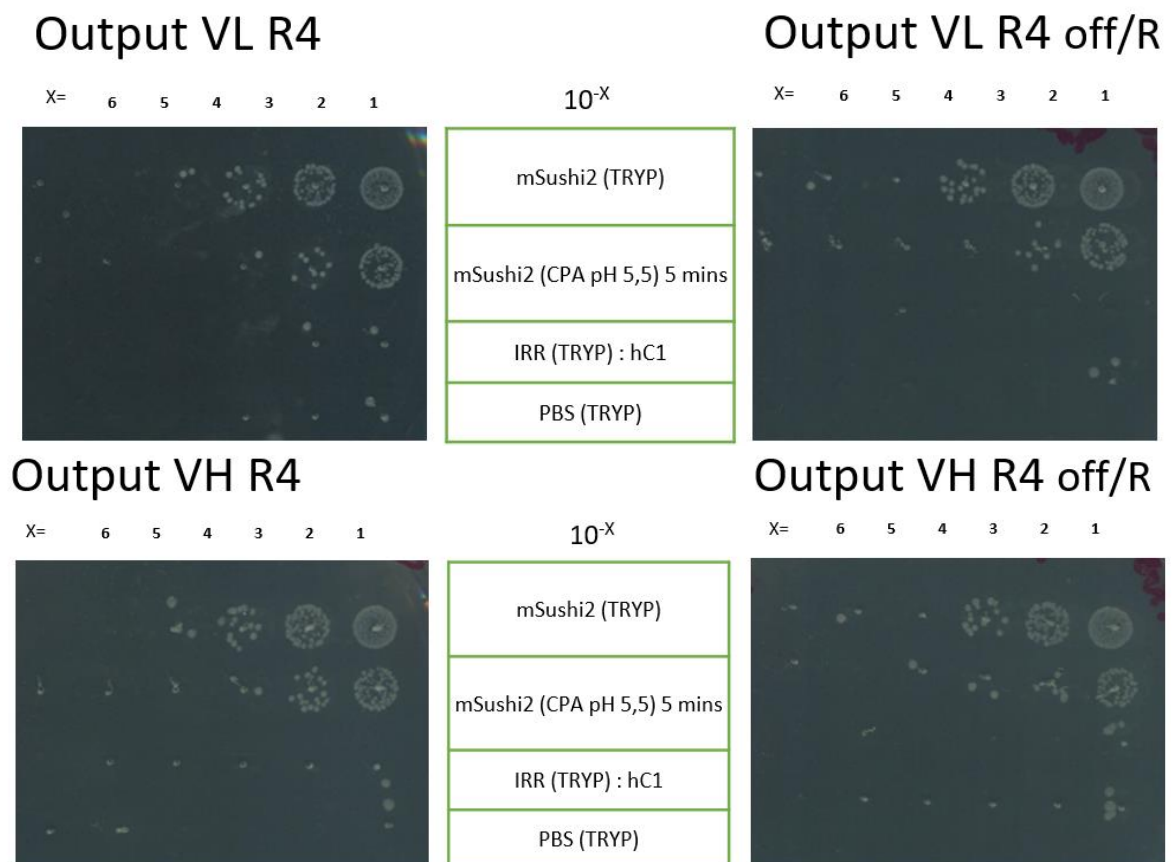


Figure 31-Spotting of the dilution series (from  $10^{-1}$  to  $10^{-6}$ ) of all outputs from Round 4 (R4) of selections, for the conditions with off-rate wash with mouse Sushi2 (right) and without off-rate wash (left), for VL (top) and VH (bottom).

Based on the colonies, a difference from normal condition to off rate was not clear. However, this seemed to happen from Trypsin to CPA elution, suggesting a selection for more potent pH-dependent clones, see Figure 31.

Therefore, 5 minutes CPA elution rescues (with and without off-rate, for VH and VL) were taken, and clones were sequenced and fabs produced and tested on peri ELISA (see 4-Peri ELISA).

## 5-Sequence analysis and peri ELISA

### 5.1-VL

From sequencing results of the clones from 5 minutes CPA elution rescues, a hotspot analysis was performed, via Antibody-Extractor™ v10.0, showing how often a histidine is introduced in a determined position or, in other words, the ratio of clones that present an histidine in each position.

Moreover, from Peri ELISA, the most pH-dependent clones (Figure 32) were selected and a further analysis of their sequence was made, in order to understand where histidine's were introduced (Figure 33, 34, 35).

pH 7,4	pH 5,5	Delta	Clone
2,9459	0,0454	2,9005	50
3,3538	0,0287	3,3251	57
2,9052	0,2874	2,6178	60
2,6957	0,0443	2,6514	71
2,9989	0,9772	2,0217	74
2,9684	0,5209	2,4475	79
2,9017	0,0805	2,8212	87
3,0416	0,9926	2,049	89
2,7853	0,631	2,1543	90
2,2086	0,1968	2,0118	92
2,7455	0,4831	2,2624	95

Figure 32- Optical density (OD 450nm-620nm) of the most pH-dependent clones tested on peri ELISA. The clones represented show the biggest delta/difference between wash at pH 7.4 and wash at pH 5.5 and therefore and considered the most pH-dependent clones.

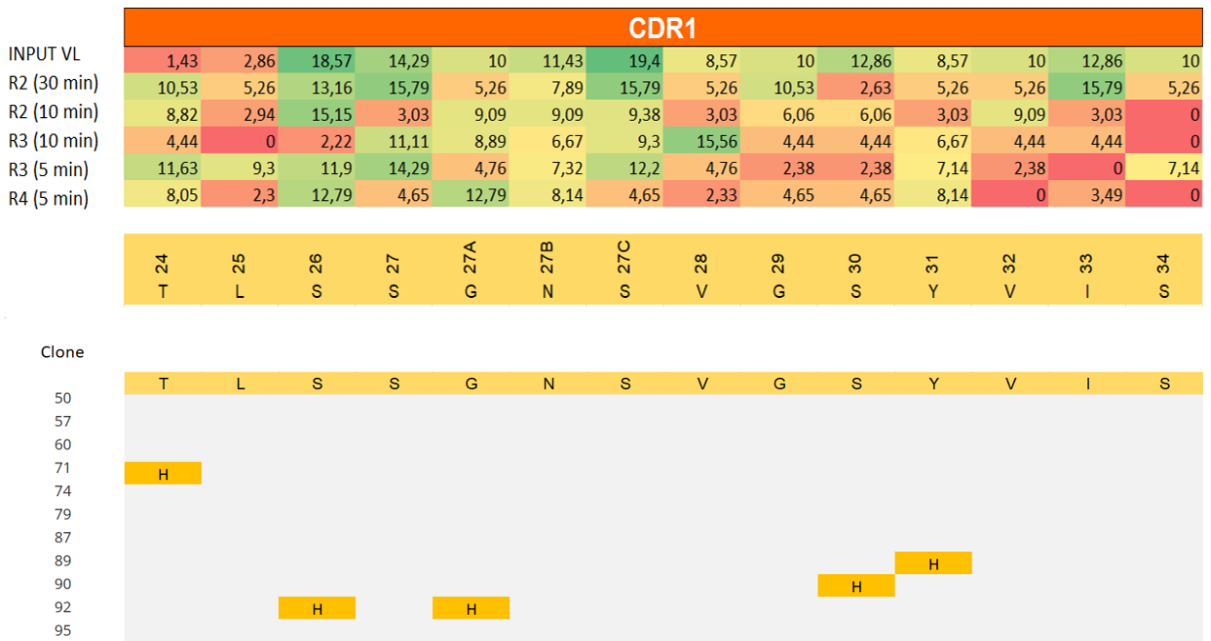


Figure 33- On top, the hotspot analysis (made via Antibody-Extractor™) considering the prevalence of histidine introduction in each position, in all generated clones, throughout the rounds of selection. At the bottom, the sequences, focused on the positions where histidine's were introduced, in the most pH-dependent clones of R4 tested on peri ELISA. Results are regarding VL CDR1.

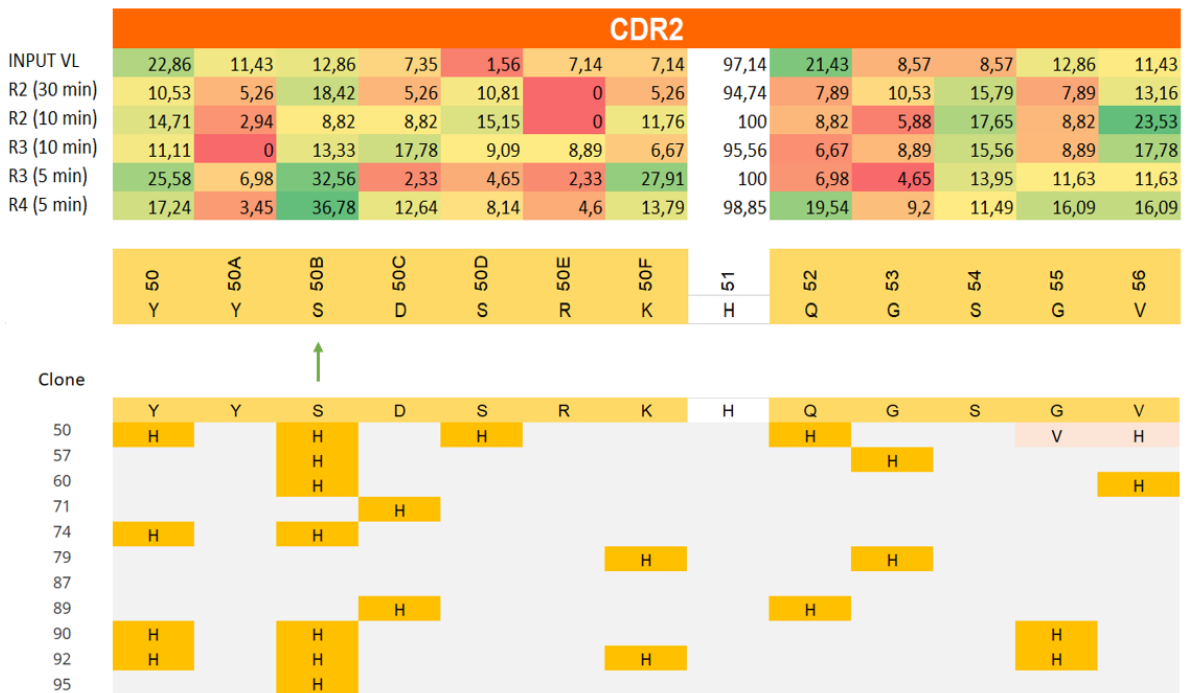


Figure 34- On top, the hotspot analysis (made via Antibody-Extractor™) considering the prevalence of histidine introduction in each position, in all generated clones, throughout the rounds of selection. At the bottom, the sequences, focused on the positions where histidine's were introduced, in the most pH-dependent clones of R4 tested on peri ELISA. Results are regarding VL CDR2. A clear prevalence of histidine in position S50B is visible and in line with data from pH-dependent clones.

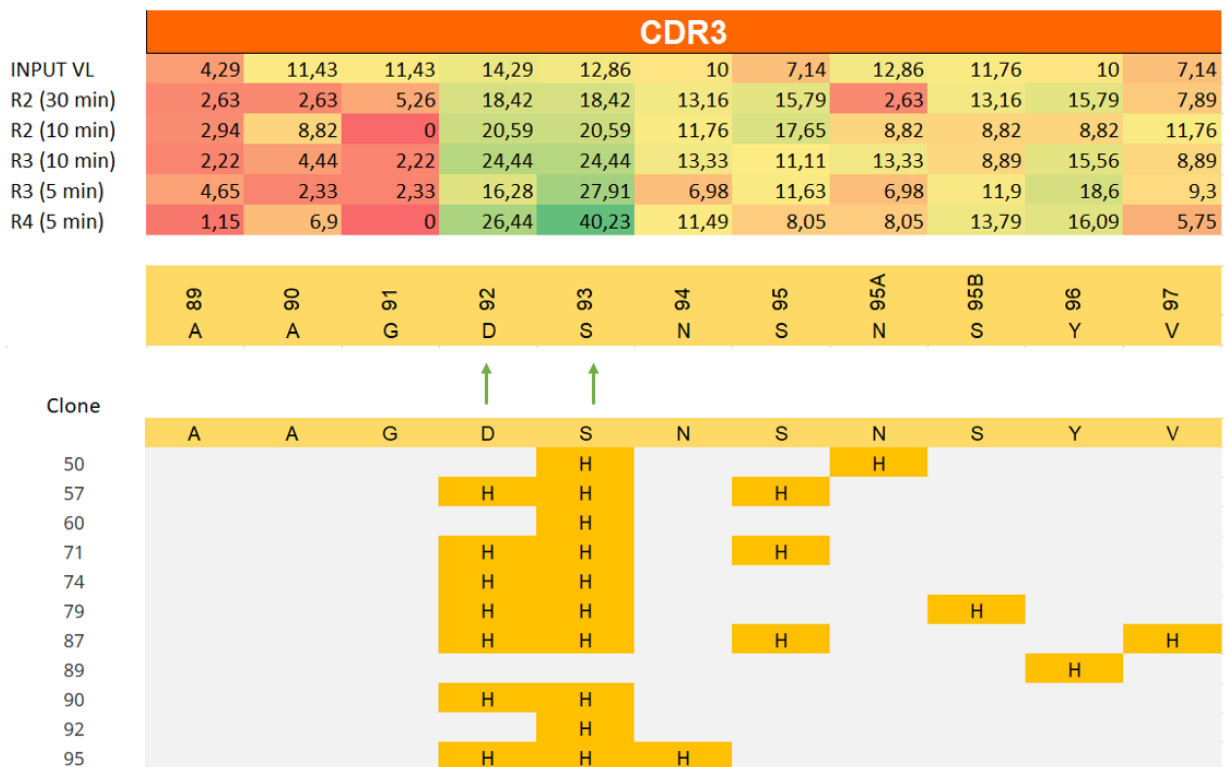


Figure 35- On top, the hotspot analysis (made via Antibody-Extractor™) considering the prevalence of histidine introduction in each position, in all generated clones, throughout the rounds of selection. At the bottom, the sequences, focused on the positions where histidine's were introduced, in the most pH-dependent clones of R4 tested on peri ELISA. Results are regarding VL CDR3. A clear prevalence of histidine in position D92 and D93 is visible and in line with data from pH-dependent clones.

Hotspot analysis of sequences clearly shows that 3 positions (1 in CDR2 and 2 in CDR3) were highly enriched in histidine throughout the selections.

Moreover, the most promising clones found in the peri ELISA show histidine mutations mainly in the same position where the enrichment in sequence analysis (throughout selection rounds) is more visible, demonstrating a strong correlation between different data. This led to the conclusion that the mutation of these positions to a histidine is very likely related to pH-dependency. Therefore, the 3 positions that stand out are: VL\_S50B, VL\_S93 and VL\_D92.

## 5.2-VH

A hotspot analysis was performed from sequencing results of the clones from 5 minutes CPA elution rescues. Next to this, peri ELISA was performed to check the pH dependent binding of different clones to mouse C2. The most pH-dependent clones (Figure 36) were selected and their sequences were in detail analyzed to detect the position where histidine's were introduced (Figure 37, 38, 39).

pH 7,4	pH 5,5	Delta	Clone
2,7698	0,3824	2,3874	49
2,1916	0,0784	2,1132	54
2,3871	0,068	2,3191	55
2,3943	0,2593	2,135	58
2,8673	0,1931	2,6742	59
2,127	0,07	2,057	66
2,7312	0,0592	2,672	76
2,9842	0,9258	2,0584	86
3,3327	0,091	3,2417	89
3,0025	0,092	2,9105	90

Figure 36- Optical density (OD 450nm-620nm) of the most pH-dependent clones tested on peri ELISA. The clones represented show the biggest delta/difference between wash at pH 7.4 and wash at pH 5.5 and therefore and considered the most pH-dependent clones.

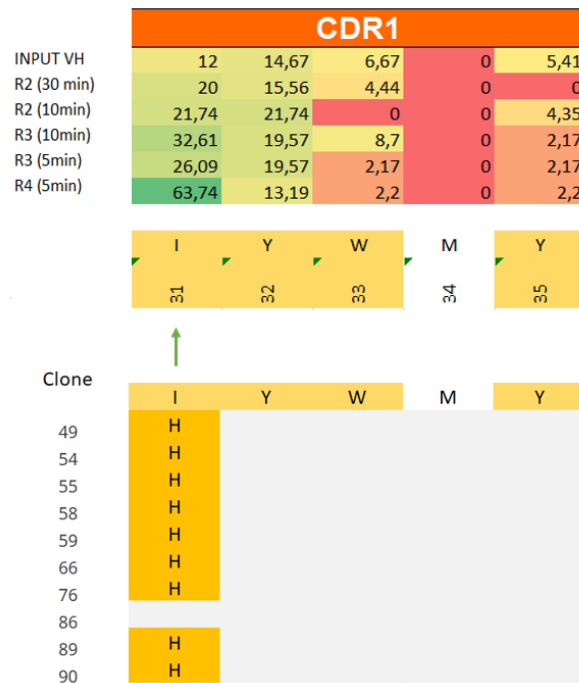


Figure 37-On top, the hotspot analysis (made via Antibody-Extractor™) considering the prevalence of histidine introduction in each position, in all generated clones, throughout the rounds of selection. At the bottom, the sequences, focused on the positions where histidine's were introduced, in the most pH-dependent clones of R4 tested on peri ELISA. Results are regarding VH CDR1. A clear prevalence of histidine in position I30 is visible and in line with data from pH-dependent clones.

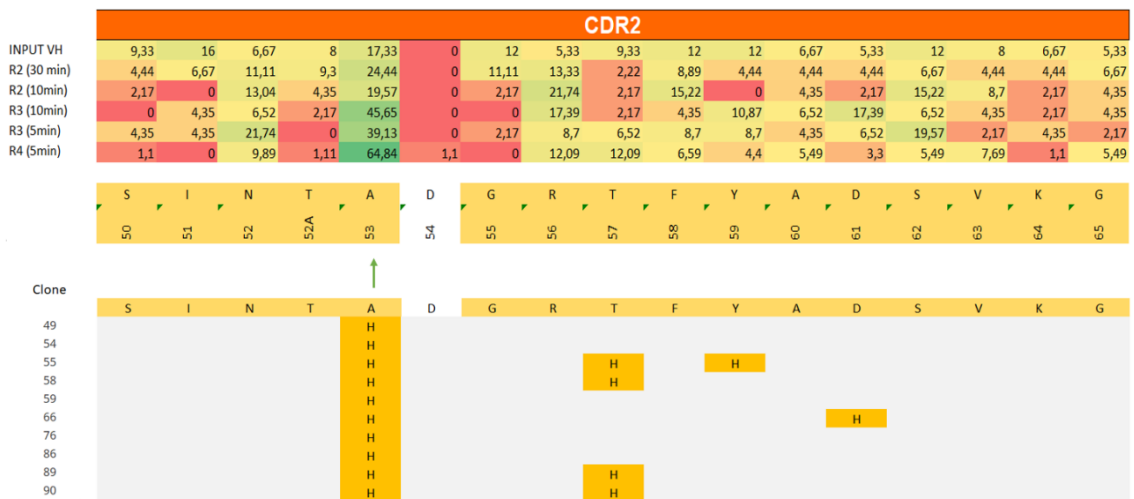


Figure 38- On top, the hotspot analysis (made via Antibody-Extractor™) considering the prevalence of histidine introduction in each position, in all generated clones, throughout the rounds of selection. At the bottom, the sequences, focused on the positions where histidine's were introduced, in the most pH-dependent clones of R4 tested on peri ELISA. Results are regarding VH CDR2. A clear prevalence of histidine in position A53 is visible and in line with data from pH-dependent clones.

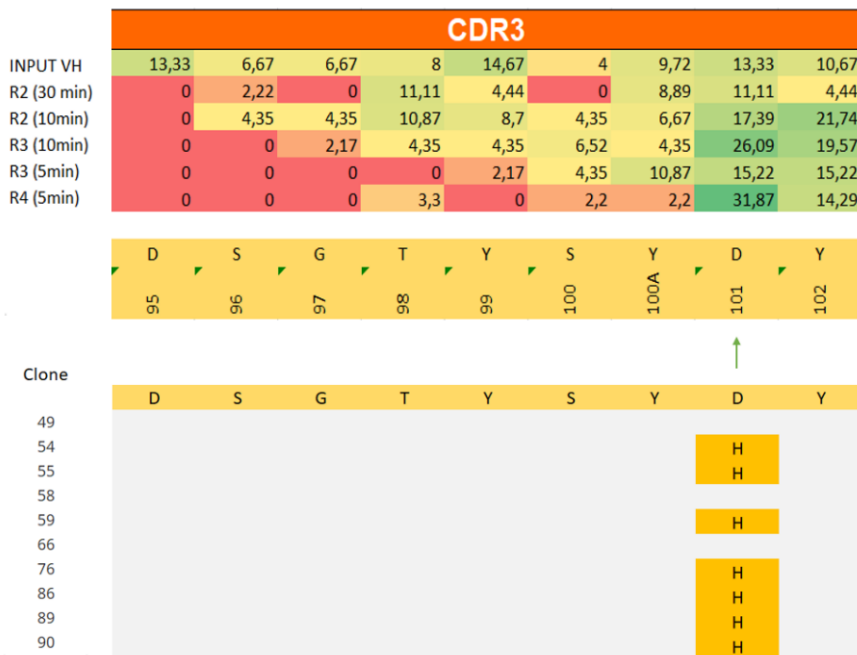


Figure 39- On top, the hotspot analysis (made via Antibody-Extractor™) considering the prevalence of histidine introduction in each position, in all generated clones, throughout the rounds of selection. At the bottom, the sequences, focused on the positions where histidine's were introduced, in the most pH-dependent clones of R4 tested on peri ELISA. Results are regarding VH CDR3. A clear prevalence of histidine in position D101 is visible and in line with data from pH-dependent clones.

For VH the correlation between the hotspot analysis and peri ELISA is even more clear compared to the VL analysis. This hints that the positions where histidine mutation(s) are found, are very likely involved in the introduction of pH-dependency.

The 3 positions that stand out are: VH\_I31, VH\_A53 and VH\_D101.

## 6- Histidine mutations combination analysis

For both chains, a deeper analysis of the sequences of the clones was performed with the goal of detecting associations between the positions and understanding if the mutations tend to be present and act alone or in combination.

### 6.1- VL

Such analysis of frequency and prevalence of combinations, suggested that VL\_S93 and VL\_D92 mutations are often correlated, but less associated with VL\_S50B, which might be involved in pH-dependency through a different point of action. Moreover, these mutations appeared to also be associated with less enriched positions, such as VL\_S50B -VL\_Y50 and VL\_S93-VL\_D92- VL\_S95, which might also affect the target-release at acidic pH.

Therefore, to study the potential interactions of these mutations with each other and the target, an analysis of their location in the predictive structure was performed.

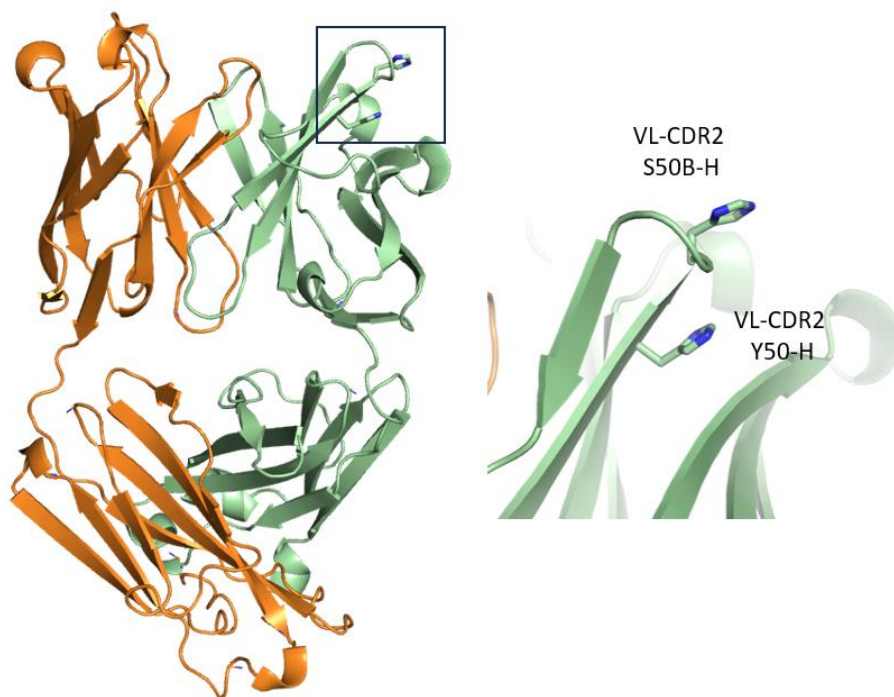


Figure 40- Mutation of VL\_S50B and VL\_Y50 in the predictive crystal structure of 12E08, shows that VL\_S50B is likely involved directly in the binding to the antigen and VL\_Y50 might play a destabilization role that allow a more pH-dependent interaction of mutated VL\_S50B with the target.

The predictive structure showed that VL\_S50B could be projected towards C2 and VL\_Y50 might destabilize the “basis” of the CDR2 loop, allowing the His substitution of VL\_S50B to modulate the binding – both in a pH-dependent fashion. See Figure 40.

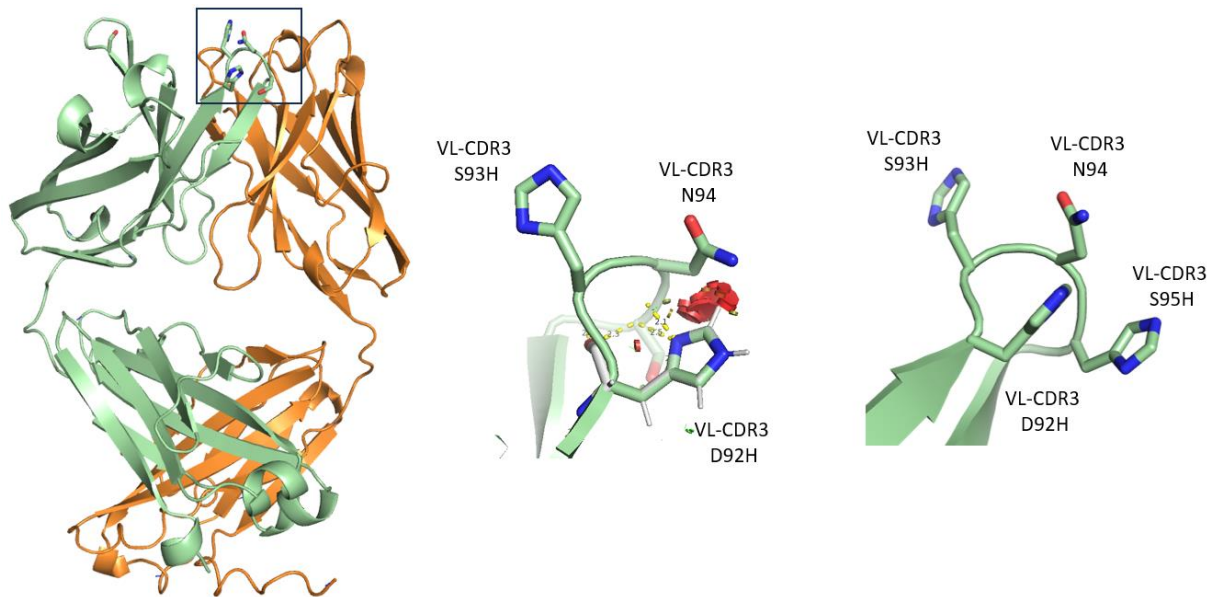


Figure 41- Mutation of VL\_D92 and VL\_S93 in the predictive crystal structure of 12E08, shows that VL\_D92 clashes with a pre-existent aminoacid (N94) and is forced to change its conformation. Such change might allow a better pH-dependent interaction of VL\_S93 to the target. Additionally, as VL\_S95 can stack with the mutated VL\_D92 (combination appears often), it might contribute to a more pH-dependent binding.

Additionally, it was also visualized that the substitution of VL\_D92 to His is not tolerated in the given predicted conformation (clash with CDR3-N94). With the limits of these predictions, this would mean that the loop needs to find a different conformation to bind C2. Possibly, this new conformation would allow binding of C2 by CDR3-S93H, in a pH dependent way (as they appear in combination very often in sequences). Furthermore, substitution of VL\_S95 into His might make this new conformation even more pH dependent, as it can stack with VL-CDR3-His92. See Figure 41.

Therefore, it is suggested that the combinations shown in Table 27 would be the most promising to generate DNA strings and to proceed to mAb production.

Table 27- Potential mutation positions for VL

VL_S50B	Relevant to test individual performance as correlation is less than 75%
VL_S93	
VL_D92	
VL_S93 + VL_D92	Associated with each other
VL_S93 + VL_D92 + VL_S95	The mutation of VL_S95 might increase pH-dependency
VL_S93 + VL_D92 + VL_S50B	Relevant to test, as they are the 3 most relevant positions and the combination of two different sites of action might be of interest

## 6.2- VH

For VH, the analysis was even more straightforward. A high correlation between VH\_I31 and VH\_A53 mutations is visible, with a lower association, although still relevant, with VH\_D101, that does not seem to show any significance when alone.

Once again, an analysis of the locations of these amino acids in the predictive structure was performed.

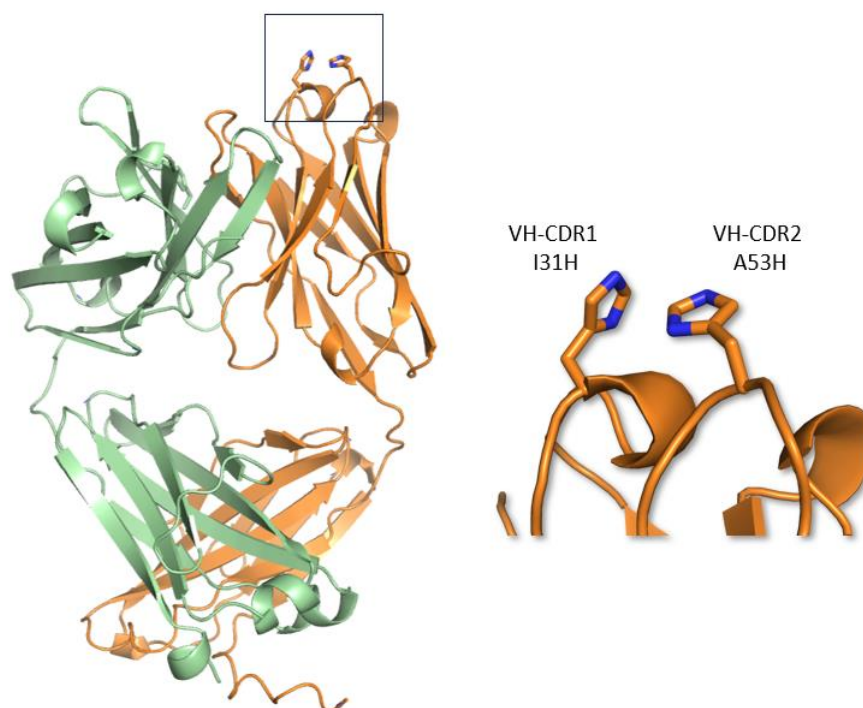


Figure 42- Mutation of VH\_I31 and VH\_A53 in the predictive crystal structure of 12E08, shows that it is possible that both are directly involved in the binding to the target. However, one might act as a support for the most optimal geometry for a pH-dependent binding. Regardless, it is very likely that they work together in a pH-dependent interaction with the antigen.

The predictive structure showed that VH\_I31 and VH\_A53 might work together to bind a single epitope in a pH-dependent fashion or one supports the orientation of binding C2 in an optimal geometry (in a pH dependent way). See Figure 42.

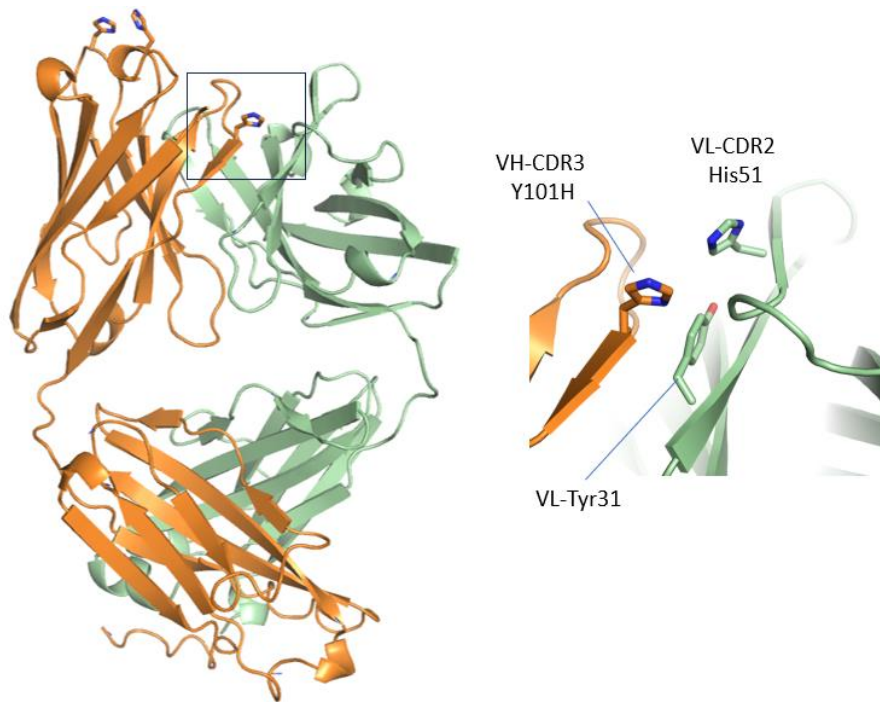


Figure 43- Mutation of VH\_D101 in the predictive crystal structure of 12E08, show that such location is very distant from VH\_I31 + VH\_A53 and, therefore, a direct interaction is unlikely. However, it is possible that the first interaction (VH\_I31 + VH\_A53) creates a destabilization that then allows VH\_D101 to better interact with aminoacids in VL (VL-His51 and VL-Tyr48), creating a destabilization between heavy and light chain and, consequently, leading to a pH-dependent target-release.

Additionally, VH\_I31 + VH\_A53 and VH\_D101 are probably too far apart to have a direct interaction. However, the “instability” of CDR1/2 (VH\_I31 + VH\_A53) might allow the His in CDR3 (VH\_D101) to destabilize the interface between the heavy and light chain, especially through the interaction with VL-His51 (His by default) and VL-Tyr48, and lead to a pH-dependent behavior. See Figure 43.

Therefore, the strings proposed in Table 28 might be the most promising combinations of histidine mutations for VH.

Table 28- Potential mutation positions for VH

VH_I31 + VH_A53	Highly associated, are very like acting together
VH_I31 + VH_A53 + VH_D101	Relevant to test to understand the role of VH_D101

# Discussion

The engineering of antibodies for a pH-dependent target release feature has been an important matter and source of great interest for the development of therapeutic mAbs with a longer half-life. In this dissertation, two approaches for the introduction pH-dependency via histidine engineering were studied: structure-based single mutations and combinatorial mutagenesis libraries.

The introduction of single histidine mutations based on the predictive model of the crystal structure of 12E08 did not lead to the generation of antibodies with the features of interest, which might be explained by several factors.

On one hand, the rationale behind the introduction of histidine relies on the generation of a positively charged region that can lead to a repulsive interaction and destabilization of the antibody-antigen complex. In that line, obtained data suggests that the introduction of a single histidine mutation is not enough to generate such destabilization and lead to antigen release at acidic pH and, most likely, a collaborative work of histidine mutations is necessary.

Moreover, the selection of positions for histidine introduction was grounded on a predictive model of 12E08 based on amino acid sequence. The model might have not accurately represented the molecule and might have led to a wrongful selection of positions, that was grounded on the conformation and spatial position of the aminoacids.

Nevertheless, two antibodies were generated (mab117\_83 and mab117\_87) that show a slight pH dependent behavior, corroborating the potential effect of histidine mutations in pH-dependency. However, these antibodies also showed a decrease in binding ability and a highly compromised functionality.

This correlation of histidine introduction and binding loss became even clearer when combinations of histidine were tested, showing that the introduction of multiple histidine's can also highly impact binding.

However, it was still believed that upon the discovery of relevant combinations, a pH-dependent target release through histidine mutations was possible.

Therefore, the combinatorial mutagenesis libraries represented a promising alternative, as a very broad range of potential histidine combinations can be assessed. In this work, phage display was used to select for the combinations implicated in pH-dependency.

It is important to note that the assessment of pH-dependent clones (obtained after phage display) was performed using Fabs in periplasmic material, simply because it is a faster alternative to produce and pre-screen a variety of clones. However, this material can present various impurities that can affect the accuracy of readouts. For that reason, full mAb characterization would have provided more reliable and precise data and conclusions.

Nonetheless, the data generated from the combinatorial histidine libraries was highly intriguing, showing a tight correlation between the positions where histidine's were introduced in the most relevant pH-dependent clones (tested on binding ELISA) and the positions where the enrichment of histidine's throughout selections was undoubtedly visible (VL\_S50B, VL\_S93, VL\_D92 for VL and VH\_I31, VH\_A53, VH\_D101 for VH).

It is relevant to mention that such correlation is more noticeable for VH than for VL. This is not surprising, as it is expected that VL plays a less crucial role in pH dependency (VL is not as involved in antibody-antigen interaction as VH). Therefore, mutations in VH are more likely to be relevant for a pH-dependent target release behavior.

Regardless, data suggests promising mutation sites for both chains. Results demonstrate a clear alignment between hotspot analysis, pH-dependent clones tested on peri ELISA and information from the predictive structure. Therefore, there is relevant evidence, hinting to specific (combinations of) histidine mutations that are likely involved in the introduction of a pH-dependent target release and should be used to proceed further development.

Moving forward to full mAb production with the proposed DNA strings, the question about the most relevant backbone for these full antibodies comes up. For a mouse model, the most interesting backbone would be a mouse IgG. Potentially mouse IgG 2b as it is common between the two main mouse strains of interest (BALB/c and C57BL/6).

However, it is difficult to measure the pharmacokinetic characteristics of a mouse antibody in mouse serum, as the therapeutic molecule cannot be discerned from the other antibodies in circulation. A human backbone would be an interesting choice, as this does

allow the study of the pharmacokinetic profile of the molecule in mice. However, a bigger immunogenicity can be expected.

Similarly to the structure-based mutants generated, FcD mutations would be important for a minimal effector function of the Fc region. Additionally, an enhanced FcRn affinity would be interesting to prolong the molecule's half-life in circulation, particularly when associated with the introduced pH-dependent target-release, as it would mimic the ARGX-117 mode of action the best.

However, NHance™ mutations in a mouse backbone or human backbone when injected in mice, lead to a constitutive blockage of FcRn, at both acidic and neutral pH, while NHance™ mutations normally increase the affinity to FcRn at acidic pH for a better rescue of the antibody from lysosomal degradation. In this situation, constitutive blockage makes it harder for the antibody to go back into circulation, which might compromise the capture of antigen as the target is a circulatory molecule (C2).

Therefore, mutations for a mouse backbone that have the same function as NHance™ in a human backbone would have to be assessed.

Another factor of research should be the study of combinations of VH mutations and VL mutations to understand if the pH-dependency can be further increased upon the combination of two histidine-mutant chains without affinity loss.

The next steps should be a full characterization of the generated antibodies in C2 binding, CP and MSD assays and proceed with the most promising molecules to *in vivo* studies in mice for a full PK/PD profile study.

Cross-reactivity with human should also be tested. 12E08 is known to be cross reactive with human, but does not show the same affinity and blocking capacity of human C2 as ARGX-117. However, the pH-dependent 12E08 variant might however show a different profile and might be better than ARGX-117.

Overall, combinatorial histidine mutagenesis libraries and consequent phage display proved to be a powerful tool for introduction of pH-dependent target release. The data generated provides interesting insights regarding the most implicated positions in such feature as well as the most promising combinations of mutations.

Therefore, with this thesis, important hints were revealed towards the development of a full pH-dependent mouse C2-blocking antibody that can be used for accurate *in vivo* studies in mice, allowing the search for new potential indications.

# References

- AKBAR, Rahmad *et al.* - A compact vocabulary of paratope-epitope interactions enables predictability of antibody-antigen binding. **Cell Reports**. . ISSN 22111247. 34:11 (2021) 108856. doi: 10.1016/j.celrep.2021.108856.
- AMENDT, Timm *et al.* - Primary Immune Responses and Affinity Maturation Are Controlled by IgD. **Frontiers in Immunology**. . ISSN 1664-3224. 12:2021). doi: 10.3389/fimmu.2021.709240.
- Antibody Diversity - Em **Immunology for Pharmacy** [Em linha]. [S.l.] : Elsevier, 2012 Disponível em WWW:<URL:https://linkinghub.elsevier.com/retrieve/pii/B9780323069472100100>. p. 79–86.
- BACKHAUS, Oliver - Generation of Antibody Diversity. Em **Antibody Engineering**. [S.l.] : InTech, 2018
- BANDA, Nirmal K. *et al.* - Essential Role of Complement Mannose-Binding Lectin-Associated Serine Proteases-1/3 in the Murine Collagen Antibody-Induced Model of Inflammatory Arthritis. **The Journal of Immunology**. . ISSN 0022-1767. 185:9 (2010) 5598–5606. doi: 10.4049/jimmunol.1001564.
- BANIN, Ehud; BRADY, Keith M.; GREENBERG, E. Peter - Chelator-Induced Dispersal and Killing of *Pseudomonas aeruginosa* Cells in a Biofilm. **Applied and Environmental Microbiology**. . ISSN 0099-2240. 72:3 (2006) 2064–2069. doi: 10.1128/AEM.72.3.2064-2069.2006.
- BOES, Marianne - Role of natural and immune IgM antibodies in immune responses. **Molecular Immunology**. . ISSN 01615890. 37:18 (2000) 1141–1149. doi: 10.1016/S0161-5890(01)00025-6.
- BURNET, F. M. - **The clonal selection theory of acquired immunity**. Nashville : Vanderbilt University Press, 1959
- CAVALLO, Federica; CALOGERO, Raffaele Adolfo; FORNI, Guido - Are oncoantigens suitable targets for anti-tumour therapy? **Nature Reviews Cancer**. . ISSN 1474-175X. 7:9 (2007) 707–713. doi: 10.1038/nrc2208.
- CHASTEEN, L. *et al.* - Eliminating helper phage from phage display. **Nucleic Acids Research**. . ISSN 0305-1048. 34:21 (2006) e145–e145. doi: 10.1093/nar/gkl772.
- CHEN, Ce-Belle; WALLIS, Russell - Stoichiometry of Complexes between Mannose-binding Protein and Its Associated Serine Proteases. **Journal of Biological Chemistry**. . ISSN 00219258. 276:28 (2001) 25894–25902. doi: 10.1074/jbc.M103539200.
- CHIU, Mark L. *et al.* - Antibody Structure and Function: The Basis for Engineering Therapeutics. **Antibodies**. . ISSN 2073-4468. 8:4 (2019) 55. doi: 10.3390/antib8040055.
- CHIU, Mark L.; GILLILAND, Gary L. - Engineering antibody therapeutics. **Current Opinion in Structural Biology**. . ISSN 0959440X. 38:2016) 163–173. doi: 10.1016/j.sbi.2016.07.012.
- Complement Inhibitors as Therapeutic Agents** - , atual. 11 jul. 2022.
- COOK, H. Terence; BOTTO, Marina - Mechanisms of Disease: the complement system and the pathogenesis of systemic lupus erythematosus. **Nature Clinical Practice Rheumatology**. . ISSN 1745-8382. 2:6 (2006) 330–337. doi: 10.1038/ncprheum0191.
- DEVANABOYINA, Siva Charan *et al.* - The effect of pH dependence of antibody-antigen interactions on subcellular trafficking dynamics. **mAbs**. . ISSN 1942-0862. 5:6 (2013) 851–859. doi: 10.4161/mabs.26389.

DUNCAN, Alexander R.; WINTER, Greg - The binding site for C1q on IgG. **Nature**. . ISSN 0028-0836. 332:6166 (1988) 738–740. doi: 10.1038/332738a0.

FERRARA, Napoleone *et al.* - Targeting VEGF-A to Treat Cancer and Age-Related Macular Degeneration. **Annual Review of Medicine**. . ISSN 0066-4219. 58:1 (2007) 491–504. doi: 10.1146/annurev.med.58.061705.145635.

FIGUEROA, J. E.; DENSEN, P. - Infectious diseases associated with complement deficiencies. **Clinical Microbiology Reviews**. . ISSN 0893-8512. 4:3 (1991) 359–395. doi: 10.1128/CMR.4.3.359.

FRASER, D.; TENNER, A. - Directing an Appropriate Immune Response: The Role of Defense Collagens and other Soluble Pattern Recognition Molecules. **Current Drug Targets**. . ISSN 13894501. 9:2 (2008) 113–122. doi: 10.2174/138945008783502476.

FRAZER-ABEL, A. *et al.* - Overview of Laboratory Testing and Clinical Presentations of Complement Deficiencies and Dysregulation. *Em* . p. 1–75.

GALVAN, M. D.; GREENLEE-WACKER, M. C.; BOHLSON, S. S. - C1q and phagocytosis: the perfect complement to a good meal. **Journal of Leukocyte Biology**. . ISSN 0741-5400. 92:3 (2012) 489–497. doi: 10.1189/jlb.0212099.

GARRED, Peter; TENNER, Andrea J.; MOLLNES, Tom E. - Therapeutic Targeting of the Complement System: From Rare Diseases to Pandemics. **Pharmacological Reviews**. . ISSN 0031-6997. 73:2 (2021) 792–827. doi: 10.1124/pharmrev.120.000072.

GEARHART, Patricia J. - The roots of antibody diversity. **Nature**. . ISSN 0028-0836. 419:6902 (2002) 29–31. doi: 10.1038/419029a.

GEIST, Brian; ZHENG, Songmao; XU, Yan - Therapeutic antibody development—Remington chapter. *Em Remington*. [S.l.] : Elsevier, 2021. p. 437–462.

GRUMACH, Anete Sevciovic; KIRSCHFINK, Michael - Are complement deficiencies really rare? Overview on prevalence, clinical importance and modern diagnostic approach. **Molecular Immunology**. . ISSN 01615890. 61:2 (2014) 110–117. doi: 10.1016/j.molimm.2014.06.030.

HADDERS, Michael A. *et al.* - Assembly and Regulation of the Membrane Attack Complex Based on Structures of C5b6 and sC5b9. **Cell Reports**. . ISSN 22111247. 1:3 (2012) 200–207. doi: 10.1016/j.celrep.2012.02.003.

HAHN, Andrew W. *et al.* - The future of immune checkpoint cancer therapy after PD-1 and CTLA-4. **Immunotherapy**. . ISSN 1750-743X. 9:8 (2017) 681–692. doi: 10.2217/imt-2017-0024.

HARBOE, Morten; MOLLNES, Tom Eirik - The alternative complement pathway revisited. **Journal of Cellular and Molecular Medicine**. . ISSN 15821838. 12:4 (2008) 1074–1084. doi: 10.1111/j.1582-4934.2008.00350.x.

HARRIS, Claire L. - Expanding horizons in complement drug discovery: challenges and emerging strategies. **Seminars in Immunopathology**. . ISSN 1863-2297. 40:1 (2018) 125–140. doi: 10.1007/s00281-017-0655-8.

HINTON, Paul R. *et al.* - Engineered Human IgG Antibodies with Longer Serum Half-lives in Primates. **Journal of Biological Chemistry**. . ISSN 00219258. 279:8 (2004) 6213–6216. doi: 10.1074/jbc.C300470200.

- IGAWA, T. *et al.* - Reduced elimination of IgG antibodies by engineering the variable region. **Protein Engineering Design and Selection**. . ISSN 1741-0126. 23:5 (2010) 385–392. doi: 10.1093/protein/gzq009.
- IGAWA, T.; MIMOTO, F.; HATTORI, K. - pH-dependent antigen-binding antibodies as a novel therapeutic modality. **Biochimica et Biophysica Acta (BBA) - Proteins and Proteomics**. . ISSN 15709639. 1844:11 (2014) 1943–1950. doi: 10.1016/j.bbapap.2014.08.003.
- IGAWA, T.; MIMOTO, F.; HATTORI, K. - pH-dependent antigen-binding antibodies as a novel therapeutic modality. **Biochimica et Biophysica Acta (BBA) - Proteins and Proteomics**. . ISSN 15709639. 1844:11 (2014) 1943–1950. doi: 10.1016/j.bbapap.2014.08.003.
- IGAWA, Tomoyuki *et al.* - Engineered Monoclonal Antibody with Novel Antigen-Sweeping Activity In Vivo. **PLoS ONE**. . ISSN 1932-6203. 8:5 (2013) e63236. doi: 10.1371/journal.pone.0063236.
- INBAR, Dan; HOCHMAN, Jacob; GIVOL, David - Localization of Antibody-Combining Sites within the Variable Portions of Heavy and Light Chains. **Proceedings of the National Academy of Sciences**. . ISSN 0027-8424. 69:9 (1972) 2659–2662. doi: 10.1073/pnas.69.9.2659.
- ITO, Wataru *et al.* - The His-probe method: Effects of histidine residues introduced into the complementarity-determining regions of antibodies on antigen-antibody interactions at different pH values. **FEBS Letters**. . ISSN 00145793. 309:1 (1992) 85–88. doi: 10.1016/0014-5793(92)80745-3.
- JAMES, K. - Complement: activation, consequences, and control. **The American journal of medical technology**. . ISSN 0002-9335. 48:9 (1982) 735–42.
- JANEWAY CA JR, Travers P, Walport M, Et Al. - **Immunobiology: The Immune System in Health and Disease**. 5th edition ed. New York : Garland Science, 2001
- JOHNSON, John B.; CAPRARO, Gerald A.; PARKS, Griffith D. - Differential mechanisms of complement-mediated neutralization of the closely related paramyxoviruses simian virus 5 and mumps virus. **Virology**. . ISSN 00426822. 376:1 (2008) 112–123. doi: 10.1016/j.virol.2008.03.022.
- KISHORE, Uday *et al.* - Structural and functional anatomy of the globular domain of complement protein C1q. **Immunology Letters**. . ISSN 01652478. 95:2 (2004) 113–128. doi: 10.1016/j.imlet.2004.06.015.
- KLAUS, Tomasz; DESHMUKH, Sameer - pH-responsive antibodies for therapeutic applications. **Journal of Biomedical Science**. . ISSN 1423-0127. 28:1 (2021) 11. doi: 10.1186/s12929-021-00709-7.
- KÖHLER, G.; MILSTEIN, C. - Continuous cultures of fused cells secreting antibody of predefined specificity. **Nature**. . ISSN 0028-0836. 256:5517 (1975) 495–497. doi: 10.1038/256495a0.
- KOLEV, Martin; KEMPER, Claudia - Keeping It All Going—Complement Meets Metabolism. **Frontiers in Immunology**. . ISSN 1664-3224. 8:2017). doi: 10.3389/fimmu.2017.00001.
- LAUGHLIN, Tosha M.; HORN, James R. - Engineering pH-Sensitive Single-Domain Antibodies. *Em* . p. 269–298.
- LI, Yue; JIN, Liang; CHEN, Tongxin - The Effects of Secretory IgA in the Mucosal Immune System. **BioMed Research International**. . ISSN 2314-6133. 2020:2020) 1–6. doi: 10.1155/2020/2032057.
- LIAO, Si-Ming *et al.* - The multiple roles of histidine in protein interactions. **Chemistry Central Journal**. . ISSN 1752-153X. 7:1 (2013) 44. doi: 10.1186/1752-153X-7-44.
- LO, Kin-Ming; LEGER, Olivier; HOCK, Björn - Antibody Engineering. **Microbiology Spectrum**. . ISSN 2165-0497. 2:1 (2014). doi: 10.1128/microbiolspec.AID-0007-12.

- LUTZ, Hans U.; JELEZAROVA, Emiliana - Complement amplification revisited. **Molecular Immunology**. . ISSN 01615890. 43:1–2 (2006) 2–12. doi: 10.1016/j.molimm.2005.06.020.
- MANNE, Kartik; NARAYANA, Sthanam V. L. - C2. Em **The Complement FactsBook**. [S.l.] : Elsevier, 2018. p. 127–134.
- MARTIN, W. Lance *et al.* - Crystal Structure at 2.8 Å of an FcRn/Heterodimeric Fc Complex. **Molecular Cell**. . ISSN 10972765. 7:4 (2001) 867–877. doi: 10.1016/S1097-2765(01)00230-1.
- MASTELLOS, Dimitrios C.; RICKLIN, Daniel; LAMBRIS, John D. - Clinical promise of next-generation complement therapeutics. **Nature Reviews Drug Discovery**. . ISSN 1474-1776. 18:9 (2019) 707–729. doi: 10.1038/s41573-019-0031-6.
- MAYES, Patrick A.; HANCE, Kenneth W.; HOOS, Axel - The promise and challenges of immune agonist antibody development in cancer. **Nature Reviews Drug Discovery**. . ISSN 1474-1776. 17:7 (2018) 509–527. doi: 10.1038/nrd.2018.75.
- MOULD, Diane R.; MEIBOHM, Bernd - Drug Development of Therapeutic Monoclonal Antibodies. **BioDrugs**. . ISSN 1173-8804. 30:4 (2016) 275–293. doi: 10.1007/s40259-016-0181-6.
- MUKAI, Kaori *et al.* - IgE and mast cells in host defense against parasites and venoms. **Seminars in Immunopathology**. . ISSN 1863-2297. 38:5 (2016) 581–603. doi: 10.1007/s00281-016-0565-1.
- MURTAUGH, Megan L. *et al.* - A combinatorial histidine scanning library approach to engineer highly pH-dependent protein switches. **Protein Science**. . ISSN 09618368. 20:9 (2011) 1619–1631. doi: 10.1002/pro.696.
- NIMMERJAHN, Falk; RAVETCH, Jeffrey V. - Fcγ receptors as regulators of immune responses. **Nature Reviews Immunology**. . ISSN 1474-1733. 8:1 (2008) 34–47. doi: 10.1038/nri2206.
- PANDE, Jyoti; SZEWCZYK, Magdalena M.; GROVER, Ashok K. - Phage display: Concept, innovations, applications and future. **Biotechnology Advances**. . ISSN 07349750. 28:6 (2010) 849–858. doi: 10.1016/j.biotechadv.2010.07.004.
- PANGBURN, M. K.; SCHREIBER, R. D.; MÜLLER-EBERHARD, H. J. - Formation of the initial C3 convertase of the alternative complement pathway. Acquisition of C3b-like activities by spontaneous hydrolysis of the putative thioester in native C3. **Journal of Experimental Medicine**. . ISSN 0022-1007. 154:3 (1981) 856–867. doi: 10.1084/jem.154.3.856.
- PICKERING, M. C. *et al.* - Systemic Lupus Erythematosus, Complement Deficiency, and Apoptosis. Em . p. 227–324.
- PODACK, E. R. - Molecular composition of the tubular structure of the membrane attack complex of complement. **Journal of Biological Chemistry**. . ISSN 00219258. 259:13 (1984) 8641–8647. doi: 10.1016/S0021-9258(17)39778-8.
- PREZ, R. M. DES *et al.* - Function of the Classical and Alternate Pathways of Human Complement in Serum Treated with Ethylene Glycol Tetraacetic Acid and MgCl<sub>2</sub> -Ethylene Glycol Tetraacetic Acid. **Infection and Immunity**. . ISSN 0019-9567. 11:6 (1975) 1235–1243. doi: 10.1128/iai.11.6.1235-1243.1975.
- RICKLIN, Daniel *et al.* - Complement: a key system for immune surveillance and homeostasis. **Nature Immunology**. . ISSN 1529-2908. 11:9 (2010) 785–797. doi: 10.1038/ni.1923.

- RICKLIN, Daniel; REIS, Edimara S.; LAMBRIS, John D. - Complement in disease: a defence system turning offensive. **Nature Reviews Nephrology**. . ISSN 1759-5061. 12:7 (2016) 383–401. doi: 10.1038/nrneph.2016.70.
- RODEWALD, R. - pH-dependent binding of immunoglobulins to intestinal cells of the neonatal rat. **Journal of Cell Biology**. . ISSN 0021-9525. 71:2 (1976) 666–669. doi: 10.1083/jcb.71.2.666.
- ROOIJAKKERS, Suzan H. M. *et al.* - Structural and functional implications of the alternative complement pathway C3 convertase stabilized by a staphylococcal inhibitor. **Nature Immunology**. . ISSN 1529-2908. 10:7 (2009) 721–727. doi: 10.1038/ni.1756.
- ROOPENIAN, Derry C.; AKILESH, Shreeram - FcRn: the neonatal Fc receptor comes of age. **Nature Reviews Immunology**. . ISSN 1474-1733. 7:9 (2007) 715–725. doi: 10.1038/nri2155.
- ROTHER, Russell P. *et al.* - Discovery and development of the complement inhibitor eculizumab for the treatment of paroxysmal nocturnal hemoglobinuria. **Nature Biotechnology**. . ISSN 1087-0156. 25:11 (2007) 1256–1264. doi: 10.1038/nbt1344.
- RYMAN, Josiah T.; MEIBOHM, Bernd - Pharmacokinetics of Monoclonal Antibodies. **CPT: Pharmacometrics & Systems Pharmacology**. . ISSN 21638306. 6:9 (2017) 576–588. doi: 10.1002/psp4.12224.
- SATHE, Abha; CUSICK, John K. - **Biochemistry, Immunoglobulin M**
- SCHRÖTER, Christian *et al.* - A generic approach to engineer antibody pH-switches using combinatorial histidine scanning libraries and yeast display. **mAbs**. . ISSN 1942-0862. 7:1 (2015) 138–151. doi: 10.4161/19420862.2014.985993.
- SHEETS, Michael D. *et al.* - Efficient construction of a large nonimmune phage antibody library: The production of high-affinity human single-chain antibodies to protein antigens. **Proceedings of the National Academy of Sciences**. . ISSN 0027-8424. 95:11 (1998) 6157–6162. doi: 10.1073/pnas.95.11.6157.
- SHEN, Chang-Hui - Gene Expression: Translation of the Genetic Code. Em **Diagnostic Molecular Biology**. [S.l.] : Elsevier, 2019. p. 87–116.
- SJÖHOLM, A. G. *et al.* - Complement deficiency and disease: An update. **Molecular Immunology**. . ISSN 01615890. 43:1–2 (2006) 78–85. doi: 10.1016/j.molimm.2005.06.025.
- SOCIÉ, Gérard *et al.* - Eculizumab in paroxysmal nocturnal haemoglobinuria and atypical haemolytic uraemic syndrome: 10-year pharmacovigilance analysis. **British Journal of Haematology**. . ISSN 0007-1048. 185:2 (2019) 297–310. doi: 10.1111/bjh.15790.
- TAEYE, Steven W. DE; RISPENS, Theo; VIDARSSON, Gestur - The Ligands for Human IgG and Their Effector Functions. **Antibodies**. . ISSN 2073-4468. 8:2 (2019) 30. doi: 10.3390/antib8020030.
- TANGE, Clare Elizabeth *et al.* - Quantification of human complement C2 protein using an automated turbidimetric immunoassay. **Clinical Chemistry and Laboratory Medicine (CCLM)**. . ISSN 1437-4331. 56:9 (2018) 1498–1506. doi: 10.1515/cclm-2017-1068.
- TONEGAWA, Susumu - Somatic generation of antibody diversity. **Nature**. . ISSN 0028-0836. 302:5909 (1983) 575–581. doi: 10.1038/302575a0.
- VAUGHN, Daniel E.; BJORKMAN, Pamela J. - Structural basis of pH-dependent antibody binding by the neonatal Fc receptor. **Structure**. . ISSN 09692126. 6:1 (1998) 63–73. doi: 10.1016/S0969-2126(98)00008-2.

VIDARSSON, Gestur; DEKKERS, Gillian; RISPENS, Theo - IgG Subclasses and Allotypes: From Structure to Effector Functions. **Frontiers in Immunology**. . ISSN 1664-3224. 5:2014). doi: 10.3389/fimmu.2014.00520.

VLAM, Lotte *et al.* - Complement activity is associated with disease severity in multifocal motor neuropathy. **Neurology - Neuroimmunology Neuroinflammation**. . ISSN 2332-7812. 2:4 (2015) e119. doi: 10.1212/NXI.000000000000119.

VLAM, Lotte *et al.* - Complement activity is associated with disease severity in multifocal motor neuropathy. **Neurology - Neuroimmunology Neuroinflammation**. . ISSN 2332-7812. 2:4 (2015) e119. doi: 10.1212/NXI.000000000000119.

WALLE, Inge VAN DE *et al.* - ARGX-117, a therapeutic complement inhibiting antibody targeting C2. **Journal of Allergy and Clinical Immunology**. . ISSN 00916749. 147:4 (2021) 1420-1429.e7. doi: 10.1016/j.jaci.2020.08.028.

WONG, Edwin K. S.; GOODSHIP, Tim H. J.; KAVANAGH, David - Complement therapy in atypical haemolytic uraemic syndrome (aHUS). **Molecular Immunology**. . ISSN 01615890. 56:3 (2013) 199–212. doi: 10.1016/j.molimm.2013.05.224.

WURM, Florian M. - Production of recombinant protein therapeutics in cultivated mammalian cells. **Nature Biotechnology**. . ISSN 1087-0156. 22:11 (2004) 1393–1398. doi: 10.1038/nbt1026.

YÉLAMOS, José - Current innovative engineered antibodies. Em [Em linha] Disponível em WWW:<URL:<https://linkinghub.elsevier.com/retrieve/pii/S1937644822000284>>. p. 1–43.

ZAFIR-LAVIE, I.; MICHAELI, Y.; REITER, Y. - Novel antibodies as anticancer agents. **Oncogene**. . ISSN 0950-9232. 26:25 (2007) 3714–3733. doi: 10.1038/sj.onc.1210372.

# Appendix

## PCR clean-up, gel extraction

Protocol at a glance (Rev. 08)

	PCR clean-up	Gel extraction	DNA clean-up (with SDS)	Single stranded DNA clean-up
<p><b>1</b> <u>PCR clean-up, DNA clean-up, or single stranded DNA clean-up:</u> Adjust binding condition</p> <p><u>Gel extraction:</u> Excise DNA fragment/ solubilize gel slice</p>		 		
	200 µL NT1/ 100 µL PCR	200 µL NT1/ 100 mg gel  50 °C 5–10 min	500 µL NTB/ 100 µL sample	200 µL NTC/ 100 µL sample
<b>2</b> Bind DNA			11,000 x g 30 s	
<b>3</b> Wash silica membrane			700 µL NT3  11,000 x g 30 s  <u>Recommended:</u> 2 <sup>nd</sup> wash  700 µL NT3  11,000 x g 30 s	
<b>4</b> Dry silica membrane			11,000 x g 1 min	
<b>5</b> Elute DNA			15–30 µL NE  RT 1 min  11,000 x g 1 min	

## Plasmid DNA purification (NucleoBond® Xtra Midi / Maxi) Protocol at a glance (Rev. 17)

	Midi		Maxi	
1–3 Cultivation and harvest	4,500–6,000 x g 4 °C, 15 min			
4–5 Cell lysis <i>(Important: Check Buffer LYS for precipitated SDS)</i>	High-copy / low-copy 8 mL / 16 mL Buffer RES 8 mL / 16 mL Buffer LYS RT, 5 min		High-copy / low-copy 12 mL / 24 mL Buffer RES 12 mL / 24 mL Buffer LYS RT, 5 min	
6 Equilibration of the column and filter	12 mL Buffer EQU		25 mL Buffer EQU	
7 Neutralization	8 mL / 16 mL Buffer NEU Mix thoroughly until colorless		12 mL / 24 mL Buffer NEU Mix thoroughly until colorless	
8 Clarification and loading of the lysate	Invert the tube 3 times Load lysate on NucleoBond® Xtra Column Filter			
9 1 <sup>st</sup> Wash	5 mL Buffer EQU !		15 mL Buffer EQU !	
10 Filter removal	Discard NucleoBond® Xtra Column Filter		Discard NucleoBond® Xtra Column Filter	
11 2 <sup>nd</sup> Wash	8 mL Buffer WASH !		25 mL Buffer WASH !	
12 Elution	5 mL Buffer ELU		15 mL Buffer ELU	
13 Precipitation	<b>NucleoBond® Xtra Midi</b>	<b>NucleoBond® Xtra Midi Plus</b>	<b>NucleoBond® Xtra Maxi</b>	<b>NucleoBond® Xtra Maxi Plus</b>
	3.5 mL Isopropanol Vortex 4,5–15,000 x g 4 °C, 30 min	3.5 mL Isopropanol Vortex RT, 2 min Load NucleoBond® Finalizer	10.5 mL Isopropanol Vortex 4,5–15,000 x g 4 °C, 30 min	10.5 mL Isopropanol Vortex RT, 2 min Load NucleoBond® Finalizer Large
14 Washing and drying	2 mL 70 % ethanol 4,5–15,000 x g RT, 5 min 10–15 min	2 mL 70 % ethanol ≥ 6 x air until dry	4 mL 70 % ethanol 4,5–15,000 x g RT, 5 min 15–30 min	4 mL 70 % ethanol ≥ 6 x air until dry
15 Reconstitution	Appropriate volume of TE buffer	200–800 µL Buffer TRIS	Appropriate volume of TE buffer	400–1000 µL Buffer TRIS